Neutronic and Burnup Studies of Accelerator-driven Systems Dedicated to Nuclear Waste Transmutation

Kamil Tuček

Stockholm 2004

Doctoral Thesis
Royal Institute of Technology
Department of Physics

Akademisk avhandling som med tillstånd av Kungl Tekniska Högskolan framlägges till offentlig granskning för avläggande av teknisk doktorsexamen fredagen den 3 december 2004 kl 10.00 i sal FA32, AlbaNova universitetscentrum, Kungl Tekniska Högskolan, Roslagstullsbacken 21, Stockholm.

ISBN 91-7283-890-6

TRITA-FYS 2004:68
ISSN 0280-316X
ISRN KTH/FYS/–04:68–SE

Printed by Universitetsservice US-AB, Stockholm 2004

Abstract

Partitioning and transmutation of plutonium, americium, *and* curium is inevitable if the radiotoxic inventory of spent nuclear fuel is to be reduced by more than a factor of 100. But, admixing minor actinides into the fuel severely degrades system safety parameters, particularly coolant void reactivity, Doppler effect, and (effective) delayed neutron fractions. The incineration process is therefore envisioned to be carried out in dedicated, accelerator-driven sub-critical reactors (ADS). However, ADS cores operating in concert with light-water reactors (two-component scenario) also exhibit high burnup reactivity swing with penalty on the system performance/economy.

In the frame of this design work, we attempted, by choice of coolant and optimisation of fuel concept and core design, to achieve favourable neutronic, burnup and safety characteristics of the transuranium ADS burner. Key thermal hydraulic and material-related constraints were respected.

A novel fuel matrix material, hafnium nitride, was identified as an attractive diluent option for highly reactive transuranics. (TRU,Hf)N fuels appeared to have a good combination of neutronic, burnup and thermal characteristics: maintaining hard neutron spectra, yielding acceptable values of coolant void reactivity and source efficiency, and providing small burnup reactivity loss. A conceptual design of a (TRU,Hf)N fuelled, lead/bismuth eutectic cooled ADS was developed. The average discharge burnup of 20% fissions per initial metal atom could be reached even without fuel reshuffling. The fission fraction ratios of even-neutron number americium nuclides are increased by a factor of two in comparison to burners with inert matrix based fuels. Hence, thanks to the reduced production of higher actinides and helium, fuel cycle economy is improved.

The coolant void worth proved to be a strong function of the fuel composition - reactor cores with high content of fertile material or minor actinides in fuel exhibit larger void reactivities than systems with plutonium-rich, inert matrix fuels. In reactor systems cooled by lead/bismuth eutectic, a radial steel pin reflector significantly lowered coolant void reactivity. For transuranic fuel, fertile and strongly absorbing matrices exhibited increasing void worth with increasing pitch, while the opposite was valid for the coolant void worth of inert matrix fuels. Large pitches also appeared to be beneficial for limiting the reactivity worth of the cladding material and improving source efficiency.

The economy of the source neutrons was investigated as a function of core and target design. An incentive to design the core with as low target radius as allowable by the thermal constraints posed by the ability to dissipate accelerator beam power was identified.

ISBN 91-7283-890-6 • TRITA-FYS 2004:68 • ISSN 0280-316X • ISRN KTH/FYS/–04:68–SE

List of Papers

I. K. Tuček, J. Wallenius, and W. Gudowski
Coolant void worth in fast breeder reactors and accelerator-driven transuranium and minor-actinide burners
Annals of Nuclear Energy, **31**, 1783 (2004)

II. K. Tuček, M. Jolkkonen, J. Wallenius, and W. Gudowski
Neutronic and burnup studies of an accelerator-driven transuranium burner in a start-up mode
Submitted to Nuclear Technology (2004)

III. J. Wallenius, K. Tuček, J. Carlsson, and W. Gudowski
Application of burnable absorbers in an accelerator driven system
Nuclear Science and Engineering, **137**, 96 (2001)

IV. K. Tuček, J. Wallenius, and W. Gudowski
Optimal distribution of fuel, poisons and diluents in sub-critical cores dedicated to waste transmutation
In Proceedings of the International Conference on Emerging Nuclear Energy Systems, ICENES 00, Petten, NRG (2000)

V. P. Seltborg, J. Wallenius, K. Tuček, and W. Gudowski
Definition and application of proton source efficiency in accelerator-driven systems
Nuclear Science and Engineering, **145**, 390 (2003)

Papers which are not included in the thesis:

VI. K. Tuček, J. Wallenius, W. Gudowski and A. Sołtan
IAEA accelerator driven system neutronic benchmark
In Feasibility and Motivation for Hybrid Concepts for Nuclear Energy Generation and Transmutation, IAEA-TC-903.3, CIEMAT (1998)

VII. J. Wallenius, K. Tuček, and W. Gudowski
Technetium-99 neutron absorbers in the reflector of Pb/Bi cooled reactors
In Proceedings of Heavy Liquid Metal Coolants in Nuclear Technology, HLMC 98, IPPE Obninsk, Russia (1998)

VIII. K. Tuček, J. Wallenius, W. Gudowski, and C. Sanders
Burnup in a sub-critical system with flat power density
In Proceedings of the Third International Conference on Accelerator-Driven Transmutation Technologies and Applications, ADTTA 99, Praha (1999)

IX. J. Wallenius, K. Tuček, W. Gudowski, and C. Sanders
Neutronics of a sub-critical system burning non-recycled LWR waste
In Proceedings of the Third International Conference on Accelerator-Driven Transmutation Technologies and Applications, ADTTA 99, Praha (1999)

X. J. Wallenius, K. Tuček, and W. Gudowski
Safety analysis of nitride fuels in cores dedicated to waste transmutation
In Proceedings of the Sixth International Information Exchange Meeting, Actinide and Fission Product Partitioning and Transmutation, Madrid, OECD/NEA (2000)

XI. M. Eriksson, J. Wallenius, K. Tuček, and W. Gudowski
Preliminary safety analysis of a Swedish accelerator driven system employing nitride fuel and burnable absorbers
In Proceedings of the Technical Committee Meeting on Core Physics and Engineering Aspects of Emerging Nuclear Energy Systems for Energy Generation and Transmutation, Argonne National Laboratory (2000)

XII. K. Tuček, J. Wallenius, and W. Gudowski
Source efficiency in an accelerator-driven system with burnable absorbers
In Proceedings of the International Conference on Back-End of the Fuel Cycle: From Research to Solutions, GLOBAL 2001, Paris, ANS (2001)

XIII. D. Westlén, W. Gudowski, J. Wallenius, and K. Tuček
A cost benefit analysis of an accelerator driven transmutation system
In Proceedings of AccApp/ADTTA'01, Reno, USA, ANS (2001)

XIV. J. Cetnar, W. Gudowski, J. Wallenius, and K. Tuček
Simulation of nuclide transmutations with Monte-Carlo continuous energy burnup code (MCB1C)
In Proceedings of AccApp/ADTTA'01, Reno, USA, ANS (2001)

XV. M. Eriksson, J. Wallenius, J.E. Cahalan, K. Tuček, and W. Gudowski
Safety analysis of Na and Pb-Bi coolants in response to beam instabilities
In Proceedings of the Third International Workshop on Utilisation and Reliability of High Power Proton Accelerators, Santa Fe, USA (2002)

Acknowledgments

I would like to express my gratitude to

- Waclaw Gudowski for inviting me to work on transmutations at the Royal Institute Institute of Technology, for his support and encouragement throughout the years.
- František Janouch for bringing me to Sweden, for his constant interest and enthusiasm initiating long discussions on any subject.
- Janne Wallenius for useful suggestions and valuable remarks.
- my colleagues, old and present, from the Department of Nuclear and Reactor Physics for providing a creative, friendly and relaxed atmosphere; particular thanks to Mikael Jolkkonen and Patrick Isaksson for linguistic advice.
- Lvíček and all other friends which made my stay here so enjoyable and cheerful.

Finally, most thanks go to my wonderful parents. Děkuji vám za všechno!

I acknowledge the financial support by the Swedish Nuclear Fuel and Waste Management Co. (SKB AB) and the Swedish Institute.

Stockholm, November 12, 2004

Kamil Tuček

Contents

Nomenclature

ABR	Actinide Burner Reactor
ADS	Accelerator-driven System
AFCI	Advanced Fuel Cycle Initiative
ALMR	Advanced Liquid Metal Reactor
An	Actinide
ATR	Advanced Test Reactor
ATW	Accelerator Transmutation of Waste
BA	Burnable Absorber
BOC	Beginning-Of-Cycle
BOL	Beginning-Of-Life
BWR	Boiling Water Reactor
CERCER	CERamic-CERamic fuel
CERMET	CERamic-METallic fuel
CAPRA	Consommation Accrué de Plutonium en Récteur rApide
CEA	Commissariat à l'Énergi Atomique
CMS	Centre-of-mass system
CNRS	Centre National de la Recherche Scientifique
DIAMEX	DIAMide EXtraction
DIDPA	Di-IsoDecylPhosphoric Acid
dpa-NRT	Displacement per atom (Norgett, Robinson, Torrens)
EdF	Électricité de France
EFR	European Fast Reactor
EFTTRA	Experimental Feasibility of Targets for TRAnsmutation
ENDF	Evaluated Nuclear Data File
EOC	End-Of-Cycle
EOL	End-Of-Life
FBuR	Fast Burner Reactor
FIMA	Fissions per Initial Metal Atom
FTF	Flat-to-Flat
FP	Fission Product
fpd	Full power day
efpy	Effective full power year
FR	Fast Reactor

GEDEPEON	GEstion des DEchets et Production d'Energie par des Options Nouvelles
GWd	Giga-watt day
GW_e	Giga-watt electric
GW_{th}	Giga-watt thermal
HLW	High Level Waste
HLLW	High Level Liquid Waste
ICRP	International Commission on Radiation Protection
IFR	Integral Fast Reactor
ITU	Institute for TransUranium elements
JAERI	Japan Atomic Energy Research Institute
JEF	Joint European File
JENDL	Japanese Evaluated Nuclear Data File
KAERI	Korea Atomic Energy Research Institute
LANL	Los Alamos National Laboratory
LBE	Lead-Bismuth Eutectic
LINAC	LINear ACcelerator
LLFP	Long-lived Fission Product
LWR	Light Water Reactor
MA	Minor Actinide
MCB	Monte Carlo Continuous energy Burnup code
MCNP	Monte Carlo N-Particle code
MCNPX	Monte Carlo N-Particle code eXtended
MOX	Mixed OXide fuel
MW_{th}	Mega-watt thermal
N/A	Not Available
NEA	Nuclear Energy Agency of OECD
OECD	Organisation for Economic Co-operation and Development
OMEGA	Options Making Extra Gain from Actinides and fission products
P/D	Pitch-to-Diameter ratio
P&T	Partitioning and Transmutation
Pb/Bi	Lead-Bismuth Eutectic
PSI	Paul Scherrer Institute
PUREX	Plutonium Uranium Recovery by EXtraction
PWR	Pressurised Water Reactor
S/A	Sub-assembly
SAD	Sub-critical Assembly Dubna
SPIN	SeParation-INcineration
tHM	Metric tonne of Heavy Metal
TRPO	TRialkyl Phosphine Oxide
TRU	TRansUranic element
TRUEX	TRansUranium EXtraction
TWh_e	Tera-watt hour electric
UOX	Uranium OXide fuel

XADS	EXperimental Accelerator-Driven System
XADT	EXperimental Accelerator-Driven Transmutation

We know only a single science, the science of history.

Karl Marx (The German Ideology, 1846)

The History of the Universe in 200 Words or Less

Quantum fluctuation. Inflation. Expansion. Strong nuclear interaction. Particle-antiparticle annihilation. Deuterium and helium production. Density perturbations. Recombination. Blackbody radiation. Local contraction. Cluster formation. Reionisation? Violent relaxation. Virialisation. Biased galaxy formation? Turbulent fragmentation. Contraction. Ionisation. Compression. Opaque hydrogen. Massive star formation. Deuterium ignition. Hydrogen fusion. Hydrogen depletion. Core contraction. Envelope expansion. Helium fusion. Carbon, oxygen, and silicon fusion. Iron production. Implosion. Supernova explosion. Metals injection. Star formation. Supernova explosions. Star formation. Condensation. Planetesimal accretion. Planetary differentiation. Crust solidification. Volatile gas expulsion. Water condensation. Water dissociation. Ozone production. Ultraviolet absorption. Photosynthetic unicellular organisms. Oxidation. Mutation. Natural selection and evolution. Respiration. Cell differentiation. Sexual reproduction. Fossilisation. Land exploration. Dinosaur extinction. Mammal expansion. Glaciation. Homo sapiens manifestation. Animal domestication. Food surplus production. Civilisation! Innovation. Exploration. Religion. Warring nations. Empire creation and destruction. Exploration. Colonisation. Taxation without representation. Revolution. Constitution. Election. Expansion. Industrialisation. Rebellion. Emancipation Proclamation. Invention. Mass production. Urbanisation. Immigration. World conflagration. League of Nations. Suffrage extension. Depression. World conflagration. Fission explosions. United Nations. Space exploration. Assassinations. Lunar excursions. Resignation. Computerisation. World Trade Organisation. Terrorism. Internet expansion. Reunification. Dissolution. World-Wide Web creation. Composition. Extrapolation?

Reprinted from Annals of Improbable Research, **3**, 27 (1997)

Chapter 1

Introduction

1.1 Background

In the present state of scientific knowledge, about 13.7 billions of years ago, some 10^{-33} to 10^{-4} s after the Big Bang, the protons and neutrons were created in baryogenesis process, hence marking the beginning of the **Nuclear Age** [1]. However, it took another $10^{5.5}$ years for first hydrogen atom to be formed, 100-200 million years for stars to be born, and some millions of years for the first supernova to explode spreading heavy elements like carbon, nitrogen, oxygen, and uranium throughout the entire Universe. At least $4.6{\cdot}10^{9}$ years ago, such a supernova explosion occurred in the vicinity of our present Solar system, providing the primordial material for its formation.

This entire historical prologue was unknown for glassmen around the village of Jáchymov (St. Joachimsthal) in the Bohemian Sudetenland as they, in the middle ages, started to use the shiny black mineral coming as a waste from local silver mines in the production of yellow coloured glass and ceramics products. An exciting mystery has been covered in these rocks, called by German miners *pechblende*, i.e. "bad luck mineral", until they came into the hands of one of the greatest scientists of his time, Henri Becquerel. In 1896, he discovered that the invisible rays emitted by these uranium rocks (a phenomenon he called *radioactivity*) are responsible for exposure of photographic plates [2].

But the major discovery was to come in December 1938. German chemists Otto Hahn and Fritz Strassmann reported that barium, an element lighter than uranium, was found in the neutron irradiated uranium samples [3]. It was Lise Meitner and her nephew Otto Frisch who first interpreted these results as a disintegration of the uranium nucleus and proposed a name for this phenomenon - *fission* [4]. A short time afterwards, Frisch and others demonstrated that the overall energetic balance of the fission reaction is positive, and that the major amount of energy is manifested as kinetic energy of the fission products. In 1939, Kowarski showed that

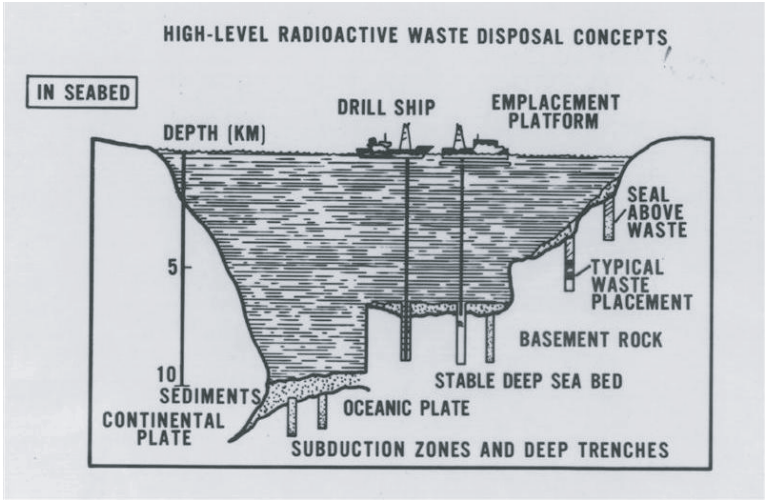

Figure 1.1. Ideas how to manage spent nuclear fuel have reached maturity since the 50s [8].

about three neutrons are liberated in one fission reaction [5, 6], which finally opened the gate for construction of a self-sustainable nuclear energy producing device.

In the shadow of World War Two, the atomic era took off as a race on the track of nuclear weapon development. Americans, being the first to succeed in 1945 and having reached considerable achievements in nuclear weapons (thermonuclear bomb in 1952) and naval reactor designs (the first nuclear driven submarine Nautilus was launched in January 1954), started to refocus their interests into the peaceful utilisation of atomic power. President Eisenhower's "Atoms for Peace" speech on December 8, 1953 and Soviet pledge of help in expanding the nuclear technology in the Eastern Block countries in 1955 had unlocked the doors to a massive and intensive development of nuclear energy on a commercial scale.

And anticipations were quite high - atomic power was supposed to turn rivers and blast valleys as well as drive rail engines and aircrafts [7]. The management of nuclear waste was similarly ambitious - such projects as dumping of nuclear wastes into the sea and launching them out into the space in rockets or depositing the waste in a seabed could be found among the proposals (Figure 1.1).

During the 60s and 70s, the spectrum of nuclear power utilisation narrowed significantly, converging into more realistic projects and focusing on designs of reactors for commercial and military purposes. Waste management strategies had got down to earth, too. Plans for geological repository were put forth proposing to bury spent nuclear fuel in deep geological formations. Such projects are under way in many countries, notably U.S.A., Sweden, and Switzerland. The moral, safety

and economic issues of this waste management option are widely discussed and especially the long-term safety of such repositories has become a major concern of enviromentalists and the general public [9].

Indeed, the safety of an underground repository is a complex function of the endurance of natural and technical barriers as well as of its volume and content of disposed nuclear waste. In the past two decades, several projects aiming to reduce the volume and content of spent nuclear fuel have taken shape and have been gathered under the general banner "partitioning and transmutation technologies" (P&T). The common denominator of all these projects is the use of an external radiation source (nuclear reactor, accelerator, or both) producing particles (neutrons, gammas, protons, etc) which in a controlled manner incinerate (transmute) certain nuclides separated/partitioned from spent fuel. Partitioning techniques are sometimes considered alone as a process of better spent fuel conditioning before final disposal. It is believed that gradual phase-in of P&T technologies into the existing fuel cycle could reduce the risks associated with spent fuel management prior to geological disposal and the long-term radiological and radiotoxic impact of the repository on the environment.

1.2 Thesis overview

This thesis investigates in part the feasibility of deploying accelerator-driven systems (ADS) as a part of a P&T scheme into the existing nuclear fuel cycle and their influence on the long-term safety performance of the geological repository. More explicitly, an attempt is made to achieve, by choice of coolant, fuel concept and core design, favourable neutronic, burnup and safety characteristics of the transuranium ADS burner. In pursuit of this goal, a conceptual design design of an ADS burner employing innovative (TRU,Hf)N fuel was developed in **Paper II**. Preparatory, design scoping studies, with respect to the coolant void worth and source efficiency were performed in **Papers I** and **IV**, respectively. In **Paper V**, a novel theoretical framework to describe the source multiplication in ADS was presented. **Paper III** investigated the feasibility of a massive introduction of a neutron absorber (B_4C) in ADS.

We begin with a presentation of the basic waste parameters of spent nuclear fuel and introduce the reader into the issue of radiotoxic fuel inventory in Chapter 2. Chapter 3 discusses the physical prerequisites for efficient transmutation of transuranics in P&T schemes and provides an overview of existing spent fuel transmutation strategies. A brief description of accelerator-driven systems and projects in this field then follows in Chapter 4. The choice of fuel, diluent matrix, cladding and coolant materials for ADS is discussed in Chapter 5. Chapter 6 accounts for neutronic, safety and burnup characteristics regarding TRU incineration in ADS. Conceptual designs of nitride fuelled lead-bismuth cooled TRU ADS burners with HfN fuel matrix and B_4C absorbers are presented in Chapter 7. Finally, Chapter 8 summarises the results presented in the appended papers.

1.3 Author's contribution

The author of the thesis is the principal author of **Papers I, II** and **IV**. He developed the framework of the study, performed neutronic, burnup and thermal hydraulic calculations, analysed and interpreted results. The author participated in the neutronic and thermal hydraulic design work of **Paper III**, was responsible for transport and burnup calculations and contributed in writing the manuscript. He was involved in the development of the theoretical framework, computational algorithm, analyses, and interpretation of the results of **Paper V**.

Chapter 2

Nuclear waste

Nuclear waste from nuclear power plants encompasses a broad spectrum of categories, inclusive high-level radioactive spent nuclear fuel, intermediate-level active parts, as e.g. water filters, and low-level waste, as protective clothing, scrap, or gaseous and liquid discharges from the plant. The spent nuclear fuel is by far the biggest contributor to the radioactivity of the nuclear waste and poses the highest risk for the environment. Nowadays, most of the countries possesses a growing stock of spent fuel, either non-processed or reprocessed with separated plutonium and vitrified high-level waste.

After the discharge from the reactor, the radioactivity of spent fuel is several orders of magnitude higher than that of the uranium ore used to manufacture the fuel [10]. This excess activity accumulated in the spent fuel is a consequence of nuclear reactions, which took place in the core during fuel burnup. In this respect, the reactions of neutron absorption, i.e., fission and capture, are of a particular importance.

2.1 Fission process

Fission absorption of neutrons in uranium leads to the disintegration of the nucleus into two or three fission fragments, so called *binary* and *ternary* fission, respectively. Fission products (FP) are neutron rich and about 2-3 neutrons are emitted from the fragments at the instant of fission. Most of the recoverable energy is released in the form of kinetic energy of fission products (85%), followed by prompt energy of gamma radiation and fission neutrons. About ten percent of the retrievable energy from fission is liberated with a certain delay as a consequence of successive radioactive decay (β^-) of fission products.

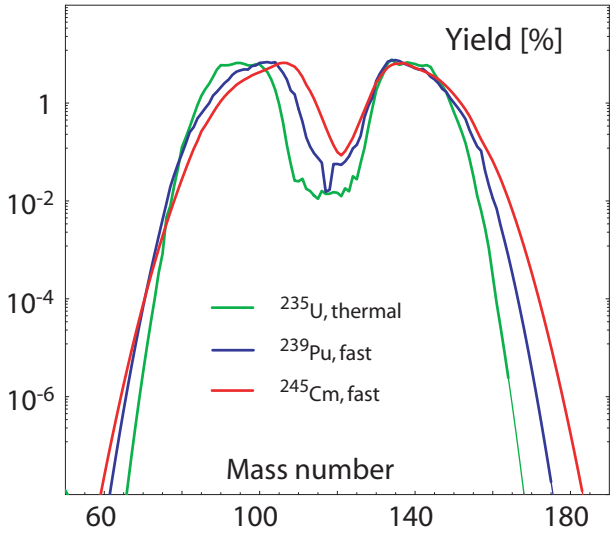

Figure 2.1. Yield of the fission products as a function of mass number given for thermal fission of ^{235}U, fast fission of ^{239}Pu, and fast fission of ^{245}Cm. JEF-2.2 data were used [11].

A typical binary fission process of an actinide, here induced by thermal neutrons on ^{235}U, may look like

$$ {}^{1}_{0}\mathrm{n} + {}^{235}_{92}\mathrm{U} \rightarrow {}^{95}_{37}\mathrm{Rb} + {}^{139}_{55}\mathrm{Cs} + 2\,{}^{1}_{0}\mathrm{n} + \tilde{\nu}_{\mathrm{e}} \qquad (2.1) $$

Fission products (FP) are typically far above the stability line (relating number of protons and neutrons) and are thus decaying by emitting β^-–particles. The mass distribution of fission products depend not only on the nature of the target nucleus, but also the energy of incoming neutron. Giving an example, fission product yields from binary *thermal* ($\overline{E_{\mathrm{n}}} \sim 0.0253$ eV) and *fast* fissions ($\overline{E_{\mathrm{n}}} \simeq$ fission neutron spectrum) of ^{235}U, ^{239}Pu, and ^{245}Cm are displayed in Figure 2.1. We observe that with increasing mass of actinide atoms, the maxima and minima of fission yield curves shift towards higher mass numbers, the difference being most pronounced for the mass range around A$\sim$90.

Transuranic elements (TRU) are produced in a nuclear reactor as a result of neutron captures on actinide nuclei, see Figure 2.2. Consecutive non-fission absorptions are eventually followed by β^- emission as the nucleus compensates for its neutron excess. Such a reaction chain can be exemplified by the production of ^{239}Pu in the fuel - neutron capture in ^{238}U is followed by two successive β^- decays of ^{239}U and ^{239}Np, with half-lifes of 24 min and 2.3 days, respectively. Almost all

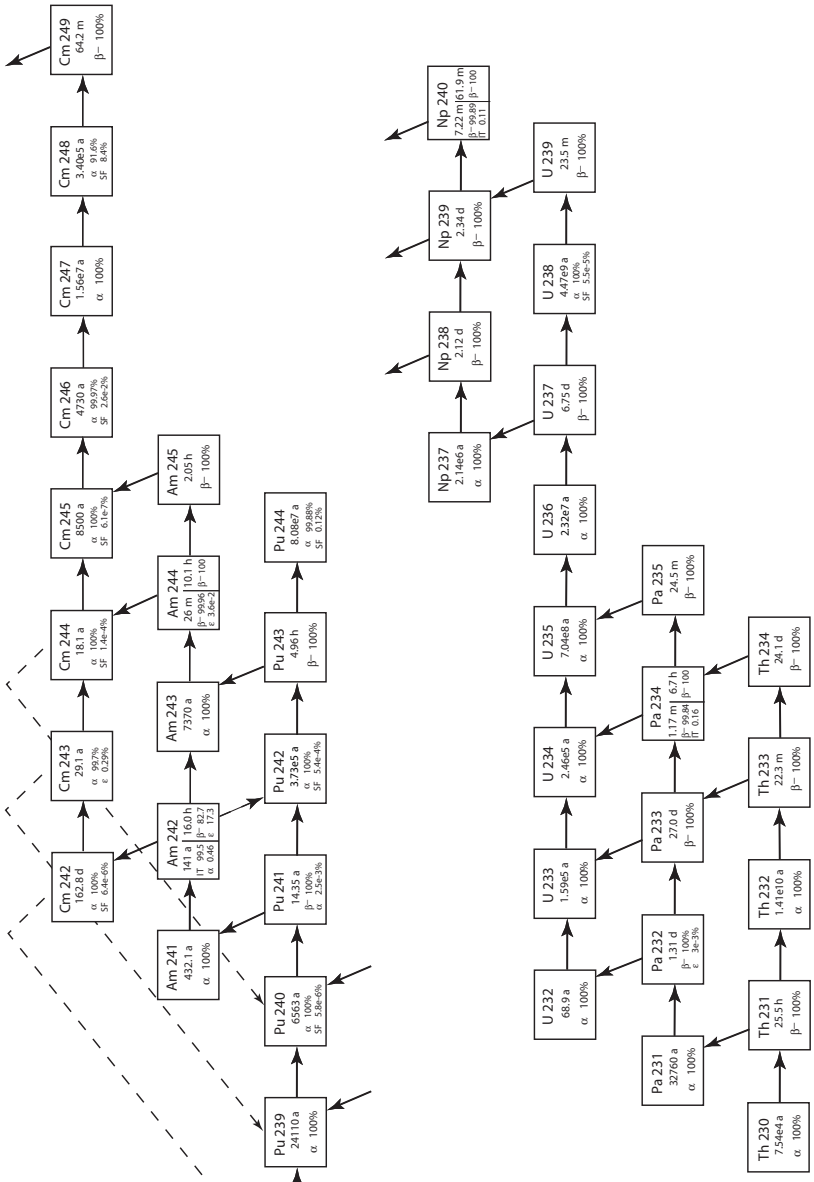

Figure 2.2. Chart of the actinides, marked transmutation paths include (n,γ) reaction, as well as α and β^- decay channels.

Nucl	Half-life [year]	UOX 41.2 GWd/t [kg/tHM]	UOX 50 GWd/t [kg/tHM]	MOX 43 GWd/t [kg/tHM]	e_{50}^{ing} [10^{-8}Sv/Bq] <1 year	adult
^{235}U	$7.04{\cdot}10^{8}$	6.6	6.5	N/A	35	4.7
^{238}U	$4.47{\cdot}10^{9}$	938	929	N/A	34	4.5
^{237}Np	$2.14{\cdot}10^{6}$	0.55	0.71	0.16	200	11
^{238}Pu	87.7	0.27	0.42	2.5	400	23
^{239}Pu	24100	5.9	6.2	21.5	420	25
^{240}Pu	6563	2.6	2.9	17.9	420	25
^{241}Pu	14.4	1.4	1.5	8.3	5.6	0.48
^{242}Pu	$3.73{\cdot}10^{5}$	0.74	0.95	7.2	400	24
^{241}Am	432.1	0.34	0.38	3.0	370	20
^{243}Am	7370	0.19	0.28	1.9	360	20
^{243}Cm	29.1	$<10^{-3}$	$<10^{-3}$	0.014	320	15
^{244}Cm	18.1	0.056	0.098	0.80	290	12
^{245}Cm	8500	0.004	0.007	0.10	370	21
^{246}Cm	4730	$<10^{-3}$	0.002	0.006	370	21

Table 2.1. The basic parameters for most important actinides from LWR-UOX (burnup 41.2 GWd/tHM and 50 GWd/tHM) and LWR-MOX (43 GWd/tHM, initial UOX fuel reprocessed after 4 years) discharges, allowing for four years of decay. Total production of TRU in the LWR-UOX and LWR-MOX is approximately 37 kg/TWh$_e$ and 187 kg/TWh$_e$, respectively. Effective dose coefficients for ingestion e_{50}^{ing} are given for an individual from general public of age under 1 year (column 6) and above 17 year (column 7). Spent fuel data are adopted from OECD/NEA study [10] and effective dose coefficients were taken from an EU directive [13].

accumulated TRU elements in spent fuel release surplus energy first by emission of α-particles and successively transform via four well-known decay chains into stable lead isotopes (^{206}Pb, ^{207}Pb, ^{208}Pb) and extremely long-lived ^{209}Bi ($T_{1/2}$ = $1.9{\cdot}10^{19}$yr [12]). In the short-term, one very important exception is the β^- decay of ^{241}Pu into ^{241}Am, relatively increasing the amount of minor actinides in the spent fuel by about a factor of 2.5 in a 40 years decay period.

2.2 Spent fuel composition

There are two main parameters, which determine the actual composition of spent fuel - burnup and reactor spectrum. On the other hand, the irradiation history is of a minor importance. A fuel burnup is the amount of recoverable energy obtained as a result of fuel fission and is, in its turn, a function of the power and duration of fuel irradiation, while the reactor spectrum depends primarily of the reactor type (choice of the core materials and lattice design). Moreover, both of these characteristics are dependent on fuel pin positions in the core and thus overall fuel

Isotope	Half-life [year]	Mass UOX 41.2 GWd/t [kg/tHM]	Mass UOX 50 GWd/t [kg/tHM]	e_{50}^{ing} [10^{-8}Sv/Bq] < 1 year	adult	workers
^{93}Zr	$1.5{\cdot}10^6$	0.87	1.05	0.12	0.11	0.028
^{99}Tc	$2.11{\cdot}10^5$	1.00	1.2	1.0	0.064	0.078
^{107}Pd	$6.5{\cdot}10^6$	0.27	0.34	0.044	0.0037	0.0037
^{126}Sn	$\sim 1{\cdot}10^5$	0.03	0.03	5.0	0.47	0.47
^{129}I	$1.57{\cdot}10^7$	0.21	0.26	18	11	11
^{135}Cs	$2.3{\cdot}10^6$	0.46	0.59	0.41	0.20	0.20

Table 2.2. The basic parameters for most important fission products from LWR-UOX fuel with burnup 41.2 GWd/tHM and 50 GWd/tHM, respectively [10]. The effective dose coefficients for occupational exposure (column 7) are age independent and in most of the cases roughly equals the effective dose coefficients assigned for the adult individuals [13]. This is with several important exceptions and e.g. the coefficient for ^{210}Po (not listed in the table) is estimated to be five times higher for general public than for workers exposure.

assembly burnup is in fact an average over local pin burnup rates. The local burnup of LWR fuel can differ as much as ten percent in individual sub-assemblies of one discharged batch corresponding to about five percent difference in the amount of TRU.

In the past 20 years, the average LWR fuel burnup increased from 30 GWd/tHM up to 50 GWd/tHM. Furthermore, it seems feasible that innovative types of fuel with target burnup rates of about 65-70 GWd/tHM could be introduced into LWR cores in the near future [14]. Spent fuel which would be considered as a subject for P&T technologies will thus have a large variety of transuranic and fission product compositions, dependent also on decay time. In order to schematically illustrate spent fuel transuranic content we further consider a typical LWR discharge with burnup of 41.2 GWd/tHM and 50 GWd/tHM after four years of decay, see Tables 2.1 and 2.2 [10]. Generally, the main part (94.5 wt%) of spent nuclear fuel still consists of the original material - uranium, containing about 0.7 wt% of fissile ^{235}U. Approximately one weight percent of spent fuel comprises plutonium and additional 0.1 wt% minor actinides (MA) - neptunium, americium, curium. Fission fragments make up the final four percent of the spent fuel mass. The amount of transuranics and minor actinides is a non-linear function of burnup due to eventual burnup of accumulated plutonium in the reactor.

An important consequence of deep burnup is a steep increase of MA content and thereafter α activity which in a long-term perspective dominates the residual heat of spent fuel and sets limiting parameters for geological repository. Note the strongly increased MA production in MOX fuel sub-assemblies which amounts around 17.5 kg/TWh$_e$ (a factor of four-five higher than for UOX), see Table 2.1.

At the end of year 2002, there were 441 reactors running worldwide with total net installed capacity of 359 GW$_e$. Additionally, 33 reactor units are under construction

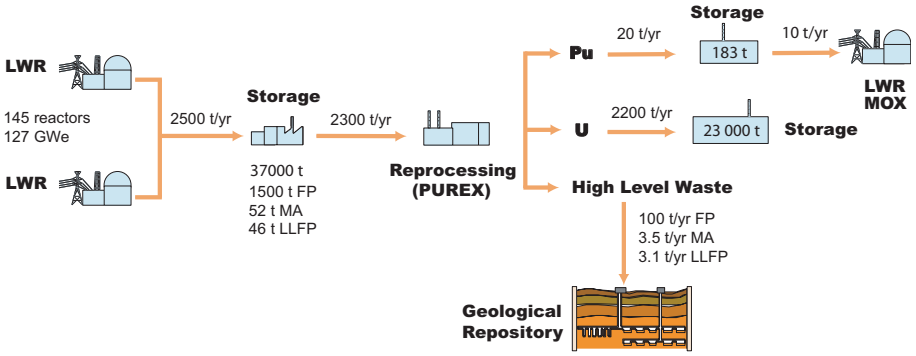

Figure 2.3. Spent and processed fuel flow sheet in the European reactor park (127 GW_e), cumulative amount and annual change as of 2001. Fuel burnup is 50 GWd/tHM. Figure is adopted from an EU roadmap report [18].

with a total capacity of 27 GW_e. The total production of electricity was 2780 TWh, being about 16% of the total world electricity supply. On the global level, about 10 500 tonnes of heavy metal spent fuel are produced annually, which is expected to increase to about 11 500 tHM/yr by 2010. Cumulatively, since the beginning of the nuclear programme, the amount of spent nuclear fuel accumulated by the beginning of 2003 was about 255 000 tHM (containing more than 2500 tonnes of transuranics), which is predicted to increase almost linearly to 340 000 tHM by the year 2010 and 445 000 tHM by the year 2020 [15]. Reprocessing and military stockpiles add approximately 170 tonnes and 100 tonnes of plutonium, respectively [16]. Almost 40% (70 000 t) of the world spent fuel stock has already been reprocessed and plutonium recycled in LWR as MOX fuel.

From the European park of nuclear reactors (Figure 2.3), amounting to 127 GW_e of nominal power, about 2500 t of heavy metal in spent nuclear fuel is produced annually, including 25 t of plutonium and about 3.5 tonnes of minor actinides (fuel burnup is 50 GWd/tHM). Additionally, there is about 100 t of fission products produced each year. We note that the annual output of spent fuel per obtained TWh_e from the European nuclear park is somewhat lower than the worldwide average due to the ongoing partial fuel reprocessing. In Sweden, the total projected amount of fuel generated, allowing for 40 years of the operation of each reactor, is 9500 tonnes [17]. Except for the main part of fuel consisting of UOX fuel sub-assemblies (both of BWR and PWR type), there is 23 t of MOX fuel and 20 t of fuel from the Ågesta reactor, which should be disposed of in geological repository. Swedish annual production of TRU corresponding to the electricity production 70 TWh_e is 2.6 tonnes, including almost 440 kg of minor actinides (around 17 wt% of TRU mass) 40 years after discharge.

2.3 Radiotoxic inventory

In order to quantify the effect of radioactivity of spent fuel on the biological tissues and assess long-term risks of its management strategy, the concept of *radiotoxic inventory* is introduced [10].

The radiotoxic inventory is a measure of the equivalent dose that is imposed to a person following the intake of a given amount of an element. It depends on the physical properties of the nuclides, such as their half-lifes, but also on respiratory deposition, clearance, and post-incorporation biokinetics in the human body (as e.g. uptake into blood). It nowadays refers almost exclusively to ingestion in favour of the earlier used values for inhalation.

Calculations of the radiation risk of a specific radionuclide take into account the type of radiation/particles emitted by the nuclide (neutrons, α, β, γ, X-rays), quantified by quality factors Q (e.g. neutrons in the energy range of 100 keV - 2 MeV and α-particles deposit around twenty times more energy than photons or electrons) as well as the effect of radiation upon the specific tissue or organ, expressed by weight factors w_T. Supposing integral body exposure time equal to 50 years, the committed effective dose intake E_{50} is then defined as

$$E_{50} = \sum_T w_T H_{50}^T, \tag{2.2}$$

where H_{50}^T is committed 50 years equivalent dose to tissue or organ T. Coefficients for committed effective dose intake (alternatively effective dose coefficients e_{50} which correspond to the committed dose E_{50} resulting from the intake of 1 Bq of a specific radionuclide) are then given in several publications, most recently in an EU directive [13] and ICRP recommendations [19, 20]. Annual limits of intake (ALI), used frequently in radiation protection for occupational exposure, can be then estimated as $ALI(Bq) = 0.20\ Sv/e_{50}(Sv/Bq)$ based on the annual average limit of committed dose of 20 mSv (100 mSv over a 5 year period).

As introduced earlier, we will consider the radiotoxic inventory of two types of spent fuel coming from present-day commercial light water reactors - spent uranium-oxide (UOX) and reprocessed mixed-oxide fuel (MOX), see Figures 2.4 and 2.5. In both cases it is assumed that separation of FP and TRU from the uranium matrix has been performed after irradiation. Note that MOX vector in this analysis corresponds to the burnup of 33.5 GWd/tHM (initial Pu content 5.3%) [10].

In the case of spent UOX fuel, the radiotoxic inventory is dominated by fission products for the first 40 years after discharge. It is mainly due to two short-lived nuclides, ^{90}Sr and ^{137}Cs, with half-lifes of around 30 yr. The contribution of plutonium isotopes and their decay daughters start to dominate the radiotoxic inventory at approximately 100 years and remains dominant until it reaches the level of the mined uranium ore used to manufacture the fuel (support factor is $\sim$3.7/0.7$\simeq$5.3). Thereafter, the radiotoxic inventory is eventually dominated by reprocessed uranium and daughters of its decay chain. Many effective dose coefficients have been

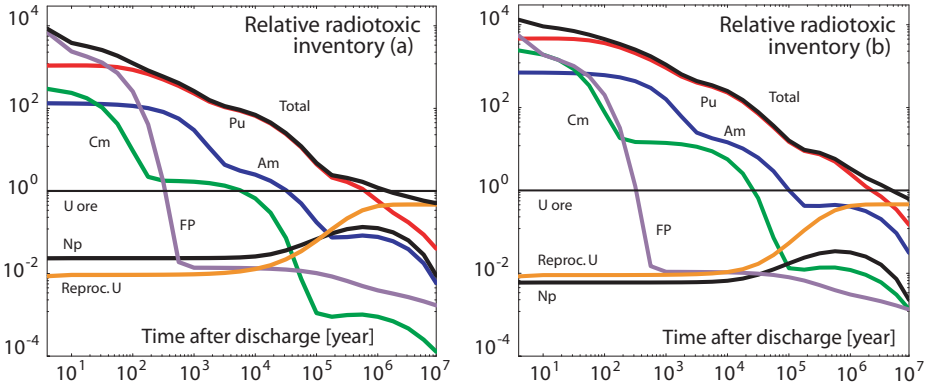

Figure 2.4. The radiotoxic inventory of spent UOX(a) and MOX(b) fuel components and their decay products relative to the radiotoxic inventory of the uranium ore that UOX fuel is manufactured from. The values are shown as a function of time relative to four years after discharge (the likely time delay for fuel reprocessing and further incineration in the P&T scheme); during this time ^{241}Am content was roughly doubled. The radiotoxic inventory of daughter products appearing as a result of decay after 4 years are included in the values of their mother nuclides. Fuel burnup is assumed to be 41.2 GWd/tHM (initial ^{235}U enrichment 3.7%) and 33.5 GWd/tHM (initial Pu content 5.3%, UOX fuel reprocessed after three years) in the case of UOX and MOX, respectively [10]. The values refer to a collective dose of the radiation ingestion intake inducing only stochastic effects. The equilibrium radiotoxic inventory of uranium ore is approximately 20 mSv/g.

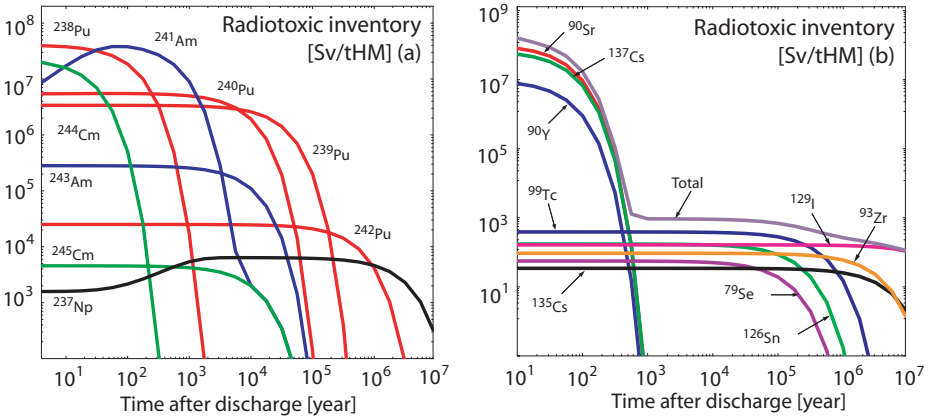

Figure 2.5. The radiotoxic inventory of transuranics (a) and fission products (b) in LWR-UOX discharge fuel, burnup is 41.2 GWd/tHM [10].

adjusted in the past few years, like e.g. those for ^{210}Po and ^{226}Ra (daughter products of ^{238}Pu and ^{238}U decay) which were increased by a factor of about 30 and 180, respectively. At the same time, the effective dose coefficient for ^{229}Th, a mem-

ber of the ^{241}Am, ^{241}Pu, and ^{237}Np family and contributing to long-term (beyond $3{\cdot}10^5$ years) radiotoxic inventory of spent fuel, was raised 25 times. The time until radiotoxic inventory reaches the level of the uranium ore needed for its manufacturing is thus prolonged up to one million years, a factor of five higher than reported in previous works [10, 21]. With respect to the mentioned uncertainties it is obvious that any quantitative estimation of the spent fuel radiotoxic inventory source term, which is an input for long-term risk assessment of repository performance inevitably has to be accompanied by extensive uncertainty analysis of input data and used models.

In the case of MOX spent fuel, the overall radiotoxic inventory is increased after 1000 years by a factor of four (considering only actinide inventory, by a factor of five) in comparison to the UOX discharges. This inventory is determined by plutonium nuclides and its decay daughters (^{241}Am), from a time 50 years after discharge till 1.5 million years when it reaches the level of uranium ore. The radiotoxic inventory of initial Am and Cm does not reach the level of uranium ore until about $2{\cdot}10^4$ years and 10^5 years, respectively, a factor of four longer than for UOX spent fuel. The radiotoxic inventory of curium isotopes is significant, mainly during the first 100 years after a discharge, due to the strong α and neutron emitter ^{244}Cm (half-life 18 year) which in conjunction with an almost doubled heat production significantly increases demands on short-term repository performance.

2.4 Spent fuel management

We see that the issue of spent fuel management spans a time of millions of years, clearly exceeding the anthropological apprehension of mankind. Spent fuel management thus inevitably becomes a question not only for scientists and experts but also for the whole society.

Of course, the most ideal waste management technique would be to reduce the radiotoxic inventories so that controlled manner disposal could be accomplished in predictable - human generation scale-time periods. In terms of spent fuel composition it would mean the complete transformation of all the long-lived actinides by means of fission and long-lived fission products via neutron capture, into stable or short-lived nuclei which would no longer pose a radiological but rather a chemical burden on the environment. However, at the present level of our knowledge, it is not feasible by technical means to reduce the radiotoxic inventory of spent fuel so that geological repository of spent fuel would become redundant [10, 22].

Alpha and Omega of any assessment of spent fuel management scenarios aiming to reduce radiological risk is the consistent consideration of the performance of the entire fuel cycle beginning from uranium mining and milling, through fuel fabrication, reactor operation and final fuel conditioning and disposal. The assessment of P&T technologies is presently a difficult and almost unrealisable task as most of the proposed technologies are still at laboratory and R&D level and e.g. the prediction

of reprocessing loss factors from advanced partitioning technologies achievable on industrial scales are very vague.

2.5 Repository performance

Some studies have been assessing the influence of P&T techniques on the fuel cycle back-end and geological repository performance (leakage resistance) accounting for the relevant exposure time, type and burnup of spent fuel, the strategy and scenario of the repository management. These analyses are very sensitive to the repository characteristics, waste conditions and types of nuclide release scenarios. As basic ones, standard water release pathways and human intrusion scenarios have been studied in different geological formations - crystalline hard rock, salt dome, and clay [23, 24, 25]. Several types of spent fuel source terms were considered, including LWR-UOX and LWR-MOX spent fuels and vitrified high-level waste.

While some nuclides (^{129}I, ^{135}Cs, ^{233}U - a daughter of ^{241}Am and ^{237}Np decay, and decay products of U and Np) have been identified as the routine prime contributors to the individual dose in all cases - there are some nuclides whose significance and contribution to the overall dose is relaxed in some conditions. The prime example of this is the problem with the high solubility of ^{99}Tc in the oxidising environment of proposed repository sites, as Yucca Mountain, U.S.A. [26, 24], which mostly disappears at reducing conditions, see Figure 2.6. The SKB study SR97 [17] assessing the long-term performance of the granite rock repository concludes that only the light mobile nuclides ^{129}I, ^{79}Se, and ^{36}Cl contribute to the geosphere dose, while still being more than four orders of magnitude below the annual limit of 0.15 mSv.

Eventually, in the long-term, the highest dose into the geosphere would be due to fission products. This was, together with non-existence of efficient partitioning techniques for trivalent actinides from lanthanides, the major reason, which made Croff in 1980 [27] and the IAEA expert team in 1982 [28] to wave aside P&T and conclude that there are no long-term safety and cost incentives for partitioning and transmutation of actinides for waste management purposes.

Truly, the water solubility of actinides is very low and their mobility in the geosphere is minimal. But the situation dramatically changes if we consider the scenario of human intrusion into the repository. There, ^{241}Am, Pu isotopes, ^{245}Cm (examination scenario) and ^{99}Tc (site occupation scenario) have been identified as key radionuclides (from clay and hard rock repositories) contributing to the *deterministic* doses for more than 10^5 year (for LWR-UOX spent fuel).

2.6 Defining goals for P&T

Without doubt, the aims of any national P&T strategy have to be merged with risk assessments of every particular repository. But is seems to be clear that *both*

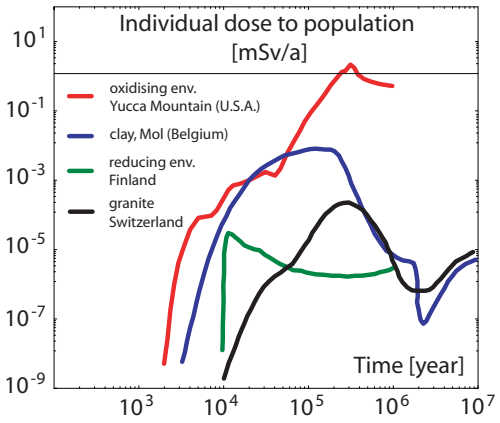

Figure 2.6. Individual doses to population for different repository concepts. In all cases, integrity of the waste canisters is assumed to be lost first after 1000 years. At that moment, the radiotoxic inventory of fuel is dominated by actinides. However, the long-term radiological hazard of spent fuel is associated mainly with fission products as these are highly mobile in ground water. Figure adapted from OECD/NEA report [25].

actinides and long-lived fission products must be considered in P&T schemes. From the viewpoint of the radiotoxic inventory reduction, in the case of the accidental intrusion to the repository, the actinides - plutonium and americium - are of major concern. On the other hand, the long term risks concerning individual doses to population are associated with fission products due to their higher mobility in water. Generally, in this context, the reduction of the radiotoxic inventory by at least a factor of one hundred is desired, thus limiting the radiotoxic risk associated with the fuel within the time when the spent fuel container is supposed to retain its integrity.

Nevertheless, the incentives for spent fuel management strategy might stem not only from the prospect of reducing radiotoxic inventory and assessment of safety and risks but also from completely different factors as e.g. ethical considerations of various management scenarios, which are in their turn influenced by professional, cultural and social factors. An OECD/NEA study [29] emphasises the importance of *inter*generational and *intra*generational equity and fairness in radioactive waste management and concludes that such an approach would minimise the risk of irreversible actions and leave doors open for other options which could be developed in the light of scientific progress and social acceptability in the future. It also cautions whether the society resources could not be used more effectively in other areas where there is a potential for greater reduction of risks to humans or the environment than from a geological repository.

This conclusion can be easily extended onto the introduction of any partitioning and transmutation strategy and thus it might be completely other factors as polit-

ical and/or social ones, which would decide about the fate of P&T technologies in a frame of spent fuel management scenarios. This was admitted also by Croff in 1990 [30] when he reexamined the incentives for actinide transmutation, claiming increased public acceptance of the repository together with higher reliance in technological barriers and predictability of geological conditions. A recent MIT study on future of nuclear power has reached similar conclusions, finding that short-term risks associated with P&T outweigh their long-term benefits [31]. The introduction of P&T technologies would be inevitable, should we give precedence to ethic incentives and the possibility to reduce the radiotoxic inventory of spent fuel at any price and not transferring the burden of its management onto our descendants. On the other hand, should we consider safeguards provided by a geological repository in both short and long terms as satisfactory, the P&T role could be reduced to development of better partitioning techniques for spent fuel conditioning prior to its final disposal.

Chapter 3

Partitioning & Transmutation

Generally speaking *partitioning* means a controlled separation (both in terms of chemical elements and isotopes) of chosen radionuclides from spent fuel. In the vocabulary of P&T technologies, it comprises the break up of inventory into components with high radiotoxic inventory and long-term risks - actinides and long-lived fission products, which are subject for further incineration.

Transmutation is in principle any change of content of nucleons in the atomic nucleus. In the case of actinides it comprises their conversion into fission products. The process can be preceded by consecutive neutron captures, β^- decays and/or isomeric transitions. An comprehensive presentation of an actinide transmutation chain was given in Figure 2.2. Fission product transmutation involves single or multiple neutron captures which are followed by β^- decays until short-lived or stable isotopes are produced.

Re-use (recycling, partitioning and transmutation) of uranium and plutonium from spent nuclear fuel was seen from the beginning of the nuclear era as the axiomatic step complementing uranium burnup and aiming to close the nuclear fuel cycle [32]. From the 50s until 70s, the ultimate goal was to achieve multiple recycling (transmutation) of U/Pu mixture in fast breeder reactors, aiming to reach maximum utilisation of uranium resources (better economy) rather than reduction of the radiotoxic inventory source term of spent fuel. First in 1964 Steinberg [33] drew the attention to the possibility of reduction of radiotoxic inventory of spent fuel focusing on the fission products ^{85}Kr, ^{90}Sr, and ^{137}Cs and their P&T in different reactor systems.

Transmutation itself can be achieved by any suitable beam of particles - neutrons, γ-rays, any reaction - (n,fiss), (n,γ), (n,2n), (γ,n), and both in multiplicative and non-multiplicative devices. However, e.g. the efficiency of γ based transmutation turned out to be unfavourable due to extremely high inventories needed to

compensate for small reaction cross-sections, being in the order of 0.2 barn at γ-energies of 15 MeV for ^{99}Tc [34]. This value is to be compared to the thermal neutron capture cross-section of ^{99}Tc that equals to 20 barn. At the same time, the high flux requirements exclude other sources than devices operating on neutrons. The possibility to directly use spallation neutrons was addressed already by Gregory and Steinberg [35] audaciously proposing a 600-850 MW proton spallation system with liquid uranium alternatively lead/bismuth target for transmutation of ^{137}Cs and ^{90}Sr from a 150 GW_e reactor park. Harada and Takahashi [36] have investigated the issue of fission product transmutation driven by a muon-catalysed neutron source claiming its positive energy balance. This was however based on overestimated deuteron-to-muon conversion factors as concluded by Wallenius [37]. It is obvious that when comparing different transmutation systems, the neutron driven incineration is superior to others due to relatively large reaction cross-sections. It also allows to build self-multiplicative devices which might eventually improve the economy of the transmutation scheme.

We will thus describe spent fuel partitioning techniques and investigate the potential of transmutation of individual spent fuel components (uranium, plutonium, minor actinides and fission products) in various neutron reactor systems (with thermal and fast neutron spectra), based both on the state-of-the-art and advanced, innovative technologies and following different types of incineration scenarios. These will be compared to the strategy of direct fuel disposal in geological formations which serves as a reference, null alternative of spent fuel management.

The strategy of a direct disposal (the fuel cycle is then called "open" or "once-through") is envisioned in some countries mainly due to the unprofitable economic conditions (cheap uranium) and proliferation risks of P&T (U.S.A.) [31]. On the other hand, some studies perceive direct storage of spent fuel as a last resort policy in awaiting a better solution for the back end of the fuel cycle [22].

3.1 Partitioning

3.1.1 Aqueous methods

The PUREX (Plutonium Uranium Recovery by EXtraction) process for separation of uranium and plutonium has been successfully developed on the basis of existing military separation technologies and is applied as a standard on industrial scale in France (La Hague, reprocessing capacity of 1600 tHM/yr) and United Kingdom (Sellafield, 680 tHM/yr) [21]. Japanese Rokkasho Reprocessing Plant (800 tHM/yr) is scheduled to start operation in 2005, Russia and India have pilot scale plants. The total worldwide capacity of reprocessing plants is around 2500 tonnes of LWR-UOX which corresponds to roughly 25% of the world's spent fuel output.

Uranium and Plutonium

In the PUREX process, the spent fuel is dissolved in nitric acid and thereafter uranium and plutonium are recovered by solvent extraction using tri-butyl-phosphate (TBP), reaching recovery efficiencies/yields up to 99.88%. Higher recovery is however obtained on a laboratory scale. At the same time, gaseous fission products as iodine, xenon and krypton are released into the environment (dispersed in sea water).

The uranium and plutonium not recovered (0.12%) are then together with minor actinides, fission products, fuel matrix material (e.g. Zr), and sub-assembly ducts treated as so called high-level liquid waste (HLLW) which is subsequently fixed in glass matrices (vitrification) and incorporated in concrete destined for final disposal. While the recovered Pu is meant to be re-used for MOX fuel fabrication, we should note that annual MOX fuel fabrication capacity is significantly under-dimensioned and amounts to only 400 tonnes worldwide (less than 20% of total reprocessing capacity).

Minor actinides

The neptunium contribution to the spent fuel TRU vector is about 5% and increases with time due to decay of ^{241}Am ($T_{1/2}$=432.6 yr). In a slightly modified PUREX process, neptunium can be treated alone and diverted directly from the U/Pu stream.

A more complex problem is the joint separation of Am/Cm from the main waste streams and, if desired, their mutual partitioning. A major difficulty is the trivalent chemical nature of americium and curium and their similarity to the lanthanide (rare-earth) fission products whose concentration is about a factor of 10-20 higher than for the MAs. As the first step, advanced aqueous methods for separation of residual actinide/lanthanide mixture from PUREX waste streams have been developed - like DIAMEX, TRUEX, TALSPEAK/DIDPA, and TRPO [25]. In order to avoid parasitic absorption of neutrons by lanthanides during transmutation, a high MA purity is required [38]. The separation of Am/Cm from lanthanides is therefore a subject of extensive research and was demonstrated on the laboratory scale for several partitioning processes as e.g. CYANEX 301 and SANEX. The SANEX process showed a 99.9% recovery yield for An/Ln separation. The process for mutual americium and curium separation is recently under investigation in the frame of the SESAME project. For both Am and Cm, a recovery yield of 99.9% was achieved on a laboratory scale.

Fuels containing minor actinides impose higher demands on fabrication and reprocessing technologies due to the increased heat generation as well as γ and neutron dose rates. As an example, reprocessing of irradiated minor actinide targets (20% of Am) has to cope with 32 times as high decay heat as compared to the standard, high burnup fuel of the EFR [39], which makes remote operation and handling of such fuels inevitable.

Fission products

The separation of relevant fission products can be achieved in a slightly modified PUREX process, with efficiencies higher than 99% for iodine and 99.8% for cesium showed on a laboratory scale. The separation of technetium is also technically feasible in the PUREX process, but a technology for recovering of the insoluble part (∼10%) has to be developed.

3.1.2 Pyrochemical methods

A major drawback of water-based reprocessing technologies is their low resistance to radiolysis of organic molecules which, in its turn, limits their capability to handle high minor actinide content fuel. Moreover, the solubility of PuO_2 in nitric acid is limited and in order to assure the reprocessibility of the fuel, the Pu-content in the $(U,Pu)O_2$ is restricted to 25-30%. Dissolution rates for metallic fuels are also very low. These difficulties are, however, relaxed when considering fuel reprocessing in non-aqueous ("dry") pyrochemical processes.

The pyrochemical reprocessing is based on fuel dissolution in molten salts (fluorides, chlorides, T=800-1000 K), from which individual actinides are selectively precipitated by electrorefining. Beside the high radiation stability of molten salts, which allows to shorten cooling times as well as reprocess fuels with high MA content, pyrochemical processes pose a comparative advantage in their relative compactness and proliferation resistance. Most of the fuels are reprocessible with pyroprocessing, which offers a necessary flexibility in P&T with respect to the composition and burnup of the fuel. The unfortunate exception is ZrN, which reprocessing by LiCl-KCl salts is problematic.

Pyrochemical processes have been developed as an option for LWR and FR oxide fuel reprocessing in Russia since 1960s. The molten eutectics salt NaCl-KCl was tested with highly irradiated UO_2 and PuO_2 fuel pins (burnup higher than 20%), reaching recovery yields of 99.8% for Pu and 99.7% for U. The LiCl-KCl eutectics used together with contact metals (Cd or Bi) is envisioned by CRIEPI [40] as a promising route for metallic and nitride fuel reprocessing. In the case of metallic fuels, recovery yields of 95% for U and 99% for mixtures of uranium and minor actinides have been reached on a laboratory scale. Pilot pyro-reprocessing plant at Argonne National Laboratory (ANL) now reprocesses one tonne of sodium-bonded spent fuel from EBR-II annually.

The current disadvantage of reprocessing techniques is the low separation yield together with low throughput of materials. The reagents used in the pyrochemical processes are very corrosive and hostile to the outer environment and steels.

Nitride fuels, on which we elaborate more later on, have been proposed by JAERI as the primary choice in order to accommodate high TRU contents. Their pyrochemical separation procedure appears to be very similar to those for metallic fuels, including molten salt electrorefining. A specific issue of nitride fuels is the necessity of high ^{15}N enrichment (99.9%) in order to avoid the massive production

of ^{14}C in ^{14}N(n,p)^{14}C reactions. While TRU nitrides have, unlike oxides, the property of being reprocessible with standard PUREX methods, pyroprocessing holds a potential of reducing cooling times and allowing efficient ^{15}N recovery. Hence, an effort to reduce the high secondary losses present in pyroprocessing appears to be justified.

3.2 Transmutation

It is customary to describe and compare the effectiveness of transmutation of radiotoxic actinides in the following terms

- burnup (consumption, depletion): $\beta = 1 - M_{\text{out}}/M$,
- specific consumption: $(M - M_{\text{out}})/W$,
- transmutation half-life: $T_{1/2} = \ln 2/(\sigma \cdot \phi)$,
- radiotoxic inventory reduction factor $R(t)$,
- waste mass reduction factor R_{f}.

where M and M_{out} are total masses of nuclides in the fuel cycle before and after the incineration, respectively, W is the energy produced by the reactor, σ is the microscopic cross-section, and ϕ denotes the neutron flux.

3.2.1 Equilibrium fuel cycle

In order to comprehend, compare and easily specify requirements for different components of P&T schemes, the concept of equilibrium cycle (i.e., a cycle with constant composition of the reactor fuel) is additionally introduced.

The actinide mass flow chart in such a cycle is displayed in Figure 3.1. Here an obvious goal is to limit the mass of actinides destined to waste, M_{waste}, in comparison to those fissioned, M_{fiss}, i.e.

$$\frac{M_{\text{waste}}}{M_{\text{fiss}}} = (1-\beta)L\frac{M}{M_{\text{fiss}}} = \delta L \tag{3.1}$$

should be minimised. L is the actinide loss fraction in the reprocessing, and $\delta = (1-\beta)/\beta$ is the burned heavy metal fraction.

Therefore, in order to reduce the amount of the waste destined to the repository, one should aim for

- high discharge burnup in each recycle, β,
- low separation losses, L.

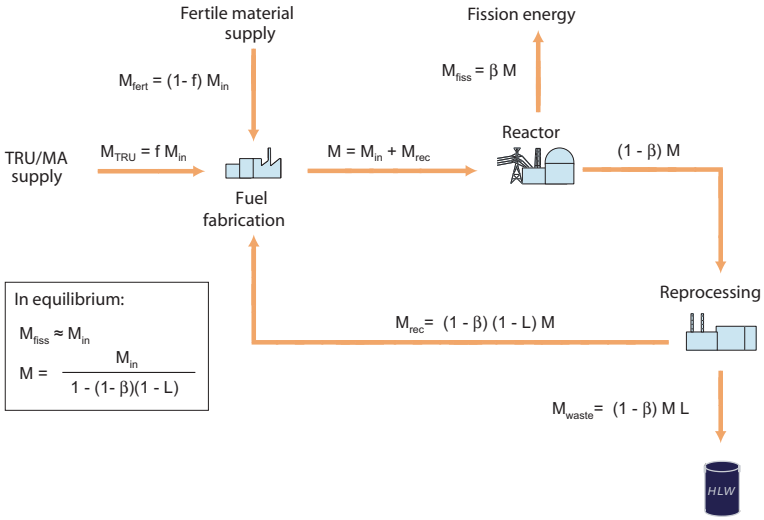

Figure 3.1. Actinide mass flow chart in closed equilibrium fuel cycle.

The amount of the fuel which enters the equilibrium fuel cycle is $M_{\rm in}$, which includes supply of TRU/MA mixture, $M_{\rm TRU}$, and fertile/diluent matrix (^{238}U, ^{232}Th), $M_{\rm fert}$. The fraction of the TRU/MA supply in the load/top-up fuel is then denoted as f.

The amount of fuel in the equilibrium cycle is a function of burnup level β and reprocessing losses L through

$$M = \frac{M_{\rm in}}{1-(1-\beta)(1-L)} \tag{3.2}$$

With the waste mass reduction factor in the fuel cycle defined as $R_{\rm f} = M_{\rm TRU}/M_{\rm waste}$, the losses in the reprocessing are consequently

$$L \approx \frac{f}{\delta R_{\rm f}} \tag{3.3}$$

The radiotoxic inventory reduction factor compares the radiotoxic inventory reduction in the equilibrium cycle to that of the top-up fuel

$$R(t) = R_{\rm neutr}(t)\frac{M_{\rm in}}{M_{\rm waste}} = \frac{R_{\rm neutr}(t)}{\delta L} \tag{3.4}$$

where $R_{\rm neutr}(t)$ is the neutronic toxicity reduction factor, depending on the core characteristics of the reactor and composition of its fuel. The factor $R_{\rm neutr}(t)$ is the radiotoxic inventory for one mole of the feed over one mole of the equilibrium

inventory after a decay time t. Considering that a majority of the transuranics have effective ingestion coefficients e_{50}^{ing} in the range of 10-26·10^{-8} Sv/Bq, we infer that the decisive contribution to the radiotoxic inventory reduction is from the waste *mass* reduction, determined in its turn by burnup level β and reprocessing losses L. In more rigourous analyses, one has shown that the $R_{\text{neutr}}(t)$-factor is in the interval 0.7-2.4 for most of the reactor systems [25]. Hence, the major contribution to the radiotoxic inventory reduction comes from the reduction of actinide mass.

We can therefore directly relate requirements which should be posed on the fuel burnup and recovery yields with respect to the desired radiotoxic inventory reduction factor. Giving the example, we assume a fertile-free top-fuel ($f = 1$) reaching an average burnup of 15%FIMA. In order to attain desired reduction factor of 100 in the radiotoxic inventory of spent fuel, the separation losses have to be under 0.18%. As higher burnups than 15-20%FIMA have not yet been proven, an actinide recovery yield of 99.9% is hence needed in order to accomplish an effective transmutation.

3.2.2 Net consumption

The main purpose of the transmutation reactors operating in radiotoxic inventory reduction schemes is to achieve as high as possible *net consumption* of plutonium and minor actinides. Therefore, in addition to the need for high burnup (and/or low separation losses), the requirement is that

- the reactors' own production of TRU should be minimised, i.e. amount of the fertile material is minimised, limiting TRU breeding ($f \sim 1$),

- the fission fraction ratio of TRU inventory should be as high as possible, i.e. a fast neutron spectrum should be applied in order to take an advantage of higher fission-to-absorption ratios (see Figure 3.2); the cycle transmutation Pu → Am → Cm → Pu is thus avoided with a positive effect on the neutron economy as explained in the next section.

However, removal of ^{238}U together with an increase of mean neutron energy of the reactor system have adverse effects on several core safety parameters, particularly Doppler effect and (effective) delayed neutron fraction. High fractions of even-neutron number (i.e., fertile) plutonium and minor actinide isotopes in the fuel further exacerbate coolant void reactivity. On the other hand, higher minor actinide content somewhat lowers the reactivity loss during burnup in the cycle, allowing to somewhat alleviate the economic penalties associated with higher fuel enrichments otherwise needed. The fuel composition, system's spectrum, and flux level influence the neutron balance in the system. The neutron economy of the TRU fuelled systems is, together with their safety parameters, thoroughly discussed in the next two sections.

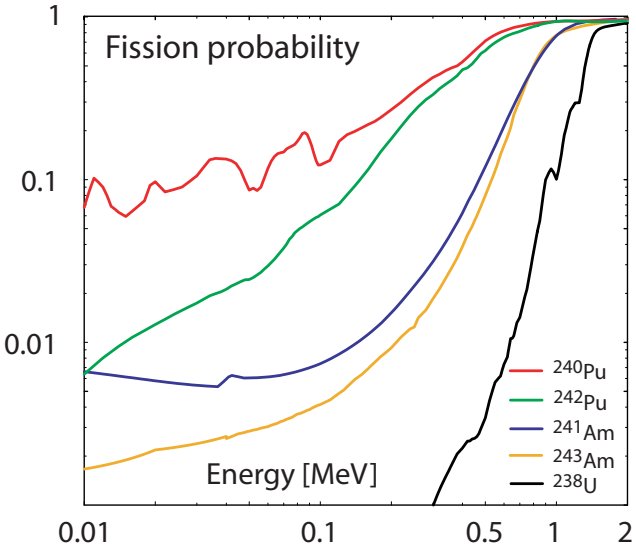

Figure 3.2. Fission probability of the actinide nuclides σ_f/σ_a as a function of neutron energy.

3.2.3 Neutron economy

In order to assess the neutron economy of different types of fuels, and reactor systems with different types of neutron spectra and magnitude of neutron flux, the neutron consumption parameter, D, was introduced for each nucleus in the fuel by Salvatores et al. [41]. The parameter D is defined as the number of neutrons needed to transform the nucleus and its reaction daughters into the required final state, i.e., in the case of actinides, into the fission products. Negative neutron consumption values mean that there is an excess of neutrons in the reactor systems supporting its neutronic needs (i.e. can be used for incineration of e.g. fission products), while neutrons have to be supplied into the reactor if a nuclide with positive D should be transmuted.

The values of D for ^{238}U, plutonium, minor actinide, and TRU vector are given in Table 3.1 for different model reactor systems.

We observe that a pure MA fuel cannot be transmuted in a thermal spectrum, due to the unfavourable neutron balance. However, the spectrum of thermal ADS is not a limiting factor for transmutation of plutonium. Thus, while the whole TRU vector can be incinerated in both thermal and fast spectrum, the fuel with high content of minor actinides is transmutable only in the fast spectrum. The issue of criticality or sub-criticality of the reactor is only the subject of consideration with respect to deteriorated safety characteristics, which we mention in the next section.

Top-up fuel	Thermal TRU ADS	Fast TRU ADS	MA ADS	FR
^{238}U	+0.24	−0.64	−0.64	−0.85
Pu	−0.40	−1.34	−1.28	−1.53
MA	+0.37	−0.86	−0.79	−1.10
TRU	−0.30	−1.29	−1.23	−1.48

Table 3.1. Neutron consumption parameters for different equilibrium cores. Thermal ADS is a graphite-moderated molten salt reactor proposed by LANL [42], fast TRU ADS is a proposal of Pb/Bi-cooled core employing metallic fuel [43], MA ADS is a nitride Pb/Bi burner proposed by JAERI [44], and fast critical reactor (FR) is of an ALMR-type. Pu and TRU vectors correspond to those of discharged LWR-UOX fuel with a burn-up of 50 MWd/tHM; MA vector is the mixture of minor actinides coming from LWRs and FRs of the first stratum reactor park of the double-strata scenario, see Section 3.3.3. Table was adopted from OECD/NEA study [25].

3.2.4 Safety aspects

Inherent stability of a nuclear reactor, as any dynamic system, can be achieved only by *negative* feedbacks acting sufficiently fast that the integrity of the reactor core is not compromised. The feedback mechanisms operating in the nuclear reactors typically constitute of an event chain where an increase in power or change in its distribution leads to decrease in reactivity through temperature dependent microscopic and/or macroscopic cross-sections.

In the sub-critical system, the requirements on the feedback mechanisms are partially relaxed due to the inferred sub-criticality [38]. However, if a substantial reactivity could be introduced into the system, e.g. during coolant voiding, such that the power is significantly increased, absence of negative feedbacks could lead to core damage in spite of the system remaining sub-critical [45]. If a large sub-criticality margin would be required ($k_{\text{eff}} \sim 0.9$) in order to prevent core damage, it would introduce penalties on the total reactor power and discharge burnup. Thus, one might be required to optimise the core sub-criticality level, while, at the same time, provide sufficiently strong negative temperature reactivity feedbacks. The latter could be also stipulated as an *a priory* requirement for successful licensing of any energy producing reactor.

3.2.5 Reactivity temperature coefficients

The total change in the reactivity of the system is given as a sum of

$$\rho_{\text{T}} = \rho_{\text{t}} + \rho_{\text{c}} + \rho_{\text{e}} \tag{3.5}$$

where ρ_{t} is the reactivity due to the temperature changes in the reactor, ρ_{c} is the reactivity introduced by control rods or other absorbing materials as e.g. fission products, and ρ_{e} is the external reactivity introduced from outside.

In the case when no reactivity is introduced from external sources and absorbing materials, ρ_{t} determines the temperature stability of the reactor. The temperature reactivity coefficients are then defined as the change in the reactivity upon temperature change of the i-th component of the reactor core

$$a_{\mathrm{i}} = \frac{\partial \rho}{\partial T_{\mathrm{i}}} \tag{3.6}$$

In a heterogeneous reactor, we usually recognise four distinctive geometrical components: fuel, structural material, moderator and/or coolant.

In the reactor core, the temperature reactivity feedback is mainly due to the following physical events

- neutron spectrum shift affecting effective scattering and absorption cross-sections in the coolant (and moderator),
- widening of the resonance absorption cross-sections, changing the probability for absorption reaction (Doppler effect),
- material density/phase change affecting macroscopic cross-sections,
- changes in the core dimensions due to thermal dilatation of materials (fuel, structure, cladding) and/or bending of the fuel elements.

Therefore, the reactivity changes as function of temperature can be decomposed as

$$\frac{d\rho}{dT} = (\frac{\partial \rho}{\partial T})_{\gamma} + (\frac{\partial \rho}{\partial \gamma})_{\sigma}(\frac{\partial \gamma}{\partial T}) \tag{3.7}$$

where the $(\partial\rho/\partial T)_{\gamma}$ is the nuclear part of the reactivity coefficients (due to the change of the nuclear properties of the material, i.e., cross-sections), and $(\partial\rho/\partial\gamma)_{\sigma}$ is the density reactivity coefficient, describing the temperature changes as a response to the change of the material density.

The total change of reactivity is then given by

$$\rho_{\mathrm{T}} = \sum_{\mathrm{i}} \frac{1}{V_{\mathrm{i}}} \int a_{\mathrm{i}}(\overline{r}) \triangle T_{\mathrm{i}}(\overline{r}) \Omega(\overline{r})\, d\overline{r} \tag{3.8}$$

where $\Omega(\overline{r})$ is the weight/importance function describing the relative spatial influence of the temperature on the reactivity, and $\triangle T_{\mathrm{i}}(\overline{r})$ is the temperature gradient corresponding to the state at which $\rho_{\mathrm{T}} = 0$.

It is important to note that apart from the changes of the reactivity induced by the temperature, one can also have reactivity change due to longer long-term events, such as swelling of cladding material or fuel pellet. Reactivity can be also introduced during a transient, e.g. if the fission gases are released from the pellet to the plenum.

Typical values of temperature coefficients for thermal and fast neutron cores are listed in Table 3.2. While all reactivity coefficients are negative in the thermal

Mechanism $10^6 a$ [K]	EBR II	Fermi	Super Phénix	BREST 1200	PWR UOX fuel
Axial fuel expansion	−3.9	−2.5	N/A	−0.8	≈ 0
Coolant density change	−9.1	−7.1	+8.0	+3.4	−50 to −8
Structure expansion	−9.7	−6.0	−11.0	−7.7	≈ 0
Doppler coefficient at nominal temperature	N/A	−2.0	−4.0	−5.4	−4 to −1

Table 3.2. Reactivity temperature coefficients for thermal and fast reactor cores [46, 47, 48, 49]. Reactivity coefficients due to the density change of *both* coolant and subassembly material are quoted for EBR-II and Fermi.

reactor, in fast systems the total temperature reactivity coefficient is the sum of positive and negative parts. Moreover, geometrical changes play more significant role in fast spectrum systems than in thermal reactors, where the coolant/moderator temperature coefficient has the major importance.

Prompt, inherent, and negative reactivity feedbacks are needed in order to mitigate positive reactivity transients. Doppler temperature coefficient is a prompt responsive feedback to power changes as it is dominated by the nuclear component involving the broadening of actinide absorption resonances. On the other hand, the coolant and moderator temperature coefficients are somewhat delayed allowing for heat to be distributed from fuel into the coolant. In the next sections, we will treat coolant and fuel temperature reactivity coefficients together with delayed neutron fractions in more detail. The objective is to give as an important theoretical background before advancing into more elaborate studies of safety aspects of transmutation reactors, which will be presented in Chapter 6.

3.2.6 Coolant temperature reactivity coefficient and void worth

The coolant temperature coefficient is not a characteristic of the coolant itself but a collective property of the core lattice and fuel design, fuel composition and coolant/moderator type. In light-water reactors, the negative coolant/moderator reactivity coefficient facilitates an important self-controlling mechanism of the system (core lattice is then so called *undermoderated*). Specifically, in BWR, an increase in steam-to-water ratio leads to a decrease of the reactivity. However, sometimes, reactor cores exhibit positive coolant reactivity coefficients, e.g., D_2O moderated and cooled reactors (CANDU), or H_2O cooled-graphite moderated reactors (RBMK). Operational stability of the reactor with positive coolant reactivity coefficient is then ensured by the strong negative power reactivity coefficients. If that is not present or is weak, one has to rely on actively operated reactor control systems rising serious safety concerns. At the same time, it is impossible to rely on natural circulation in order to cope with the cooling accidents.

Loss of coolant has two distinctive consequences on the reactor operation. First, the ability of the heat removal is lost leading to overheating and possibly also to loss of core integrity. The loss of heat removal capability was one of the main reasons for core melting accidents, e.g. at the Three Mile Island nuclear reactor at Harrisburg, Pennsylvania. Second, it can introduce reactivity into the system. The coolant temperature reactivity is one of the most prominent characteristics of fast reactors and some existing designs of liquid metal cooled reactors have coolant temperature reactivity coefficient positive, e.g. Super Phénix reactor in France (see Table 3.2). The negative temperature reactivity feedback is then ensured by strong contributions from expansion of grid structure and from fuel temperature coefficient.

The coolant density change or occurrence of the void in the core can be a result of the following events

- temperature increase of the coolant due to pump failure, human errors, inadequate instrumentation and prediction of hot-channel factors, crud deposition, and plugging of the coolant channels; ultimately, this leads to a coolant phase change - boiling. Note that accident scenarios assuming coolant boiling are less relevant for systems cooled with lead-alloys due to the high boiling temperature of both Pb and Pb/Bi (Pb: T_{b}= 2023 K; Pb/Bi: T_{b}= 1943 K), while in sodium cooled systems (T_{b}= 1156 K) coolant boiling can occur before any significant damage to the fuel, clad, or structural material would be inflicted.

- blocking of the coolant circulation as a consequence of coolant freezing in the steam generator, i.e. overcooling.

Additionally, void cavities can appear in the core due to

- gas leakage from ruptured pins,

- steam ingress from ruptured steam generator,

- blow-down of bubbles from gas injection system,

- coolant leakage caused by brittle failure of the reactor vessel.

The coolant acts in the reactor not only as a neutron absorber, but also as moderator, affecting the neutron spectra. The reactivity change when decreasing the density of the coolant in fast neutron cores from coolant is mainly due to two effects

- spectral hardening, i.e. reduction of the neutron moderation, with a concurrent increase of actinide fission probabilities,

- reduction of neutron parasitic absorption in fuel, coolant, and cladding.

Coolant	ρ [g·cm^{-3}]	A [u]	N [10^{-22}·cm^{-3}]	T_m [K]	T_b [K]	ξ
Na	0.847	22.99	2.22	371	1156	$8.45{\cdot}10^{-2}$
Pb/Bi	10.15	208.1	2.94	398	1943	$9.59{\cdot}10^{-3}$
Pb	10.48	207.1	3.05	601	2023	$9.63{\cdot}10^{-3}$
He	$4.13{\cdot}10^{-3}$	4.003	0.06	1.05	4.15	$4.25{\cdot}10^{-1}$

Table 3.3. Density (ρ), mass number (A), atomic density (N), melting (T_m) and boiling (T_b) temperatures, and average logarithmic decrement of energy (ξ) of coolants considered in the study. Coolant densities are given at 700 K, helium pressure is 6 MPa [50].

3.2.7 Neutron slowing down

In this section we therefore analyse the neutronic (slowing-down) properties of candidate coolants for the fast reactor systems, see Table 3.3.

With an assumption that the neutron elastic scattering is isotropic in the centre-of-mass system (CMS), we can describe neutron slowing-down process in terms of the averaged logarithmic decrement of energy as

$$\xi = \overline{\ln E_1 - \ln E_2} = 1 + \frac{(A-1)^2}{2A} \ln \frac{A-1}{A+1}, \qquad A > 1 \tag{3.9}$$

where A is the nuclide mass number and E_1 and E_2 are the energies before and after the collision, respectively.

In order to apprehend the nature of the slowing-down process, the moderating power of the respective coolants is usually defined as

$$\xi \Sigma_\mathrm{s} = \Sigma_\mathrm{i} N_\mathrm{i} \xi_\mathrm{i} \sigma_\mathrm{i} \tag{3.10}$$

where N_i is the atomic density of the i-th nuclide and σ_i is its elastic scattering cross-section. However, to include also slowing-down process from the inelastic scattering in the evaluation, the energy-loss cross-section should be studied. It is defined as

$$\overline{\Sigma_{\Delta E}} \equiv \frac{\Sigma_\mathrm{el}\overline{\Delta E_\mathrm{el}} + \Sigma_\mathrm{inel}\overline{\Delta E_\mathrm{inel}}}{E}, \tag{3.11}$$

where

$$\overline{\Delta E_\mathrm{el}} = \frac{1}{2}(1-\alpha)E_\mathrm{n}, \;\; \alpha = (\frac{A-1}{A+1})^2 \tag{3.12}$$

and

$$\overline{\Delta E_\mathrm{inel}} = E_\mathrm{n} - (\frac{A}{A+1})^2[E_\mathrm{n} - Q\frac{A+1}{A}] \tag{3.13}$$

is the average energy loss in elastic scattering and inelastic scattering, respectively; Q denotes the excited energy levels of the target nuclei, E_n is the neutron energy, and A is the target nucleus mass number (see **Paper I**).

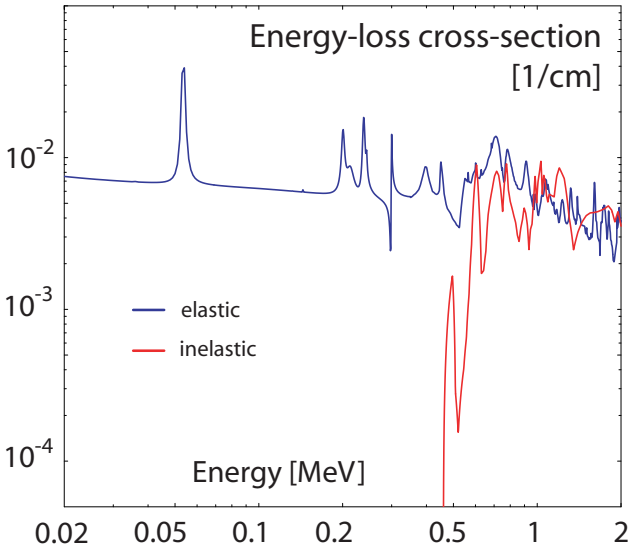

Figure 3.3. Energy-loss cross-section for ^{23}Na. Data from JEF-2.2 library were used. Macroscopic scattering cross-sections were taken at T = 600 K. According to **Paper I**.

Nuclide	Abundance	1st	2nd	3rd
^{23}Na	100%	459.1	2166	2495
^{206}Pb	24.1%	806.9	1171	1347
^{207}Pb	22.1%	572.5	902.1	1641
^{208}Pb	52.4%	2628	3213	3492
^{209}Bi	100%	900.6	1617	2455

Table 3.4. Threshold energies [keV] for inelastic scattering of liquid metal coolants used in this study. ^{206}Pb features additional five excited energy levels yielding threshold energies below or close to 2 MeV limit: 1474, 1692, 1713, 1793, and 2008 keV. Table adapted from **Paper I**.

Threshold energies for the inelastic scattering (i.e., kinetic energies of the neutron in the laboratory system, E_{n}) are higher than excited level energies Q of the system. Considering the kinematics of the inelastic scattering

$$E_{\mathrm{n,CMS}} + E_{\mathrm{N,CMS}} + Q = \frac{A}{A+1} E_{\mathrm{n}} \tag{3.14}$$

$$\text{where} \quad E_{\mathrm{n,CMS}} + E_{\mathrm{N,CMS}} \geq 0 \tag{3.15}$$

we obtain a requirement for the laboratory kinetic energy of the neutron, $E_{\mathrm{n}} \geq \frac{A+1}{A} Q$. $E_{\mathrm{n,CMS}}$ and $E_{\mathrm{N,CMS}}$ are kinetic energies of the neutron and the nucleus in the centre-of-mass system, respectively.

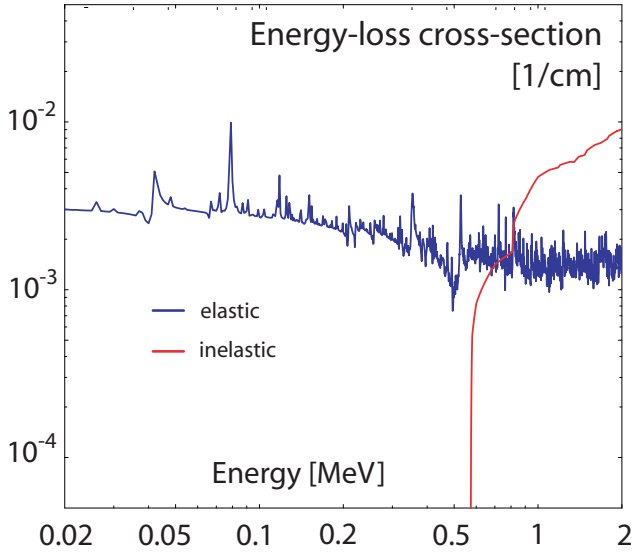

Figure 3.4. Energy-loss cross-section for natural lead. Cross-section data were taken from ENDFB/VI-8 cross-section library. Σ_{el} and Σ_{inel} at T = 600 K were used. Figure adopted from **Paper I**.

The energy-loss cross-section for sodium decomposed into the contributions from elastic and inelastic scattering is displayed in Figure 3.3. The same comparison for natural lead is made in Figure 3.4. In the whole energy range investigated (100 keV - 2 MeV), lead energy-loss cross-section due to the elastic scattering is significantly smaller than for sodium. However, due to the presence of several thresholds for inelastic scattering in the energy interval from 0.57 to 2 MeV, the energy loss in inelastic scattering is notably larger than for sodium. Therefore, neutron spectrum of lead and lead/bismuth cooled reactors will be somewhat suppressed for energies above 1 MeV. On the other hand, the magnitude of neutron flux for sodium-cooled reactor is suppressed in the energy interval of 0.7-1.5 MeV, where contributions to the neutron slowing down from elastic and inelastic scattering reactions are merely equal, see Figure 3.5.

Additionally, the neutron mean free path, (λ=1/Σ_t), in sodium is larger than that of Pb/Bi. Therefore, the leakage of neutrons and their contribution to overall neutron balance in the system is more significant for Na. Further, higher scattering in Pb/Bi without increasing the moderation for neutrons below 0.5 MeV would prevent the neutrons from escaping from the internal parts of the Pb/Bi-cooled cores and, at the same time, provide an excellent reflecting capability for the neutrons which escape the system, see Figure 3.6. Hence, we can also infer that the neutron economy of the Pb/Bi systems would be better than for Na-cooled counterparts and a smaller actinide fraction would be required for Pb/Bi than Na to reach

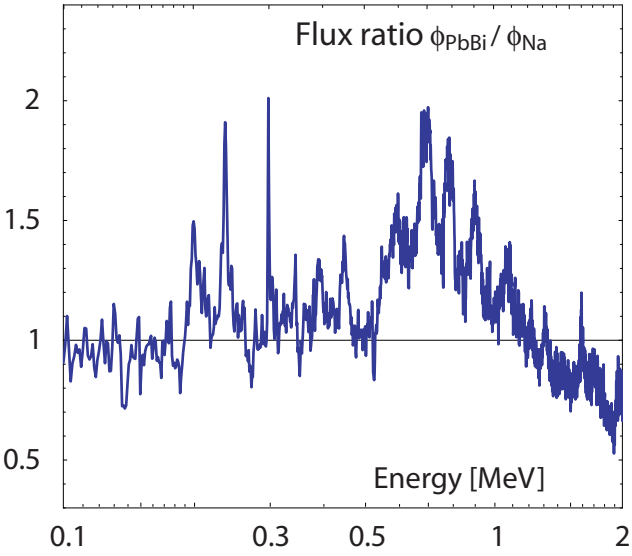

Figure 3.5. Neutron spectrum of the Pb/Bi-cooled system in comparison to the Na-cooled reactor having the same fuel and geometry design parameters. Redrawn from **Paper I**.

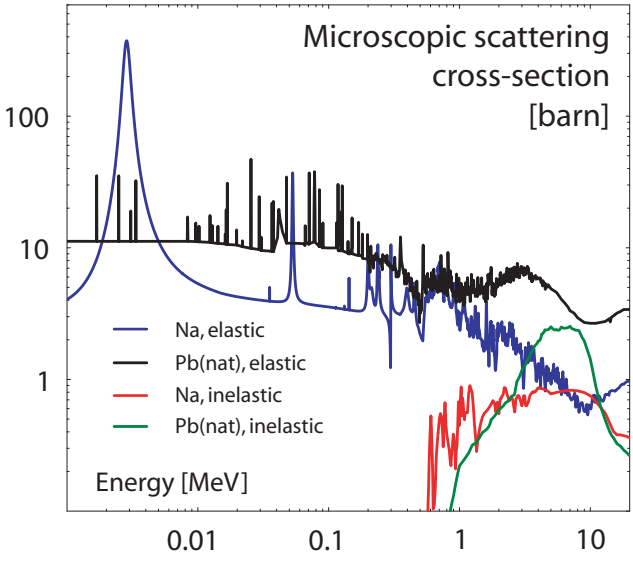

Figure 3.6. Elastic and inelastic scattering cross-sections for Na and Pb. Data were taken from JEF-2.2 library.

criticality/same sub-criticality. On the other hand, e.g. power peaking issues are more relaxed in sodium system as neutrons more easily escape the high reactivity regions. We develop on the subject in Chapter 6.

3.2.8 Feedback through material dilatation

A temperature rise causes expansion of core materials with concomitant changes in geometry. This influences the macroscopic cross-section ($N \cdot \sigma$), affecting the interaction rates ($N \cdot \sigma \cdot \phi$), neutron mean free path, resonance self-shielding effect in the fuel, neutron leakage probability, and consequently changes overall criticality of the system. Moreover, the material dilatation can alter the relative position of core parts, individual fuel pins or whole sub-assemblies. E.g. fuel sub-assembly bowing was the initiator of the accident at the experimental breeder reactor EBR-1 Mark II in November 1955. The subsequent analysis of the core have shown that the transient had resulted in melting of 40%-50% of the fuel elements.

Temperature changes causes a dilatation of all materials in the core. However, the most important reactivity contribution with respect to the geometrical changes appear to be

- axial expansion of fuel column,
- radial expansion of the core lattice grid, changing spacing in-between fuel elements and effective radius of the core,
- thermal bowing of sub-assemblies.

Change in length of the i-th core component per change in temperature is given by the linear expansion coefficient defined as

$$\alpha_{\mathrm{i}} = \frac{1}{l_0} \frac{dl}{dT}_{\mathrm{i}} \tag{3.16}$$

where dl is the change in length, l_0 is the initial length of the material, and dT is the change in temperature. The density of the material then changes as

$$\rho = \frac{\rho_0}{1 + \beta \Delta T} \tag{3.17}$$

where β is the volumetric expansion coefficient ($\beta \approx 3\alpha$), ρ_0 is the initial material density, and $\Delta T = T - T_0$ is the temperature difference.

The linear expansion coefficient is usually itself dependent on the temperature and for actinide nitrides and relevant diluent matrices, ZrN and HfN, it slightly increases with temperature, see Figure 3.7. For comparison, the linear expansion coefficients of uranium, plutonium, uranium dioxide, and structural material are given in Table 3.5. For the mixture of the nuclides, the linear expansion coefficient is obtained by using Vegard's law.

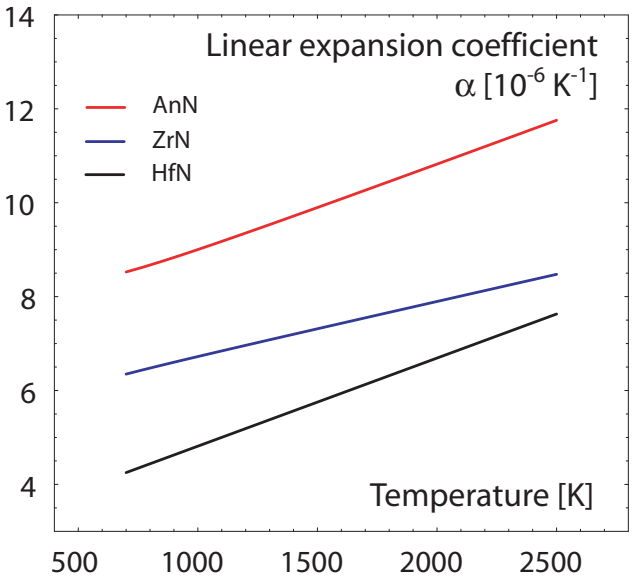

Figure 3.7. Linear expansion coefficient of AnN [51], ZrN [51], and HfN [52] as a function of temperature.

Material	α $[10^{-6}\cdot\mathrm{K}^{-1}]$	Note
U	13.9 (α)	300 K
Pu	55 (α), 35 (β)	300 K
UO_2	11.1 to 13	700−1600 K
AnN	8.5 to 11.8	600−2500 K
SS-316	18.6 to 21.6	300−1300 K

Table 3.5. Linear expansion coefficients of some core materials [53, 32, 50].

The dilatation of the material in the core affects neutron mean free path, which is increased as $\lambda = 1/\Sigma_t = 1/(N \cdot \sigma_t)$. At the same time, the core dimensions increase and the densities of the material in the core decrease, which has positive and negative effect on the system reactivity, respectively.

Increase in the core dimensions, assuming the cylindrical core, decreases the neutron leakage probability as surface-to-volume ratio becomes smaller with larger R and/or H

$$\frac{2\pi r(r+H)}{\pi r^2 H} = 2(\frac{1}{H}+\frac{1}{r}) \tag{3.18}$$

where r and H are the radius and the height of the core, respectively. In the case of the axial expansion of the fuel column, the density of the fuel changes as

$$\frac{\Delta\rho}{\rho_0} \approx -\frac{\Delta l}{l} \tag{3.19}$$

while in the case of the radial displacement of the core grid the density varies with the square of the core radius

$$\frac{\Delta\rho}{\rho_0} \approx \frac{r_0^2 - (r_0 + \Delta r)^2}{r^2} \approx -\frac{2\Delta r}{r} \tag{3.20}$$

Thus, the reactivity change upon the core expansion is actually the result of two components, a positive one due to the core expansion, and a negative one due to smaller densities. In fast reactors, the former effect is usually smaller than the latter, yielding the negative overall expansion coefficient [54]. We also expect that an increase in the core radius is approximately twice as effective in reducing the reactivity than the axial fuel expansion.

3.2.9 Doppler feedback

The Doppler effect involves changes of reactivity due to variation of fuel temperature. This effect has a premium significance in nuclear reactor safety, providing immediate reactivity feedback, which responds to the changes in the fuel temperature. In fact, the absorption cross-section of an actinide is dependent on the relative velocity between the nuclide and neutron. While the area under the resonance integral [55]

$$I^{\mathrm{res}} = \int_{\mathrm{E}}^{\mathrm{E}_0} \sigma_{\mathrm{a}}(E') \frac{dE'}{E'} \tag{3.21}$$

remains constant upon temperature changes, the effective resonance integral is then dependent on temperature through Σ_{a} in the denominator

$$I_{\mathrm{eff}}^{\mathrm{res}} = \int_{\mathrm{E}}^{\mathrm{E}_0} \sigma_{\mathrm{a}}(E') \frac{\Sigma_{\mathrm{s}}}{\Sigma_{\mathrm{s}} + \Sigma_{\mathrm{a}}} \frac{dE'}{E'} \tag{3.22}$$

The probability of neutrons escaping the resonance capture then changes as

$$p = \exp(-\frac{N}{\xi\Sigma_s} I_{\mathrm{eff}}^{\mathrm{res}}). \tag{3.23}$$

The fuel temperature reactivity coefficient can be approximated for most reactor designs by a $1/\mathrm{T}^{\mathrm{a}}$-dependence (a$\sim$1 for oxide-fuelled sodium-cooled fast reactors) and thus the Doppler effect is often in the literature quantified in terms of the Doppler constant

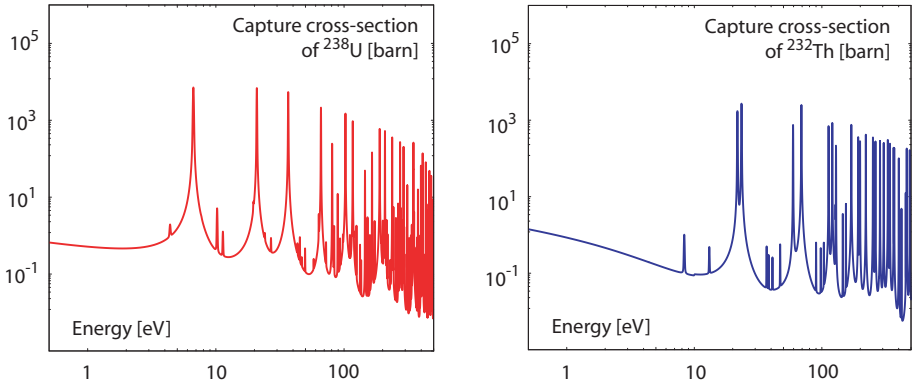

Figure 3.8. The neutron capture cross-section for ^{238}U and ^{232}Th. JEF-2.2 data were used.

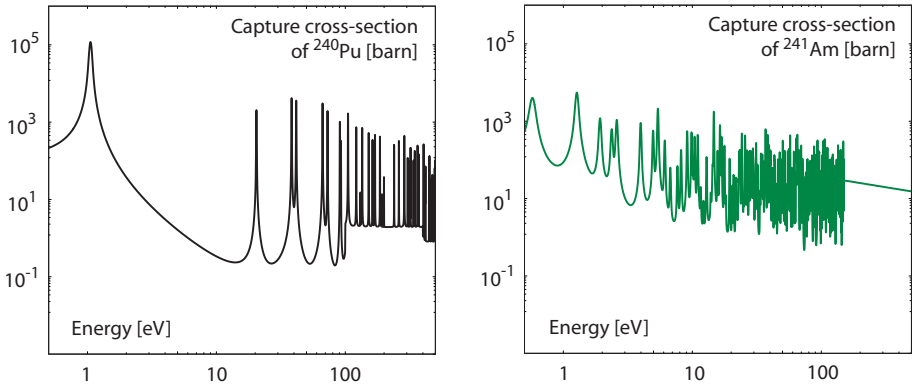

Figure 3.9. The neutron capture cross-section for ^{240}Pu and ^{241}Am. Data were taken from JEF-2.2. Note large ^{240}Pu resonance at ∼1 eV.

$$K_{\mathrm{D}} = T\frac{dk}{dT} \tag{3.24}$$

The Doppler effect itself is prominent in an energy range of well-separated resonances around 1 keV (higher energies cross-section variations with temperature are minimal) and for fertile nuclei it results in a decrease of resonance escape probability [46]. As shown experimentally, mainly fertile materials as ^{238}U, ^{232}Th, and to a minor extent ^{240}Pu, contribute to the Doppler effect, see also Figures 3.8 and 3.9. On the other hand, the Doppler effect of most of the fissile isotopes as ^{239}Pu and ^{235}U appear to be almost zero or even positive [54]. In the thermal spectrum, plutonium fuel can provide positive Doppler feedback due to the huge 0.3 eV resonance of ^{239}Pu.

In the standard FBR design, the major contribution to the negative Doppler effect comes from broadening of ^{238}U resonances. In hard neutron spectra, only small portion of neutrons is moderated down to the region of pronounced resonances (below 100 eV), where the contribution to the Doppler effect is the most profound. At the same time, as uranium content is significantly reduced in transmutation reactors, the Doppler coefficient becomes small. Extensive studies of properties of different fuel carrier material which would help to at least partially regain the Doppler effect were reported e.g. by Lombardi [56] and Conti [57]. It appeared that a certain degree of Doppler could be obtained using materials with significant resonances in the fast energy range - W, Mo, Nb - which, on the other hand, exhibit adverse effect on coolant void worth.

3.2.10 Delayed neutron fractions

The deterioration of kinetic parameters as delayed neutron fraction β and neutron lifetime also imposes constraints on transient behaviour of reactor systems. The delayed neutron fractions are specific characteristics of individual nuclei determined by their distribution of fission yields. In Table 3.6, the values of total delayed neutron yields ν_{d} and average number of neutrons per fission ν_{therm} are listed together with estimated delayed neutron fractions.

Two regularities can be observed from listed data: the total delayed neutron yield increases with the atomic mass of a given element but, on the other hand, decreases with increasing proton number. Furthermore, the delayed neutron yields remain energy independent until 4 MeV when they quickly drop by about a factor of two. For a fast neutron spectrum, the average neutron yields are slightly increased resulting in a further reduction of delayed neutron fractions.

The effective delayed neutron fraction, β_{eff}, is the number of delayed neutrons *inducing* fission in the system $\mathrm{N_{d,i}}$ compared to number of all neutrons *inducing* fission in the reactor $\mathrm{N_i}$. The most rigourous mathematical definition of β_{eff} was given by Keepin [58] as

$$\beta_{\mathrm{eff}} = \frac{\int \Psi(\overline{r}, E', \Omega')\chi_{\mathrm{d}}(E')\nu_{\mathrm{d}}(E')\Sigma_{\mathrm{f}}(\overline{r}, E, \Omega)\phi(\overline{r}, E, \Omega)dEd\Omega dE'd\Omega' d\overline{r}}{\int \Psi(\overline{r}, E', \Omega')\chi(E')\nu(E')\Sigma_{\mathrm{f}}(\overline{r}, E, \Omega)\phi(\overline{r}, E, \Omega)dEd\Omega dE'd\Omega' d\overline{r}} \tag{3.25}$$

where ϕ is the neutron flux at position $\overline{r}$ with energy E and solid angle Ω, ν is the averaged neutron yield per fission, ν_{d} is the averaged delayed neutron yield, Σ_{f} is the macroscopic fission cross-section, χ_{d}, χ is the energy spectrum function of delayed and all neutrons in the system, respectively, and $\Psi(\overline{r}, E, \Omega)$ is the neutron importance function (i.e. function proportional to the asymptotic power level resulting from introduction of a neutron into the critical system). In sub-critical systems, $\Psi(\overline{r}, E', \Omega')$ is proportional to the probability of neutron to induce fission.

In Monte Carlo code MCNP [59], β and β_{eff} are not given explicitly. Moreover, $\mathrm{N_{d,i}}$ and $\mathrm{N_i}$ cannot be obtained directly. We therefore write

$$\beta_{\mathrm{eff}} = \frac{N_{\mathrm{d,i}}}{N_{\mathrm{i}}} = \frac{P_{\mathrm{d,i}}}{P_{\mathrm{i}}}\frac{N_{\mathrm{d}}}{N} = \frac{P_{\mathrm{d,i}}}{P_{\mathrm{i}}}\beta \tag{3.26}$$

Isotope	ν_{d}		ν_{therm}		β [pcm]	
	ENDF	JENDL	ENDF	JENDL	ENDF	JENDL
^{232}Th	0.0527	–	1.949	–	2704	–
^{233}U	0.0074	0.0067	2.495	2.493	297	275
^{235}U	0.0167	0.0160	2.437	2.439	685	656
^{238}U	0.0440	0.0481	2.492	2.489	1766	1933
^{237}Np	0.0108	0.0122	2.636	2.541	410	480
^{238}Pu	0.0042	0.0047	2.895	2.895	145	162
^{239}Pu	0.0065	0.0062	2.881	2.884	226	215
^{240}Pu	0.0090	0.0091	2.803	2.784	321	327
^{241}Pu	0.0162	0.0160	2.945	2.931	550	546
^{242}Pu	0.0197	0.0183	2.810	2.859	701	640
^{241}Am	0.0043	0.0045	3.264	3.224	132	140
$^{242\mathrm{m}}$Am	0.0069	0.0065	3.264	3.275	211	198
^{243}Am	0.0080	0.0095	3.273	3.210	244	296
^{242}Cm	0.0014	0.0021	3.440	3.252	41	65
^{243}Cm	–	0.0030	3.430	3.433	–	87
^{244}Cm	–	0.0044	3.460	3.244	–	137
^{245}Cm	0.0059	0.0063	3.606	3.531	164	178
^{246}Cm	–	0.0092	3.480	3.199	–	288

Table 3.6. Thermal total delayed and average neutron yields per fission together with estimated delayed neutron fractions as obtained from ENDFB-VI, revision 5 and JENDL 3.2 data libraries. Note the large differences in delayed neutron fractions evaluated, which are as high as 50% for some minor actinides.

where $\beta = \mathrm{N_d/N}$ is the number of delayed neutrons compared to number of all neutrons in the reactor, $\mathrm{P_i}$ and $\mathrm{P_{d,i}}$ are the probabilities that the average neutron and delayed neutron induce fission in the reactor, respectively. The values of β, $\mathrm{P_i}$ and $\mathrm{P_{d,i}}$ can be assessed in two separate MCNP calculations.

The probability that the average neutron induce fission is given by

$$P_{\mathrm{i}} = L_{\mathrm{f}} = \Sigma_{\mathrm{f}}\phi \tag{3.27}$$

In the calculation, the transport of both prompt and delayed neutrons is considered, explicitly modelling their respective spectra. Similarly, simulating the transport of prompt neutrons only, we obtain

$$P_{\mathrm{p,i}} = L_{\mathrm{f,p}} = \Sigma_{\mathrm{f,p}}\phi \tag{3.28}$$

In this approach, we assume that the shapes of the ϕ function are same as in both cases, which is almost true as ν_{d} is two orders of magnitude lower than ν.

The probability that the delayed neutrons induce fission is then determined from

$$\nu L_{\mathrm{f}} = \nu_{\mathrm{p}} L_{\mathrm{f,p}} + \nu_{\mathrm{d}} L_{\mathrm{f,d}} \quad \Rightarrow \quad L_{\mathrm{f,d}} = \frac{\nu L_{\mathrm{f}} - \nu_{\mathrm{p}} L_{\mathrm{f,p}}}{\nu_{\mathrm{d}}} \tag{3.29}$$

Assembly	Experimental values [pcm]	JEFF-3.0		ENDF/B-VI		JENDL-3.3	
		β	β_{eff}	β	β_{eff}	β	β_{eff}
Godiva	659 ± 10	600	683	633	662	627	635
Jezebel	194 ± 10	191	189	187	176	189	181
^{242}Pu	–	565	–	594	247	545	183

Table 3.7. Effective delayed neutron fractions for Godiva, Jezebel and ^{242}Pu critical configurations. Note that the delayed neutron energy distribution for ^{242}Pu is not given in JEFF-3.0. Experimental values were taken from ref. [60].

where ν_{p} is the prompt neutron yield.

In order to test the reliability of the devised approach, the β_{eff} was calculated for two benchmark configurations, Godiva and Jezebel. Godiva is an unreflected sphere of the highly enriched metallic uranium (^{234}U 1.02 wt%, ^{235}U 93.71 wt%, ^{238}U 5.27 wt%, radius 8.7414 cm, density 18.74 g/cm^3), Jezebel is the similar sphere configuration with weapon grade plutonium (^{239}Pu 95.2 at%, ^{240}Pu 4.5 at%, ^{241}Pu 0.3 at%) enclosed in a thin nickel shell. A critical metallic ^{242}Pu sphere was also modelled. Rather good agreement with the experimental values was obtained, see Table 3.7.

3.3 Transmutation strategies

After defining incentives for P&T of spent nuclear fuel and identifying the basic physical characteristics and constraints which accompany this process, we now give a comprehensive overview of different P&T schemes, involving both thermal and fast nuclear reactors. Most recently, the subject was studied by OECD/NEA [25].

In general, transmutation of transuranics are envisioned to be accomplished in either so called *homogeneous* mode, where TRU nuclei are homogeneously dispersed in the whole reactor core, or *heterogeneous* mode, where the irradiation takes place in dedicated target sub-assemblies or in dedicated reactors operating exclusively TRU fuel.

Transmutation scenarios are considered to be either "once-through", i.e. irradiation takes place until a significant depletion is reached and fuel/targets are directly disposed of, or with multi-recycling when fuel/dedicated targets are discharged from the reactor, reprocessed and again returned to the transmutation process.

In a broad perspective, the different fuel cycle concepts investigated can be categorised as follows

- once-through fuel cycle, without spent fuel recycling, entailing the direct disposal of spent fuel in a geological repository; this strategy is applied in countries without recycling possibilities or with proliferation concerns,

- plutonium burning strategy, where plutonium is first incinerated in light water reactors, and afterwards in critical fast reactors; minor actinides and fission products are concurrently destined into the geological repository,
- closed fuel cycle which, in addition to the preceding scheme, involves burning of MA homogeneously distributed in FRs (BREST [48], EFR [61], IFR [62]) or in dedicated reactor systems, e.g. ADS; such complete recycling entails that secondary waste streams to the repository are limited.

Variations of these basic principle schemes are displayed in Figure 3.10 and will be discussed in detail below. From the system point of view, P&T is proposed to be achieved in two different scenarios: an *evolutionary*, with reactor systems and reprocessing technologies of the present knowledge (aqueous), and *innovative*, where pyrochemistry technologies and advanced reactor systems are used for TRU burning in the closed fuel cycle.

The different fuel cycle/transmutation strategies will be discussed in the next sections with respect to the reactor spectrum. In order to address the safety issues associated with introduction of minor actinides into the fuel, *dedicated* reactor systems operating in both critical and sub-critical mode have been proposed. We will treat these systems in more technological detail in Chapter 4.

3.3.1 Thermal reactors

Thermal neutron spectrum systems encompass both commercial light-water reactors (LWR), i.e., pressurised water reactors (PWR) and boiling water reactors (BWR), and heavy water CANDU type reactors.

Plutonium

The transmutation of Pu from spent LWR-UOX fuel is industrially accomplished in light-water reactors in the form of so called mixed-oxide fuel (MOX). It involves extraction of plutonium and uranium from spent fuel and re-use of plutonium mixed with uranium tailings (^{235}U enrichment of about 0.25%-0.3%) in fabrication of new fuel sub-assemblies. Plutonium reprocessed from about five to eight UOX spent fuel sub-assemblies having a burnup of 40 GWd/tHM is sufficient to produce one MOX sub-assembly with 5% to 8.2% Pu content. Reprocessed uranium has so far been applied in some test MOX sub-assemblies, but its use has not become an industrial praxis also because of the large stocks of depleted uranium (about 7 tonnes is produced per each tonne of enriched uranium). Its usage is also unfavourable due to the presence of a neutron poison (^{236}U), and because of its increased radioactivity due to the strong γ-emitters ^{208}Tl and ^{228}Th, daughter products of ^{232}U (half-life 70 year).

The plutonium fission fraction ratio in the first MOX recycle is only about 25% while additional 10% is transformed into minor actinides [10]. The latter figure highlights the major drawback of plutonium recycling in LWRs, which is the build

up of minor actinides, as even neutron number nuclei have virtually zero fission-to-capture probability ratios in the thermal spectrum. Thus, despite the Pu mass reduction, radiotoxic inventory actually increases.

Indeed, further mass reduction can be achieved by multiple recycling of plutonium. This is, however, accompanied with constraints on core neutronic behaviour and limitation at reprocessing plants as plutonium quality decreases. The quality is defined as a mass fraction of fissile isotopes in the Pu-vector

$$Q_{\mathrm{Pu}} = 100 \cdot \frac{m(^{239}\mathrm{Pu}) + m(^{241}\mathrm{Pu})}{m(\mathrm{Pu_{tot}})}. \tag{3.30}$$

It diminishes in subsequent generations and drops from the value of about 70 for LWR Pu discharge down to about 45 at the fifth recycle generation in standard lattices of LWRs [63]. Due to the lowered plutonium reactivity, its enrichment in the U/Pu mixture has to be increased in further generations which influences several safety characteristics of the reactor - particularly moderator void and temperature reactivity coefficients, the Doppler coefficient and boron reactivity worth. This is due to a spectrum hardening in MOX sub-assemblies which is further pronounced, e.g. in the case of loss-of-coolant accident, when fast fission of fertile Pu isotopes become significant. In order to keep the boron reactivity worth on the same limit, the concentration of the boric acid in the water has to be increased, which however further deteriorate coolant void reactivity. Thus, due to the positive void worth, the plutonium content in standard PWR lattice MOX sub-assemblies cannot exceed 12 wt% [64].

These safety drawbacks may be mitigated by changes of sub-assembly lattice design in order to achieve satisfactory spectrum thermalisation. This is accomplished either by an increase of moderator/fuel ratio (up to 3.5 - 4) - so called high moderation PWR (HM-PWR) [65], or by a radical decrease of the fuel smear density from 9 g·cm^{-3} to 3.5 g·cm^{-3} keeping the same lattice geometry [66]. Another innovative method was presented by CEA, proposing heterogeneous distribution of uranium and plutonium pins in a fuel sub-assembly (Advanced Plutonium Assembly - APA and CORAIL MOX sub-assemblies) allowing to keep also an acceptable power shape [67, 68, 69, 70]. A further possibility to mitigate void problems is to increase the ^{235}U fraction in the fuel keeping plutonium content fixed at 4% (so called MIX approach) which on the other hand result in higher fabrication costs and lower Pu fission fraction ratios [71]. Combining the previous design approaches, an over-moderated ^{235}U-enriched MOX sub-assembly (MOX-UE) was recently developed [72]. In the S/A lattice with slightly increased moderation ratio, the neutron spectrum is sufficiently thermalised such that reasonable value of the void reactivity is maintained also during Pu recycling. In order to compensate for a degradation of the Pu vector (and respect 12% Pu limit), ^{235}U enrichment in the fuel has to be gradually increased (to 3% after 7 recyclings).

An additional major problem with high plutonium content fuels is the small delayed neutron fraction, which entails faster reactor response on reactivity and

power transients. In this respect, the potential of LWRs to recycle stocks of weapon grade Pu (95% ^{239}Pu, 5% ^{240}Pu) seems to be questionable.

Safety of reactor cores is proven up to 30%-50% of MOX fuel assemblies with plutonium enrichment up to 5%. At this level as much plutonium is consumed in MOX sub-assemblies as is produced in UOX. For MOX-UE, stabilising Pu inventory requires that 25-28% of the energy is generated in the MOX sub-assemblies. Maximum plutonium consumption in LWRs would be reached in 100% MOX cores, whose feasibility, however, needs to be further investigated.

Obviously, due to the presence of uranium in the U/Pu matrix, plutonium depletion is somewhat diminished. Use of an inert matrix instead of uranium could gain higher plutonium consumption, which is, however, at the expense of fuel temperature feedback. Some studies have been also done on the use of thorium as a plutonium support in MOX fuel showing improved void characteristics [73, 74].

Nevertheless, recycling of plutonium in LWR does not meet our objectives for P&T technologies as it does not significantly reduce the radiotoxic inventory of spent fuel. The amount of minor actinides produced in a MOX sub-assembly is 3-4 times higher than in corresponding UOX sub-assemblies having increased requirements on interim storage and short-term repository performance as consequence.

Minor actinides

Possible transmutation strategies for minor actinides are with certain limitations determined by the performance and abilities of chemical separation processes. The general problems accompanying addition of minor actinides to the fuel are similar to those already mentioned for plutonium - deterioration of physical characteristics of reactor cores, particularly coolant void temperature coefficient, Doppler feedback, and delayed neutron fractions. An additional serious difficulty is the helium production due to α-decaying ^{242}Cm, ^{244}Cm, and ^{238}Pu which enhances fuel swelling and results in pin over-pressurisation. Thus the content of minor actinides in reactor cores has to be somewhat limited.

Americium and curium Transmutation of *both* americium and curium has to be accomplished if a reduction of radiotoxic inventories higher than a factor of 100 is to be reached [75, 25]. Moreover, incineration of pure curium in a standalone facility can not be considered due to the very high heat production from the α and neutron emitters ^{242}Cm and ^{244}Cm. The only remedy is either its incineration together with americium or transmutation of curium as ^{240}Pu allowing for a decay of ^{244}Cm (half-life 18.1 yr) in a time period of 100 years or so, which still leaves ^{245}Cm untransmuted.

Studies of the homogeneous recycling of americium show a significant deterioration of the coolant void reactivity coefficient. Taking into account limits on uranium enrichment ($< 5\%$) or plutonium content (less than about 12%) in the case of MOX fuels, the maximum concentrations of americium in fuel were identified as 1% for standard PWR and 2% for highly moderated lattices [21]. It results in a

10% decrease of Doppler coefficient while the moderator temperature coefficient is diminished by 25%. The specific consumption of americium in UOX fuel (total inventory of about 1.1 tonne) reaches about 19 kg/TWh$_e$ (annual production of about five 1000 MWe-LWRs). Adding 1% Am into MOX-UE sub-assembly requires that ^{235}U enrichment is increased by about 2% and Pu content decreased to ∼8%. If both plutonium and americium inventory should be stabilised, 40% MOX-UE cores have to be applied [72]. As the fission-to-absorption ratio for ^{241}Am is very low (virtually zero) in thermal spectra, most of the americium (70%) is converted via ^{242}Am into ^{242}Cm which consequently α-decays into ^{238}Pu, resulting in increased fuel swelling rates due to the formation of He bubbles.

Targets A much more attractive option with respect to core neutronic characteristics was thought to be heterogeneous americium recycling in separate subassemblies placed at the core periphery, thus having lower influence on core characteristics. As thermophysical properties of AmO_2 are not favourable owing to the low thermal conductivity and melting temperature, several materials have been investigated as suitable matrices for americium incineration. E.g., the EFTTRA-T4 experiments [76] study behaviour of americium incorporated in spinel ($MgAl_2O_4$) matrix (11 wt% of Am) during irradiation in Petten's thermal high flux reactor. Another compound - MgO-AmO_{2-x} - was fabricated and irradiated by ITU [77], having americium particles homogeneously dispersed in the matrix as well as in the macroscopic solution with it.

Due to anticipated significant difficulties with reprocessing of such target fuels, a once-through transmutation scheme is envisaged for thermal americium incineration. Dedicated americium targets are left in the reactor until a significant depletion takes place and are thereafter directly disposed of. The residence time of such assemblies in the reactor is limited by the maximum radiation damage which inert matrix and cladding can withstand and by the maximum capacity of the target pins to accommodate produced helium.

As the preliminary calculations show, consumption of americium in dedicated targets is rather low, reaching about 9 kg/TWh$_e$ in the best case (depletion 74%) having 30 wt% AmO_2 in a mixture with an inert matrix. This corresponds to half the annual LWR americium production (4 years after decay). Furthermore, due to the low reaction rates, the equilibrium incineration of americium in LWRs implies very large fuel inventories - about several hundreds of tons of TRU - much more than waste discharges.

Indeed, the radiotoxic inventory is again increased due to the massive curium production which, together with reactivity and swelling problems, makes LWRs unsuitable for effective MA incineration in a P&T scheme. The fuel swelling problems are only partially relaxed in the fast neutron spectra and need to be addressed in dedicated systems with favourable minor actinide fission-to-absorption ratios and where gasses may be released into the plena, which is not possible in standard LWRs.

Fission products

As discussed in Chapter 2, there are some long-lived fission products (LLFP), which contribute to the long-term geosphere dose, also when considering a human intrusion scenario into the repository. These are hence candidates for partitioning and transmutation schemes - ^{129}I (production rate 5 kg/GW$_e$ ·year), ^{135}Cs (12 kg/GW$_e$·year), and in an oxidising environment ^{99}Tc (21 kg/GW$_e$·year).

The transmutation of fission products is considered to be accomplished in heterogeneous mode fixing individual LLFP nuclides in suitable target forms. The target material/matrix has to be stable upon irradiation and withstand high burnups, the melting point has to be high and compatibility with cladding and coolant must be ensured. Transmutation of selected fission products can be accomplished by single neutron capture, resulting in stable nuclei

$$^{99}\mathrm{Tc} + \mathrm{n} \rightarrow ^{100}\mathrm{Ru} + \beta^- + \tilde{\nu}_\mathrm{e} \tag{3.31}$$

and

$$^{129}\mathrm{I} + \mathrm{n} \rightarrow ^{130}\mathrm{Xe} + \beta^- + \tilde{\nu}_\mathrm{e} \tag{3.32}$$

The superiority of transmutation of these isotopes is that even further double neutron capture would lead to stable nuclei (^{101}Ru, ^{102}Ru, ^{131}Xe, ^{132}Xe). The cross-section for neutron capture is highest at thermal energies with significant resonances in the epithermal region. It is therefore attractive to place LLFP pins in the moderator of thermal reactors. On the other hand, as high fluxes as possible are favourable, which would suggest the placement of LLFP into the specially moderated sub-assemblies of fast reactors. A major drawback of a such approach is a strong self-shielding causing dips in neutron flux at the centre of LLFP pins and, as we will show, the fast neutron induced LLFP transmutation performs at least equally well (see **Paper III**).

The transmutation of long-lived fission products has been studied in the frame of the EFTTRA collaboration since 1992 [76].

In the case of ^{99}Tc, the metallic form was chosen as the most attractive option due to the highest technetium concentration and compatibility with transmutation product (^{100}Ru). The irradiation of sample targets has been done in thermal positions of Petten's high flux reactor reaching burnups from 6% to 16% [78, 79]. Neither swelling nor microstructural changes in the pellets have been observed and it seems that metallic technetium is a good candidate for transmutation. However, its behaviour in fast reactor environments remains to be confirmed. Theoretical predictions of transmutation half-lifes are from 15 to 18 years in fast reactors and 40 to 77 years in LWRs. Due to the limitations posed by radiation damage of cladding materials, the transmutation has to be accomplished in multi-recycling mode in order to achieve a significant reduction of Tc content.

The choice of target material is more complex for iodine. ^{129}I mass proportion is about 80% in a mixture with stable ^{127}I which seems to be rather affable. In elemental form, iodine is rather volatile (melting point 387 K) and thus some binary compounds seem to be more suitable - CeI_3, PbI_2, and NaI. The irradiation

experiments in Petten HFR have revealed incompatibility of PbI_2 with the 15-15Ti stainless steel capsule, which corroded. At the same time, serious difficulties have been encountered while manufacturing CeI_3 and thus NaI seems to be so far the best candidate for iodine incineration. Another important question, limiting iodine transmutation rate, is the accommodation of gaseous ^{130}Xe, which has to be accomplished either by a large gas plenum in the LLFP pin or by special vented design.

In the case of cesium, isotopic separation of ^{133}Cs, ^{135}Cs, and ^{137}Cs has to be accomplished prior to incineration, which makes transmutation of ^{135}Cs economically hardly feasible.

3.3.2 Fast reactors

Plutonium

The development of a self-sustaining U-Pu fuel cycle based on MOX fuelled fast breeder reactors engaged thousands of nuclear scientists during the 60s and 70s. The technical complexity and associated difficulties have together with economical disadvantages (cheap uranium) and political reasons considerably slowed down their introduction into the nuclear reactor parks. Furthermore, in terms of partitioning and transmutation technologies, the incentives for fast reactor deployment changes and are shifting from plutonium/transuranic *breeding* to *burning*.

While incineration of plutonium in thermal neutron spectra is limited due to the deterioration of plutonium vector composition and core neutronic and safety aspects, and the limitation in the PUREX reprocessing technologies, the infinite multiple-recycling of plutonium in fast reactors is theoretically feasible [73]. The superiority of fast spectrum in actinide transmutation and radiotoxic inventory reduction of spent fuel is recognised by most authors [39, 80, 81]. All actinide isotopes are in principle fissionable and in a high flux neutron spectrum of fast reactors act as neutron producers, see also Section 3.2.3 [41, 82].

Special type of fast *burner* reactors (FBuR) without breeding blanket and thus with maximised plutonium consumption are extensively studied. The CAPRA reactor [83] was proposed in 1992 utilising MOX fuel with up to 45% of plutonium enrichment. The CAPRA core can work in symbiosis with about one MOX-LWR and five UOX-LWRs achieving significant reduction of the Pu inventory as only reprocessing losses are treated as a waste. However, due to the massive production of minor actinides, the radiotoxic inventory is reduced only by a factor of three for several thousand years and by five-six afterwards. The plutonium depletion reaches 55% and its concentration in spent CAPRA fuel is reduced to 25% which is the maximum concentration in MOX fuel being compatible with the PUREX process. Obviously, this difficulty could be solved by applying other types of fuel matrices as nitrides or metallic fuels together with pyro-reprocessing.

Minor actinides

The neutron surplus when transmuting minor actinides is positive in fast spectrum for fluxes over 10^{15}n·cm^{-2}s^{-1} [41]. MA incineration is again envisioned in homogeneous and heterogeneous modes considering either a once-through or multi-recycling scheme.

Neptunium As in the case of LWRs, the homogeneous introduction of neptunium in the MOX fuel is the preferred option. Due to the limitations in Doppler feedback and moderator void coefficient (sodium), the content of neptunium in the fuel has to be limited to about 2.5%. However, more strict limitation is posed again by the PUREX reprocessing due to the α and heat emitter ^{238}Pu. Specific consumption rates of Np are not significantly increased when compared to the thermal spectrum and amount to about 10 kg/TWh$_e$ in an EFR-type core.

Extensive calculation studies of MA transmutation in fast reactors have been performed in the frame of European activities on feasibility and cost assessment of P&T [84]. Regarding heterogeneous once-through recycling of neptunium, the targets (40% of Np in an inert matrix material) were placed in the reflector of an EFR-type core and burnup calculations were performed for 4500 effective full power days, after which radiation damage to cladding steels had reached the limit of 200 dpa-NRT. The Np depletion appeared to be rather low, reaching 60% at the very modest fission fraction ratio 24%. Thus, about 60% of the depleted neptunium was converted to non-fissile plutonium isotopes with a high portion of ^{238}Pu.

Americium Due to the limitations on ^{238}Pu concentration, remember

$$^{241}\mathrm{Am} + \mathrm{n} \;\rightarrow\; ^{242}\mathrm{Cm} \;\rightarrow\; ^{238}\mathrm{Pu}, \tag{3.33}$$

the americium content in homogeneous MOX mixtures has to be reduced, as in the case of neptunium homogeneous recycling, to 2.5%. The americium consumption is accordingly very low, only 9 kg/TWh$_e$, and the fast reactor can accommodate the annual production of about 3 LWRs. The fabrication costs of fuel containing americium increase by about 20% compared to standard FBR MOX.

In the case of once-through heterogeneous recycling of americium, targets containing 20%, 40%, and 100% of americium in an Al_2O_3 inert matrix were placed in the reflector of an EFR-type reactor core. It appeared that depletion and fission fraction ratios depend strongly on the americium content. The optimum concentration of americium in the targets was around 40% with respect to power profile characteristics, depletion rates and influence on core performance. The americium consumption was calculated to be comparatively high amounting to 14 kg/TWh$_e$ (which is a factor of 2-3 higher than the internal americium production of the EFR). The irradiation time was, as above, limited to the maximum steel damage of 200 dpa-NRT. In this respect, we note that 200-dpa NRT is probably unrealistic limit considering latest results obtained by Budylkin et al. [85]. For further discussion on this issue, see Chapter 5.

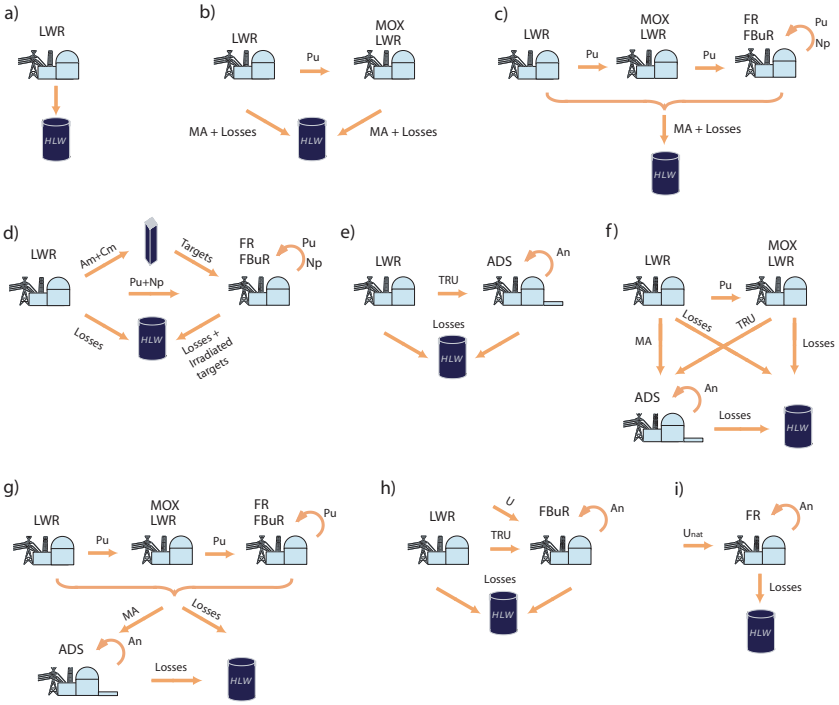

Figure 3.10. Fuel cycle/P&T scenarios: a) open "once-through" cycle; b) Pu MOX burning in LWRs; c) Pu MOX burning in LWRs & fast reactors (∼70% LWR-UOX − ∼10% LWR-MOX − ∼20% FR); d) Pu burning & heterogeneous MA recycling in fast reactors; e) two-component strategy, TRU burning in ADS, ADS support ratio ∼21%; f) two-component strategy, Pu MOX recycling in LWR prior to TRU burning in ADS, fraction of ADS ∼15%; g) double-strata (multi-component, two-tier) scheme, fraction of ADS ∼ 5-10%; h) TRU burning in FBuR, the reactor park consists of 63% LWRs and 37% FBuRs; i) one-component fast reactor cycle.

Neptunium and americium Multiple heterogeneous recycling of neptunium and americium was studied by Baetslé [86] in an admixture with plutonium and depleted uranium (67%U-33%TRU). It was revealed that 1 tonne of Pu+MA mixture from LWR-MOX fuel can be completely transmuted after 15 cycles (255 years) in a CAPRA-like reactor (1 cycle = 5 years of irradiation and 12 years of cooling down) allowing, of course, for reprocessing losses. A fast reactor could thus support 1-2 LWRs of the same power.

Curium Due to the strong α and neutron emission, fabrication of curium target fuels becomes extremely costly and curium is thus preferably diluted with americium. Alternatively, one may, prior to any transmutation, allow ^{244}Cm to undergo α-decay into ^{240}Pu.

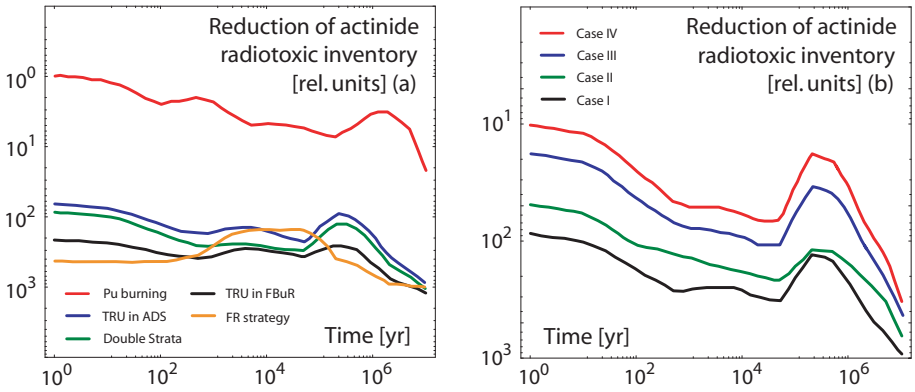

Figure 3.11. Reduction of radiotoxic inventory for different P&T schemes (a) and an impact of fuel losses in separation technologies on a performance of double-strata scenario (b). Reprocessing losses in advanced PUREX of the first stratum were assumed to be either 0.1% for all actinides in Case I, or 0.1% for U&Pu and 1% for MA in Cases II-IV. Losses in pyro-reprocessing are 0.1% (Case I&II), 0.5% (Case III) and 1.0% (Case IV), respectively. Figure courtesy of OECD/NEA [25].

3.3.3 Scenarios

Now, we are ready to discuss the different P&T scenarios involving both evolutionary and innovative reactor system components, recall Figure 3.10, and assess their performance with respect to the reduction of the radiotoxic inventory of spent fuel. A comprehensive analysis of this subject was provided most recently in OECD/NEA study [25]. The results for some principal schemes are given in Figure 3.11(a).

It was shown that multirecycling the *Pu alone* (in either LWRs or in LWRs-FRs schemes, i.e., strategy b) and c)) significantly reduces the losses of TRU to the repository, but its performance with respect to the reduction of the radiotoxic inventory disqualifies it as an effective transmutation strategy. The radiotoxic inventory is reduced by about a factor of two and five for the b) and c) strategy, respectively.

The best strategy for *minor actinide* transmutation in *fast critical reactors* seems to be homogeneous incineration of neptunium in MOX fuel sub-assemblies, while americium together with curium needs to be recycled and irradiated in dedicated sub-assemblies positioned in the core periphery, i.e., scheme d). However, cooling times for the irradiated Am/Cm assemblies become excessive (7-12 years) if aqueous reprocessing is to be used, and the support ratio, i.e. the number of fast neutron cores needed to manage MA production of one LWR, becomes larger than 0.5 with adverse effect on the economy of the P&T fuel cycle. A 90% reduction of TRU would thus be reached in time scales of 100-250 years. As mentioned above, significantly smaller cooling times are possible for pyrochemical technologies, which could reduce the length of an irradiation reprocessing cycle by more than a factor

of two.

But all in all, unfavourable safety characteristics appearing when burning minor actinides in both thermal and fast reactors of the standard design have led to the idea of dedicated actinide and LLFP transmutation in special reactors, conceived originally both as critical and sub-critical. The dedicated systems are envisioned to work either in TRU burning mode - in symbiosis with light-water reactors in a two-component scenario - i.e. strategies e) and f), or in concert with LWRs and FRs - in a so called double-strata (multi-component, two-tier) scheme [87, 82] - strategy g).

The double-strata concept was first proposed by JAERI in 1984 [88]. It comprises dividing the fuel cycle into two rather distinct parts - the first stratum which is based on modestly changed state-of-the-art technologies (reprocessing, fuel fabrication, core design - LWRs and FRs) and the second relying, in all respects, on advanced, innovative processes. The plutonium incineration in the LWRs and FRs of the first stratum is thus seen as an effective way to reduce transuranic mass rather than radiotoxic inventory, which allows to keep the fraction of innovative reactors managing minor actinides at a minimum level.

The impact of the different separation losses on the capability of the double-strata scheme is illustrated in Figure 3.11(b). The losses in the pyroprocessing of the MA burning stratum showed to be decisive with respect to the transmutation performance of the scenario. The actinide radiotoxic inventory can be reduced to 1% of its original value within 100 years after fuel reprocessing, if actinide losses in pyroprocessing are limited to 0.1% - a similar requirement we already imposed on the recovery yields of the separation technologies in the model equilibrium cycle, see Section 3.2.1. In the first stratum, the losses in advanced PUREX were assumed to be limited to 0.1% for U & Pu and 1.0% for minor actinides (Case II).

TRU burning in FBuR and *pure*, one-component fast reactor strategy have been both also identified as promising P&T routes, closing also the fuel cycle for all transuranics. It appeared that if MOX recycling is not pursued in LWR and the whole TRU vector is directed into FBuR, minor actinide fraction in the FBuR fuel can be kept under 2.5% limit (set by deteriorating Doppler feedback and coolant void coefficient). Thus, if whole TRU vector is recycled, the scheme performs equally well or better than scenarios including dedicated systems, see Figure 3.11(a). Therefore, there may be an incentive to re-evaluate the decisions to *continue* with MOX-recycling in LWRs. Fast reactor scenario, strategy i), involves an introduction of a completely new fuel cycle scheme, relevant only for countries not utilising nuclear power today.

Chapter 4

Dedicated reactors

As discussed in the previous chapter, removal of ^{238}U and/or admixture of large amounts of minor actinides into the fuel severally deteriorates the safety parameters of reactor cores, significantly decreasing Doppler temperature feedback and effective delayed neutron fractions. In addition, high content of even-neutron number nuclei in the fuel elevates coolant void worth and/or coolant temperature reactivity coefficient. The possibility to operate dedicated MA burning cores critical hence become doubtful.

Already in 1974, the introduction of slightly sub-critical cores for MA burning was therefore envisioned by Los Alamos scientists [89]. The idea was revived again by Japanese scientists ten years later, proposing a separate management of minor actinides in *dedicated* facilities and adopting fast reactors for recycling of plutonium [88]. Thus, handling of a strong α and neutron emitters is confined only to a very small fraction of the reactor park. Nowadays, another important reason for introduction of dedicated MA burners is the excess of ^{241}Am present in spent fuel due to the long delay in commencing of P&T in most countries. Both critical and sub-critical dedicated MA burners were proposed originally, but in recent years, the focus is naturally on the sub-critical systems. Note that the review provided here is neither complete nor exhaustive.

4.1 Critical actinide burners

In JAERI investigations, two concepts of dedicated critical actinide burner reactors (ABR) have crystallised - lead-cooled pin fuel (L-ABR) and a helium-cooled particle fuel (P-ABR) [80]. For these reactors, JAERI proposed a nitride fuel consisting of 65% of minor actinides (Np,Am,Cm) and 35% of highly enriched uranium. Enriched uranium is mixed into the fuel in order to counterattack problems with extremely low delayed fractions. However, β_{eff} still remained rather low at the level of 260 pcm (about 20% lower than CAPRA reference core). As also neutron lifetimes became

very small (in the order of 0.13 μs), safety margins of the ABRs were significantly deteriorated.

CEA studied a fast modular critical ABR based on the lead-bismuth coolant technology and nitride fuel. The thermal output of these cores was rather modest in the order of 130 MW_{th} with MA consumption rate of about 78 kg/TWh_e. The delayed neutron fraction were again very low on the level of about 170 pcm.

4.2 Accelerator-driven systems

The ADSs couple the technology of high-intensity particle accelerator with spallation targets, which provide neutrons for a multiplicative sub-critical blanket/core. The accelerator is either a linac as proposed by LANL [90] and JAERI [91] or a cyclotron as advertised by CERN [92].

Several types of targets are studied, including a solid one where tungsten is cooled by sodium flowing through holes in the target, and a liquid one - based on lead-bismuth eutectic serving both as a spallation material and coolant. In terms of minor actinide transmutations, ADSs offer much higher flexibility what concerns fuel composition, irradiation times and overall system performance as requirements on safety margins are somewhat relaxed. ADSs can accommodate excess americium and curium and use uranium-free fuel, allowing to reach the theoretical maximum TRU net consumption 360 kg/GW_{th}·year. A majority of the sub-critical cores envisioned for MA transmutation are designed to be operated in a fast or coupled fast/thermal spectrum in order to achieve the most favourable neutronic spectrum for effective MA and LLFP burning. As shown by Salvatores and coworkers [93], the ADSs in comparison to the critical systems supply a higher excess of neutrons which can be used for additional transmutation purposes.

While some of the safety issues of ADSs are common with those considered for critical reactors (e.g. heat removal), there some problems which are ADS specific. They, in particular, occur on the interface and in connection with accelerator and core (blanket) coupling and involve, e.g. irregularities/oscillations in particle beam intensity (e.g. beam-overpower accident) or issues of radiation damage of accelerator beam window and target walls in neutron and proton fields. Reliability and availability of the accelerator beam is another important question. Namely, a frequency of beam trips long enough to cause the shut-down of the system has to be significantly limited.

4.3 Review of ADS related projects

The research on accelerator-driven systems or material/component-related subjects is pursued worldwide. We give a brief overlook and summary of relevant projects.

4.3.1 Japan

In the frame of the OMEGA programme, JAERI studied two types of solid fuel ADSs [94]. The first relied on the established technology of sodium and the second employed lead-bismuth as coolant. The latter option was further developed in recent years [95]. The reactor core 800 MW_{th} is fuelled with minor actinides (60%) mixed with initial plutonium loading, thus mitigating the burnup reactivity swing. The fuel is diluted with ZrN. Ductless fuel sub-assemblies are envisioned in order to avoid crud blockage accidents and enhance self-circulation of Pb/Bi hence improving decay heat removal capabilities. JAERI operates the Pb/Bi material test loop in order to study corrosion stability of structural materials, beam window thermal hydraulics and behaviour of radioactive impurities. Moreover, transmutation experimental facility is planned to be build in the Tokai Research Establishment. The facility would comprise Transmutation Physics Experimental Facility which would be a zero-power sub-critical system coupled with low power proton beam, and ADS Target Test Facility being able to accept 200 keV-600 MeV proton beam in the Pb/Bi spallation target that would be used for material irradiation testing purposes. Studies on fast spectrum molten salt cores were also made, but are given secondary priority due to safety and material compatibility problems. The molten salt chlorides were proposed as a primer choice, having a multifold purpose of fuel carrier ($64PbCl_2$-$36TRUCl_3$), target material and coolant [94].

4.3.2 France

Alluding to the 1991 Law on Nuclear Waste Management, the Separation - Incineration research programme was started in France, investigating the potential of P&T in the spent fuel management scheme [96]. Research in the area of ADS is coordinated in France by the GEDEPEON group, including research organisations (CEA, CNRS) as well as industrial bodies (EdF, Framatome). Development of ADS was considered in a broader frame of advanced nuclear fuel cycles - potentially serving both as dedicated MA burners and being a basis of new, thorium burning reactor generation. Two systems were studied, based on the technology of molten salts [82] and heavy metal (Pb/Bi) cooled, nitride-fuelled blankets [97]. Recently, the activities have refocused from the ADS neutronic and system studies and the priority is given to development of novel sub-assemblies for multi-recycling of Pu in PWRs [71], design of gas-cooled fast neutron reactors [98] (in coherence with Generation IV activities [99]), and development of fuel and targets for FRs and ADSs [100]. R&D concerning spallation target (MEGAPIE), advanced separation technologies for minor actinides and cesium, regarding high energy nuclear data, and development and testing of new materials for ADS (SPIRE) is also pursued. The MUSE experiments at the MASURCA fast critical assembly has been recently concluded gaining an invaluable understanding and experience with physics of sub-critical systems. TRADE (TRIGA Reactor Accelerator Driven Experiment) experiments are planned to be started around 2006-2007 as a follow-up of the MUSE

programme [101]. TRADE will demonstrate the coupling of the spallation target source with a sub-critical reactor at power sufficient to observe reactivity feedback effects. Complementary experiments are also under way in Minsk at YALINA facility coupling the thermal spectrum sub-critical core with a neutron generator. In the frame of SAD project in Dubna, 600 MeV proton accelerator will be connected with a low power MOX core.

4.3.3 U.S.A.

In the past years, a research programme on ADSs in U.S.A. experienced a turbulent development. First, the interest has shifted from thermal spectrum designs [102, 103] to fast spectrum systems [104], based on Pb/Bi coolant technology. The ATW (Accelerator Transmutation of Waste) programme at LANL envisioned incineration of TRU and LLFP coming directly from LWRs in a sub-critical reactor using metallic fuel - an admixture of TRU with zirconium (85%Zr-15%TRU). In 1999, a federal road-mapping activity was performed, defining goals for further transmutation research in the U.S.A. [105]. Rather short-lived AAA (Advanced Accelerator Application) programme was then replaced by Advanced Fuel Cycle Initiative (AFCI) in 2003. AFCI is a common initiative by a team of national laboratories, universities, and industrial bodies aiming at development of advanced fuels and separation technologies. In a broader perspective, it also strives to revitalise U.S. nuclear science and engineering infrastructure.

4.3.4 CERN

The loudest advocate of ADSs was a team at CERN under the leadership of Carlo Rubbia. In 1993, this group presented the so called Energy Amplifier (EA) - a 200 MW_{th} sub-critical reactor core driven by an 800 MeV-6.25 mA cyclotron for "clean" energy production based on the thorium fuel cycle. This concept was originally conceived as thermal, water cooled using thorium metallic fuel [106]. Lately, the design features have shifted to fast spectrum systems driven by a 1 GeV-12.5 mA cyclotron. The Energy Amplifier in energy producing mode was oxide-fuelled with a power output of 1500 MW_{th} [107], while metallic-fuelled in LWR spent fuel incineration mode [108].

4.3.5 EU related projects

The EU 5^{th} Framework Programme on P&T includes significant experimental work on materials (Pb/Bi coolant, ferritic steels and nitride fuels) for accelerator-driven systems. Congruently with these activities, the development of a prototype ADS, eXperimental Accelerator Driven System (PDS-XADS) was started. The project focused on the design of an ADS system based either on heavy metal coolant (Pb/Bi eutectic), so called Ansaldo design (80 MW_{th}), or cooled by gas (He), so called Framatome design.

Within the frame of PDS-XADS, the Belgian MYRRHA project was also envisioned [109]. MYRRHA facility is a multipurpose prototype research fast spectrum sub-critical device driven by a 350 MeV-5 mA proton accelerator. The Pb-(Pb/Bi) spallation target is planned to be windowless in order to avoid problems with the radiation damage.

Considerable effort in ADS research also takes place in several other countries such as Spain (CIEMAT), Italy (ENEA), and Korea (HYPER facility, KAERI).

4.4 Role of ADS in P&T schemes

Obviously, the role of ADSs in the transmutation of the long-lived radiotoxic inventory has to be considered in the symbiosis with existing fuel cycle schemes. As emphasised by Salvatores [39], the minor actinide management is inevitably connected to the plutonium incineration strategy. We already know that a radiotoxic inventory reduction factor higher than ten is achievable only if curium is treated in a P&T process in a special manner. Of course, the easiest way (from the point of view of technology demands) is to let curium decay in the time period of about 100 years and transmute it afterwards as plutonium. This option, however, shifts responsibilities to the future and might not be accepted for ethical reasons. Truly, there is a theoretical possibility of immediate curium transmutation achieving fission fraction ratios as high as 90-95%. As discussed earlier, such incinerations have to be accomplished together with americium in once-through heterogeneous mode placing target dedicated assemblies of fast burners, or in dedicated reactors. This would, however, require very long irradiation times (as high as ten years), posing significant radiation damage to the cladding materials. As studies reported by Beaumont [110] show, MA target residence times in the periphery of the CAPRA high burnup core are limited to five years corresponding to the maximum cladding damage of 180 dpa-NRT. We remind the reader that this figure can be unrealistic considering recent results from low dose rate irradiations of ferritic and austenitic steels in BOR-60 [85]. In addition, the pin plenum length needed to accommodate produced helium (due to ^{242}Cm decay) becomes exceedingly long reaching 3.5 m. In this regime, as high as 80% percent of americium/curium is actually transmuted/fissioned *via* plutonium, with associated constraints on neutron economy.

As we will discuss further in the following chapters, much more favourable fission fraction ratios for *direct* fissioning of even-neutron americium and curium isotopes can be achieved in a novel type of accelerator-driven, sub-critical burner design, presented in **Paper II** and **III**. In the next chapter, we start by by reviewing and motivating the choice of materials for such a system.

Chapter 5

Choice of materials for ADS

The materials which are proposed to be applied in ADS are innovative in many aspects. The fuels should preferably fertile free (without U or Th support) and be able to accommodate large amounts of minor actinides. In order to facilitate efficient transmutation, a hard neutron spectrum should be maintained, imposing demands on the irradiation stability of the construction materials.

General requirements on materials in the ADS can be summarised as follows

- good high-temperature mechanical and irradiation performance,
- chemical stability and inertness to outer environment (air, water, steam), with no hydrogen-forming substances,
- acceptable level of induced activity,
- prolonged in-pile lifetime, achieving high fuel burn-up,
- sufficient abundance in nature.

5.1 Fuel

There are several types of fuel matrices, which could be considered for ADS - oxides, nitrides, and metallic fuels. Sometimes carbide and coated particle fuels are also envisioned. The primary goal for the development of transmutation fuels is to achieve a high burnup, hence fertile-free matrices are preferable in order to maximise TRU consumption and reduce void worths [111]. However, current reactors operate on uranium based fuels. New and innovative fuel types are thus needed. Transmutation fuels have high decay heat and high neutron and gamma emission rates. The decay heat is a factor of 20 higher in the spent fuel than for ordinary LWR fuels, being an incentive for refinement of radiation resistant reprocessing technologies. The irradiation performance of the fuel is also an unanswered question.

5.1.1 Nitride fuel

Already since the 1960s, nitride fuels have been studied in Japan as promising candidates to accommodate high plutonium fractions. The advantages of the nitrides in comparison to the more customary used oxide fuel is higher thermal conductivity (3-4 times), good compatibility with construction and coolant materials, and high solubility in nitric acid in the whole range of Pu compositions.

High thermal conductivities enables low operating temperatures of fuel, limiting fuel swelling and fission gas release. However, the specific feature of nitrides is their susceptibility to decomposition into a liquid or gaseous metal and nitrogen gas at high temperature (e.g. during transient involving power excursion)

$$2\ \mathrm{AnN} \ \rightarrow\ \mathrm{N_2} + 2\ \mathrm{An} \tag{5.1}$$

In this case, the presence of the liquid metallic phase thus precedes the melting of the nitride compound itself and decomposition of the fuel continues until concentrations of An and N_2 reach a level of equilibrium relative to the decomposing nitride.

It was shown that the decomposition behaviour of the AnN fuel is a strong function of the chemical composition of the surrounding gas. Adding nitrogen into the gas effectively lowers actinide vapour pressure, thus delaying the onset of the nitride decomposition by several hundreds of Kelvin. As the thermal conductivity of nitrogen is significantly lower than that for helium, only a small portion of nitrogen (a few per cent) in the gas can be applied. Experiments with UN in frame of the CONFIRM project show that decomposition of UN samples occurred at about 2700 K in inert atmosphere. PuN decomposition values ranges from 2857 to 3103 K in 1 bar N_2, while decomposition occurs at 2200 K in pure He and 1923 K in vacuum at 1 bar [112]. Experimental results indicate that vaporisation of $(U_{0.8},Pu_{0.2})N$ in He atmosphere is small for temperatures below 2150 K [113] and onset of the decomposition can be delayed by at least 400 K in nitrogen atmosphere [112].

The dissociation behaviour of higher actinide nitrides (AmN, CmN) is less well known. Under inert atmosphere, AmN dissociates when temperatures exceed 1600 K [114, 115, 116]. On the other hand, under 1 bar of flowing nitrogen, the dissociation rate decreases by two orders of magnitude [115, 116]. CmN was so far only fabricated in solid solution with PuN and AmN, but appears to feature a vapour pressure similar to that of PuN [117].

Nitrides are obtained from oxide powder by the carbothermic reduction method. The oxides are mixed with an excess of graphite and then heated under flowing nitrogen, resulting in the reaction

$$2\ \mathrm{AnO_2} \ +\ 4\ \mathrm{C} + \ \mathrm{N_2} \ \rightarrow\ 2\ \mathrm{AnN} \ + 4\ \mathrm{CO} \tag{5.2}$$

When oxygen removal is complete, hydrogen is added to the gas flow in order to remove residual carbon by formation of HCN. Limiting both carbon and oxygen impurities is of a crucial importance for the stability and irradiation behaviour of the fuel. E.g. the thermal conductivity has been shown to decrease significantly

Material	Lattice parameter [nm]	k [W/(m·K)]	T_{limit} [K]	T_m [K]
ThN	0.5167	47	–	3098
UN	0.4888	25	2700	3128
PuN	0.4905	13	∼2150	2862
AmN	0.4991	∼9	1570	N/A
CmN	0.5041	∼6	N/A	N/A
ZrN	0.4576	37	–	3250
HfN	0.4520	17	–	3660
β-BN (cub.)	0.3615	29	2550	3270
YN	0.4891	N/A	–	>2970

Table 5.1. Lattice parameters, thermal conductivities, dissociation and melting temperatures for actinide nitrides and nitride inert and absorbing matrices. The thermal conductivity of AnN is a decreasing function of atomic number and the presented values for AmN and CmN were extrapolated from PuN data. The nitride limit(decomposition) temperature is given at p = 1 atm in inert atmosphere; thermal conductivity is given at 1273 K, except for ThN, where a value for 1000 K is used. Table adapted from **Paper II**.

by about 10% for 1% concentration of oxygen. In the present state of technology, the oxygen and carbon content could be reduced to less than 1000 ppm for actinide nitrides.

Mutual solubility of actinide nitrides is desired, as the composition of fuel is going to be very much dependent on the previous history of the sub-assembly in the fuel cycle. It seems that the flexibility of the fuel composition can be achieved with nitride fuels, as the solubility of AnNs has been either successfully demonstrated (in the case of (U,Np,Pu)N, and (Pu,Am,Cm)N) or is expected due to the small differences in the lattice parameters.

Fast reactor irradiation experience includes two full core loads of UN in BR-10. (U,Pu)N pins have been irradiated in Phénix, BOR-60 and JOYO to about 5% FIMA. Irradiation of sodium bonded americium bearing nitride fuels is presently taking place in the Advanced Test Reactor (ATR) in Idaho, as part of the US Advanced Fuel Cycle Initiative (AFCI). Similar fuels are planned to be irradiated in Phénix in the FUTURIX programme.

Japanese and Russian experiments show that the radiation swelling is appreciably small, of the order of 1%/%FIMA, in fuels operated at low temperatures (< 1270 K). Hence, burnup of ∼15%FIMA is attainable [118]. It is assumed that the melting temperature will decrease with burnup similarly as for oxides as, i.e. by 3.4β Kelvin, where β is burnup (see Section 3.2.1). The temperature gradient in the nitride fuel is much lower than in oxides, thus the mobility of the actinide metals and fission products along this gradient is rather reduced.

The thermal conductivity of AnN is a decreasing function of atomic number [119], strongly depending also on the fuel impurities and pellet porosity [120].

Nitrides are also fully compatible with liquid metal coolants (Na, Pb/Bi) and construction materials. The nitrogen reaction with the cladding is less of the problem than the oxidising of the clad is for oxide fuels. In Russian studies, PuN proved compatible with austenitic steels up to 873 K.

As already mentioned, the major economic difficulty associated with nitride fuels is the necessity of nitrogen enrichment by ^{15}N (natural abundance is 0.366% in a mixture with ^{14}N) up to 93-98% in order to avoid the production of radiologically hazardous ^{14}C through the reaction ^{14}N(n,p)^{14}C [121].

5.1.2 Diluent for nitride fuel

In order to compensate for the excess reactivity of fertile free ADS fuel, a diluent matrix has to be provided. Its selection process involves a complex assessment of physical and chemical characteristics, irradiation behaviour, as well as compatibility with reprocessing technologies. High conductivity, melting point, and compatibility with cladding and coolant are necessary requirements. Thus, maximum allowable fuel ratings can be increased, fuel has larger margins to damage, and cycle burnup can be prolonged. Higher diluent matrix fraction fuels also feature improved irradiation performance. The matrix provides more space to accommodate fission products, hence allowing for higher discharge burnups.

A number of different nitride matrices have been investigated. It was shown that UN is completely miscible and forms solid solution with YN, LaN, CeN, PrN, NdN, and ZrN, while TiN and BN form a heterogeneous mixture with AnN [51, 122]. Some heterogeneous nitride fuels are also considered, such as PuN-Si_3N_4 and nitride-metallic AnN-Mo. Their major disadvantage is the risk for hot-spot formation, especially for micro-dispersed fuels. At the same time, the dimensional stability of fuel is affected.

In **Paper II**, we investigated a neutronic and burnup performance of some diluent matrix candidates, namely ZrN, YN, HfN and BN. Basic characteristics of the nitride compounds considered in this study are displayed in Table 5.1.

Different fabrication routes for inert matrix nitride fuels are under development. In JAERI, solid solution ($Pu_{0.1}$,$Zr_{0.9}$)N pellets were fabricated by blending of PuN obtained by carbothermic reduction of plutonium with commercial ZrN powder. Sintering yielded densities above 90% of the theoretical density (TD). (Am,Zr)N has been fabricated for two different concentrations of Am. A single phased solid solution of ($Am_{0.1}$,$Zr_{0.9}$)N was obtained without an oxide phase. However, for Am content of 30% in Am+Zr mixture, two solid solutions were present. The reason for formation of these two phases is not known, but one speculates that the cause were high carbon and oxygen impurities. In the CONFIRM project, solid solution ($Pu_{0.20}$,$Zr_{0.80}$)N and ($Pu_{0.30}$,$Zr_{0.70}$)N pellets were produced by carbothermic nitridation of the corresponding oxide powders. In spite of the high affinity for oxygen of zirconium, the residual level of oxygen could be reduced to about 0.2 weight percent, performing the nitridation process under optimised conditions [123]. The

porosity of the pellets could however not be decreased below 18%, even when sintering at 2023 K. For the BORA-BORA experiment in Russia, PuN and ZrN were fabricated by nitridation of metals. The compounds were then mixed and sintered to 85% of the theoretical density. In Los Alamos, (Pu,Zr)N, (Pu,Np,Zr)N and (Pu,Am,Zr)N were fabricated using carbothermic nitridation of oxide powders in argon atmosphere, resulting in high losses of Am during sintering and high levels of residual carbon/oxygen [114].

Inert matrix has a stabilising effect on the fuel, delaying the onset of the fuel decomposition. Experiments have been performed on $(U_{0.2},Zr_{0.8})N$ heated up to 3073 K, with solidus and liquidus temperatures determined to be 2885 and 3038 K, respectively, while dissociation occurred in pure UN at 2700 K [124]. The behaviour of (Pu,Zr)N was assessed in calculations for 49 at% fraction of Zr, showing that melting does not occur below 2804 K. There is an assumption that due to the chemical similarities between actinide compounds, the melting point of (Np,Zr)N system is the same as for (U,Zr)N and (Am,Zr), and that of (Cm,Zr)N same as (Pu,Zr)N. Recent studies have shown that $(Pu_{0.21},MA_{0.09},Zr_{0.7})N$ stability may be expected up to 2400 K in N_2 saturated atmosphere [116]. Some experiments are under way, e.g. irradiation in JMTR and CONFIRM, but the irradiation of minor actinide fuel including inert matrix are pending.

At PSI, $(Zr_{0.75},Hf_{0.25})N$ pellets have been fabricated by carbothermic reduction from mixed oxides and a solid solution was obtained [125, 126]. Due to the similarity of the lattice parameters, actinide nitrides are assumed to form a homogeneous solution also with HfN. Hafnium is a good absorber of neutrons in the thermal and resonance energy regions, effectively hardening the neutron spectrum (see **Paper II**). Moreover, our simulations have shown that the temperature stability of (TRU,Hf)N is maintained at least up to 2400 K. Due to the chemical similarity of Hf and Zr (hafnium and zirconium are both group IV transition metals), the chemical behaviour of the hafnium nitride is thus supposed to be very similar to that of ZrN. Accordingly, we expect that HfN is soluble in HNO_3.

5.1.3 Metallic fuel

Another option considered for advanced TRU burning is their incorporation in metallic fuels. Several reactor concepts as the Integral Fast Reactor (IFR) and Advanced Liquid Metal Reactor (ALMR/PRISM) have been proposed mainly in the U.S.A. [62]. The advantage of metallic fuels is their relatively high thermal conductivity. The ternary compounds, as U-Pu-10wt%Zr, have been envisioned and considerable experience was gained during irradiations in the EBR-II reactor [127]. The fuel burnup of 18%FIMA was reached at linear ratings up to 50 kW/m without pin failure. The metallic fuels allow to reach harder neutron spectra than nitride/oxide fuels, which partially mitigate problems with minor actinide production. However, in order to control swelling for metallic alloys, excessive fuel porosities about 75% are required.

In the dispersion fuels, e.g. TRU-10wt%Zr, the fission products are supposed to be accommodated within the fuel particles mixed in the matrix. It is therefore assumed that these fuels would have much better swelling behaviour than alloy-based counterparts. However, fuel particle volume fraction in the matrix should not exceed 25% [43].

In the frame of Advanced Fuel Cycle Initiative, non-fertile and low-fertile metallic compounds with ∼70 vol%Zr are envisioned. Irradiation of two pairs of samples in Advanced Test Reactor began in 2003 with target burnups of 5-8%FIMA and 15%FIMA, respectively.

5.1.4 Oxide fuel

In comparison to the nitride and metallic fuel, there is a vast experience with in pile operation of oxide fuels. Oxide fuels feature high thermal (melting temperature) and chemical stability, but the thermal conductivity of oxides is significantly lower than that for nitrides, resulting in high temperature gradients in the fuel pellet. The major difficulty is also the plutonium solubility limit in nitric acid (∼25%). Additionally, in order to ensure stability of americium and curium oxides at higher temperatures, the oxygen-to-metal ratio must be considerably less than 2.0, which further lowers their thermal conductivity in comparison with standard oxides. The high MA-content fuels are hence supposed to be stabilised by some inert material (matrix) - either ceramic or metallic.

Ceramic matrices as spinel ($MgAl_2O_4$), zirconium oxide (ZrO_2), and magnesium oxide (MgO) were considered as the promising candidates with respect to their neutronic characteristics (transparent for neutrons) and high thermal conductivities [128, 129, 130, 131, 132, 133]. However, low temperature irradiation experiments of AmO_{2-x} micro-dispersion fuels in spinel showed that this fuel is susceptible to radiation damage. On the other hand, PuO_{2-x}-MgO performed well and high linear power ratings up to 165 kW/m could be achieved. Irradiation tests with AmO_{2-x}-MgO targets are currently under way in Phénix. A candidate matrices for CERMET fuels have to feature both high melting point and low absorption cross-section. The latter condition is posed by the requirement to keep inert matrix volume fraction higher than 50 vol% to ensure fabricability and stability of the fuel. In a recent study, two fuel candidates for MA ADS burner were proposed, a ceramic-ceramic one - $(Pu,Am,Cm)O_{2-x}$-MgO and a ceramic-metallic one - $(Pu,Am,Cm)O_{2-x}$-^{92}Mo [134].

5.2 Coolant

The requirement of a fast neutron spectrum for MA transmutation implies usage of coolants with low moderating power, such as Na, Pb, Pb/Bi and He, see also Section 3.2.7. Basic properties of these coolants are summarised in Table 5.2. Liquid metals allow to operate the system at atmospheric pressures, while gas

Coolant	ρ [g·cm^{-3}]	T_m [K]	T_b [K]	c_p [kJ/(kg·K)]	v [m/s]	k [W/(m·K)]
Na	0.847	371	1156	1.3	∼10	70
Pb/Bi	10.15	398	1943	0.15	2.5	13
Pb	10.48	601	2023	0.15	2.5	16
He	$4.13{\cdot}10^{-3}$	1.05	4.15	5.2	70-120	0.25

Table 5.2. Density (ρ), melting (T_m) and boiling (T_b) temperatures, specific heat (c_p), velocity (v) and thermal conductivity (k) of coolants considered for ADS given at 700 K [50]. Maximum coolant velocities of liquid metals are stated, while typical velocities are given for helium. Helium pressure is 6 MPa.

cooled systems requires high pressures in order to achieve similar heat transfer capability. Problems related to usage of liquid metals include increased corrosion rate and lack of visual inspection possibilities.

The sodium has superior thermal hydraulic capabilities, allowing for small pin pitches. There is a large experience of operation of sodium cooled fast reactors. While several power reactors have been shut down, BOR-60, JOYO, Phénix and BN-600 are still operating, the latter being in quasi-commercial operation since 1982. New reactors are under construction in Russia, China and India. Sodium features reasonably low melting temperature, but the low boiling point (1156 K), which raises safety concerns in connection with transients. Sodium exhibits high chemical activity with water and water vapour, and a sodium fire stopped operation of MONJU in 1998.

Understandably, gas coolants (helium, CO_2) allow to maintain the hardest neutron spectrum. However, high pressurisation (50-70 bars) and special profiling of the cladding is required to ensure appropriate heat removal. Gases do not impose any compatibility issues with the structural material or fuel. On the other hand, a serious safety concerns arise concerning decay heat removal in the case of the accident involving loss of pressure. Thus, the designs with low specific power densites have to be applied in order to allow for a heat removal by a natural circulation of an ambient air.

The choice of lead-alloys as coolants is motivated primarily by their high boiling temperatures, making risks for coolant boiling small. Lead-bismuth eutectic also provides a low melting point (398 K) limiting problems with freezing in the system and features low chemical activity with outer environments (water) excluding the possibility for fire or explosions. In comparison to sodium, lead-alloys also have beneficial effects on coolant void worth in TRU-fuelled systems (for detailed discussion see Chapter 6). On the other hand, Pb/Bi flow rates are limited by erosion concerns to about 2.5 m/s [135]. Typical sodium velocities are around 10 m/s, hence Pb/Bi in practice has a lower heat removal capacity. In addition, poorer heat transfer coefficients and more stringent temperature limits set by corrosion require higher pin P/D to stay below those limits. Using oxygen control the temperature

limit for long term operation of ferritic steels like HT-9 and T91 is roughly 820 K, while silicon modified steels like the Russian EP-823 may operate at temperatures reaching 890 K [136, 137]. Pure lead has a melting temperature of 601 K, which significantly narrows reactor's operational interval to about 680-890 K. A drawback interconnected with Pb/Bi is the accumulated radioactivity in Pb/Bi (mainly due to α-emitter ^{210}Po, $T_{1/2} \simeq 138$ d), which would pose difficulties during fuel reloading or repair work on the primary circuit [138]. A conservative estimation of the bismuth resources on Earth limits the capacity of Pb/Bi-cooled reactors to 280 GW_e [139].

Lead-bismuth eutectic offers a favourable combination of three characteristics. It provides low void worths (see Chapter 6) and features low melting and high boiling temperatures. In this study, we therefore choose Pb/Bi as a primary coolant candidate for a TRU ADS.

5.3 Construction material

The choice of liquid metals as coolant imposes significant challenges with respect to in-pile performance of the structural materials. Ferritic-martensitic steels feature good radiation and corrosion resistance, but are inferior to austenitic when comparing mechanical properties at high temperature. Example given, the rapid burst limit measured for SS-316 (1330 K) is about 200 K higher than that of HT-9 [140].

For high dose rates, certain ferritic-martensitic steels have exhibited very small swelling rates up to doses of 200 dpa-NRT, corresponding to a fast neutron fluence of $4{\cdot}10^{23}$ n/cm^2. Note however that the threshold for swelling appears to be dose dependent. Recent results from irradiations of ferritic as well as austenitic steels indicate that lowering the dose rate (fast neutron flux magnitude) by a factor of three decreases the swelling threshold significantly [85].

Concerning corrosion resistance, nickel has a high solubility in lead alloys, hence ferritic steels generally perform better. Raising the silicon content of the steel improve the corrosion resistance of both austenitic and ferritic steels [141]. The silicon modified Russian steel EP-823 has been shown to withstand temperatures up to 890 K. The price to be paid is however a reduced radiation resistance. Recently it was shown that EP-823 looses ductility and becomes brittle after irradiation at 720 K to relatively modest doses [142].

At the moment it thus appears as there is no obvious choice of cladding material for lead-alloy cooled reactors. In the present thesis, EP-823 was used as reference material, in lack of better options.

5.4 Neutron absorber

Boron carbide is widely used in fast breeder reactors as a control rod absorber material. In this study, the use of B_4C for stationary reactivity compensation was

suggested in **Paper III**. B_4C offers high thermal stability, with melting temperature $T_m = 2720$ K and a thermal conductivity comparable to that of AnN (∼5-10 W/m·K at the operational temperature range 600-900 K). However, the thermodynamical stability of boron carbide is small in reactions with steel materials at temperatures above 970 K, resulting in formation of $(Fe,Cr)_2B$. There is considerable amount of gas released into the fission gas plenum from $^{10}B(n,\alpha)^7Li$ reactions. B_4C is introduced into the fuel sub-assembly in the form of separated absorber pins. The boron carbide is enriched in ^{10}B up to 90%-95% in order to increase its burnup efficiency.

Chapter 6

Neutronic and burnup aspects of TRU incineration

The design and choice of materials for ADS blanket strongly influences its neutronic and burnup performance, and has an impact and imposes demands on other components of the system (spallation target, accelerator, separation technologies). As we mentioned, the fast spectrum is widely established as being favourable with respect to the transmutation performance of the system because of the high fission-to-absorption probabilities, especially for even-neutron numbered nuclides (see Figure 3.2). In the softened spectrum, build-up of the higher actinides adversely affects the neutron balance and influences the neutronic and safety performance of the system. Furthermore, it complicates fuel reprocessing due to the heat and radiation damage caused by high power of americium and curium.

The fast spectrum leads to a positive void worth. Even though the high boiling point of lead and lead-alloys makes coolant boiling a hypothetical event, void cavities may be introduced into the core by, example given, a Steam Generator Tube Rupture (SGTR) event. This type of accident is far from hypothetical, as it actually occurred in one of the Russian Pb/Bi cooled sub-marine reactors [143].

6.1 Design challenges

Our goal is an effective and safe consumption of TRU, i.e. reduction of their mass and thus decreasing the radiotoxic inventory of spent fuel (see Chapter 3). To summarise and develop on this subject, the aim is to

- maximise the discharge burnup,
- minimise the reactivity loss over one irradiation cycle, thus decreasing the accelerator beam power swing and associated power peaking,

- lower coolant void worth in order to reduce the necessary sub-criticality margin at BOC,
- ensure the core integrity at accidental conditions,
- provide efficient multiplication of source neutrons.

We will show that these goals will lead to somewhat contradictory requirements on the system design parameters.

6.1.1 Reactivity loss

The fuel discharge burnup β_{d} (%FIMA) is proportional to the product of total fuel residence time in the reactor T_{res} (fpd) and average power density q_{V} (W/m^3) divided by the mass of actinide inventory m_{act} (kg)

$$\beta_{\mathrm{d}} \propto \frac{T_{\mathrm{res}} q_{\mathrm{V}}}{m_{\mathrm{act}}} \tag{6.1}$$

Hence, in order to maximise β_{d}, one should aim to design the system with high power density and in-pile fuel residence time, while limiting actinide mass in the fuel.

The burnup reactivity loss over an irradiation cycle is given as the product of the reactivity swing rate, $\Delta k^{\mathrm{t}}_{\mathrm{eff}}$ (pcm/fpd), and the cycle duration, T_{i} (fpd), $\Delta k^{\mathrm{c}}_{\mathrm{eff}} = \Delta k^{\mathrm{t}}_{\mathrm{eff}} T_{\mathrm{i}}$. Similarly, discharge burnup is proportional to specific power P_{s} (W/kg) and total fuel irradiation time $T_{\mathrm{res}} = n\ T_{\mathrm{i}}$, where n is the number of the irradiation cycles. For fertile-free fuels, the reactivity loss over one irradiation cycle is, in the first approximation, proportional to the cycle burnup β_{c}. Then,

$$\Delta k^{\mathrm{c}}_{\mathrm{eff}} \propto \beta_{\mathrm{c}} = \frac{\beta_{\mathrm{d}}}{n} \propto P_{\mathrm{s}} T_{\mathrm{i}} \tag{6.2}$$

Thus, intuitively, in order to attain high discharge burnup β_{d} and low reactivity swing over a irradiation cycle, a sufficient number of irradiation batches n is required.

Low reactivity burnup swing can hence be accomplished in designs with low specific power, i.e., low power densities and high TRU inventories, these parameters being, however, in a clear contradiction with aforementioned requirements for high target burnup.

An alternative way is to design the core with high specific power and choose short irradiation periods such that the core's design limits are not exceeded. This option is attractive as it provides for more compact cores facilitating better system economics. However, a very high frequency of outages (every $\sim$ 40-50 days) would negatively influence the system capacity factor. Hence, irradiation cycle has to be sufficiently long ($>$ 100 full power days). The cores with low specific fuel inventories feature high burnup rates, the fraction of transuranics remaining in the discharged fuel thus being low. Additionally, the amount of the untransmuted material at the end of the system operation (the last core) is also minimised.

6.1.2 Power peaking

Reactivity losses exacerbate power peaking behaviour, which effectively limits the cycle length due to thermal hydraulic constraints of the clad/fuel. Design options to explicitly mitigate power peaking are

- enrichment zoning, an excessive number of different zones however complicates fuel fabrication and management,
- fuel shuffling, where high burnup assemblies are placed in the vicinity of the target, the shuffling procedure in liquid metal cooled reactors is however a delicate and time consuming procedure, reducing system availability significantly,
- employment of fewer irradiation cycles for the innermost S/As, which however reduces the discharge burnup.

6.1.3 Burnup reactivity swing & coolant void worth

Options to decrease the burnup reactivity swing and, at the same time, to reduce the coolant void worth, have been extensively studied for fast critical breeder reactor designs with metallic fuel by Khalil & Hill [144]. As the most promising option, an introduction of tightly coupled radially heterogenous pancake-like cores was suggested. However, it appeared that the void worth and burnup reactivity losses can not be reduced *simultaneously* to an acceptably low level, the conclusion, which was confirmed in a subsequent study even for a highly unconventional design, involving BeO moderating layers and movable fuel sub-assemblies [145]. For fast critical burner reactors, strongly heterogenous cores with other solutions like inner B_4C shielding regions [146] or streaming fuel sub-assemblies with double-entry control rod drives [147] have been proposed. These investigations were performed for metallic-fuelled reactors.

Several studies have shown that the coolant void worth is significantly reduced in Pb/Bi-cooled TRU and MA burners in comparison with sodium-cooled systems [148], see also **Paper I**. We note that providing a negative coolant reactivity is not *a priory* a prerequisite for a safe accommodation of coolant voiding transients in accelerator-driven systems since the reactor safety margins can be adjusted by an appropriate choice of initial level of sub-criticality, so that the increase in source multiplication, and thus core power, is not detrimental. On the other hand, if substantial reactivity would be introduced into the system *together with* or as a consequence of an inadvertent increase of the accelerator beam power (unprotected beam overpower transient), this could lead to the loss of core integrity with subsequent potential for core material restructuring and recriticalities. It was shown that providing substantial margin to prevent core damage in the cases with high coolant void reactivity would require very high sub-criticalities, with penalties on the total reactor power, discharge burnup, and/or extensive requirements on the beam power as a result ($\sim$100 MW) [149, 150].

Therefore is appears relevant to find design options that allow to operate the ADS with smaller sub-criticality margins. In order to optimise the core's performance, the choice of materials and the design of the core lattice are most decisive. Therefore, in the next sections we will treat neutronic, safety and burnup characteristics of different core and fuel designs in order to arrive into an optimised core design, as presented in Chapter 7 and **Paper II**. What follows below is a summary of the results presented in the appended papers.

6.2 Source efficiency

The balance of neutrons in a neutron multiplying system without an external source is described by a homogeneous Boltzmann transport equation

$$A\phi = F\phi \tag{6.3}$$

where F is the production operator in matrix form, A is the consumption operator in matrix form, and $\phi \equiv \phi(\vec{r}, \vec{\Omega}, E, t)$ denotes the neutron flux. In a system with an external neutron source, the neutron balance equation reads as

$$A\phi = F\phi + S, \tag{6.4}$$

where $S = S(\vec{r}, \vec{\Omega}, E, t)$ is the spatial distribution of the external neutron source.

In the sub-critical state, the effective multiplication coefficient k_{eff}, which is the largest positive eigenvalue of the homogeneous transport equation

$$A\phi = \frac{1}{k_{\text{eff}}} F\phi \tag{6.5}$$

does not describe the true physical state and actual neutron multiplication in the system.

Rather, the multiplication characteristics of system should be expressed in terms of a number of neutrons released in the multiplication reactions *per source particle*. The multiplication of spallation neutrons exiting target can be evaluated either as

$$M_{\text{ext}}^{\text{n}} = 1 + k_0 + k_0 \cdot k_1 + k_0 \cdot k_1 \cdot k_2 + \cdots \tag{6.6}$$

where k_0 is the external source neutron multiplication factor, and k_i $(i > 0)$ is the generation dependent multiplication factor, or estimated in terms of fission multiplication as

$$M_{\text{ext}}^{\text{f}} = 1 + \bar{\nu} N_{\text{f}} \ , \tag{6.7}$$

where $\bar{\nu}$ is the average number of neutrons emitted per fission, and N_{f} is the number of fissions per source particle.

The resulting difference in neutron multiplication is then often parameterised in terms of the neutron source efficiency ϕ_{i}^{*}, normalising the $M_{\mathrm{ext}}^{\mathrm{f}}$ and $M_{\mathrm{ext}}^{\mathrm{n}}$ per source *neutron* as

$$\phi_{\mathrm{i}}^{*} \equiv \frac{M_{\mathrm{ext}}^{\mathrm{i}} - 1}{M_{\mathrm{fiss}} - 1} \quad \mathrm{i} = \mathrm{f}, \mathrm{n} \tag{6.8}$$

where the fundamental mode multiplication is given by

$$M_{\mathrm{fiss}} = \frac{1}{1 - k_{\mathrm{eff}}} \tag{6.9}$$

The neutron source efficiency is thus a parameter, which describes the difference between the real external source multiplication and the multiplication inherent to the distribution of neutrons corresponding to the fundamental mode.

Then we can, equivalently to $\mathrm{k_{eff}}$, define the source multiplication coefficient as

$$k_s = \frac{\overline{\nu} N_f}{1 + \overline{\nu} N_f} \tag{6.10}$$

The generation dependent multiplication factors k_{i} can be found by running MCNP [59] in KCODE mode, and extracting the track length estimate of k_{i} for individual fission generations. An example of the resulting generation dependence is shown in Figure 6.1 for a model $(\mathrm{U,Th})\mathrm{O_2}$ fuelled lead-cooled ADS [151].

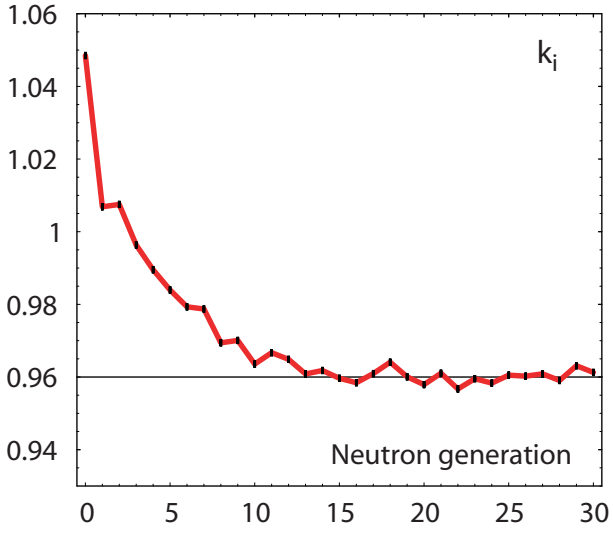

Figure 6.1. Generation dependent multiplication factor $\mathrm{k_i}$.

As can be seen, the first 10-12 generations are subject to significantly lower neutron losses than in the asymptotic limit (fundamental mode). This can be partially attributed to the probability of a fission neutron to enter the spallation

target, where it is allowed to decelerate, avoiding capture in cladding materials and fertile actinides, and then to enter the core again, with a high probability of inducing (epithermal) fission in fuel. Since the first few k_{i}:s may be larger than unity, even for deeply sub-critical systems, this phenomenon enhances the power peaking in the vicinity of the target, and was carefully analysed in design and safety studies of systems with liquid metal coolant/target.

On the other hand, spallation neutrons can also slow down or are absorbed in the target media before entering the core. Thus, *for thick targets*, the probability of spallation neutron induced fission would be smaller than for the average fission neutron and $k_0 < k_{\mathrm{i}}$.

By introducing k_0, the physical model of a neutron chain propagation in the system can be conveniently separated into the *source* and *fission* parts. Such decomposition of a neutron multiplication is a practical tool for scoping calculations while simulations of a whole neutron cascade are inevitable in order to determine the value of the source efficiency.

The neutron source efficiency ϕ^* generally depends on the position of the neutron source and the dimensions and material composition of the reactor core and target. Thus, a comparison of the performance of different ADSs in terms of source efficiency can be done only for systems with the same target/blanket geometry. A novel concept of the proton source efficiency was therefore developed in **Paper V**. The proton source efficiency ψ^* of a sub-critical system may be defined as

$$\psi^* \equiv \frac{M_{\mathrm{ext}}^{\mathrm{p}} - 1}{M_{\mathrm{fiss}} - 1} = \frac{P\overline{\nu}}{\overline{Q}S_{\mathrm{p}}} \frac{1 - k_{\mathrm{eff}}}{k_{\mathrm{eff}}} \tag{6.11}$$

where $M_{\mathrm{ext}}^{\mathrm{p}}$ is the actual multiplication of source spallation neutrons per source *proton*, P is the thermal power of the system, and $\overline{Q}$ is the averaged recoverable energy released in fission.

We have shown that the relationship between neutron source efficiency ϕ^* and proton source efficiency ψ^* is then given by

$$\phi^* = \frac{M_{\mathrm{ext}}^{\mathrm{i}} - 1}{M_{\mathrm{fiss}} - 1} = \psi^* \frac{S_{\mathrm{p}}}{S_{\mathrm{n}}} = \frac{\psi^*}{Z} \quad \mathrm{i} = \mathrm{f}, \mathrm{n} \tag{6.12}$$

where S_{n} is the neutron source intensity [n/s], and $Z = S_{\mathrm{n}}/S_{\mathrm{p}}$ is the number of neutrons per proton (neutron spallation yield).

Consequently, the ADS accelerator current can be determined from

$$I_{\mathrm{p}} = \frac{e\overline{\nu}(1/k_{\mathrm{eff}} - 1)}{\psi^*} \frac{P}{\overline{Q}} \tag{6.13}$$

where $e = 1.609 \cdot 10^{-19}$ C is the elementary charge.

In our parametric, scoping studies, the source efficiency was studied as a function of target radius and axial position of the accelerator beam. We considered a single Pb/Bi target module located in the centre of the core and contained in a 5 mm

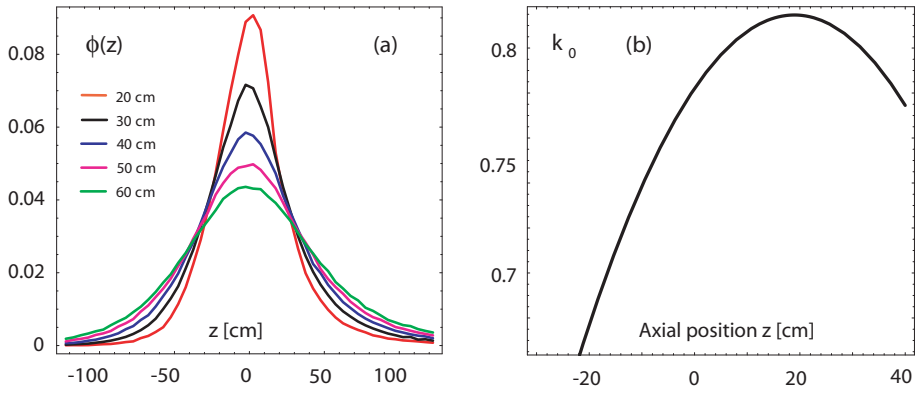

Figure 6.2. The axial distribution of normalised neutron flux exiting target of a given radius (a). The external source multiplication factor k_0 as a function of beam impact relative to the core centre (b).

thick ferritic steel container. Beam tube radius was 15 cm. The incident proton energy was set to 1 GeV, which is approximately the level where increasing the energy does no longer increase the effective neutron yield per energy unit. The simulations were performed with the Monte Carlo code MCNPX [152] using the LA150 cross-section library.

6.2.1 Axial position of beam impact

The optimal relative axial position of the spallation target beam impact was investigated in terms of minimising leakage of neutrons to axial reflectors. Leaked neutrons have lower probability to enter the reactor core and, consequently, induce fission. The neutron leakage is minimised when the target surface was placed 17.6 cm above the core centre for a radius of 20 cm, while for R = 50 cm, the optimal position is z = 19.7 cm, see Figure 6.2(a). The slight shift of the optimal position can be attributed to enhanced diffusion of neutrons in the target material.

In more detailed studies, performed in **Paper V** aiming at maximising the proton source efficiency, the optimal shift of axial position of the target beam impact from the core centre was found to be also ∼20 cm. In Figure 6.2(b), the corresponding external neutron multiplication factor k_0 is shown.

The total number of neutrons leaking out of the target without entering the core is shown in Figure 6.3. Considering a typical active core length of 100 cm, about 8.5% of the neutrons leak outside the core (2.6% in the forward, 5.9% in the backward direction), which is to be compared to the 25.6% in the case of target radius of 50 cm (forward 10.8%, backward 14.8%). More than 95% of the neutrons enters the core when the fuel pin length is larger than 1.3 m, for the 50-cm target the corresponding figure is 2.1 m. This would suggest increasing the height of the fissile column in order to maximise the source efficiency. However, thermal

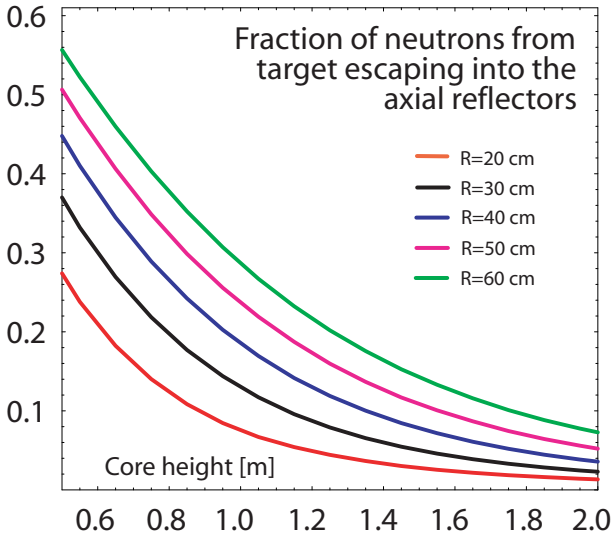

Figure 6.3. The fraction of neutrons not directly entering the reactor core as function of active pin length. R is the radius of the spallation target.

hydraulic constraints and deterioration of the void worth disqualify the choice of extensive core heights [153].

6.2.2 Target radius

The spectrum of neutrons escaping the target has been determined for five different target radii, see Figure 6.4. An increase of target radius implies an increase of probability for axial leakage of neutrons, which diminishes the chances of neutrons to induce fission in the core. At the same time, the absorption of neutrons in the target and core increases as neutrons subsequently slow down. The median energy of neutrons exiting the target thus drops from 1020 keV to 730 keV as target radius is increased from 20 cm to 30 cm. Remembering that fission neutrons are born with a mean energy of about 2 MeV, it is clear that the neutron source efficiency may fall well bellow unity for targets of any reasonable size, i.e., $k_0 < k_\mathrm{i}$. Only 0.4% neutrons are above 20 MeV in the case of the 50 cm target radius and 3.2% in the case of a 20 cm radius.

We conclude that a small target radius is favourable not only from the viewpoint of gaining fast neutron spectra but also for minimising neutron losses to the axial reflector, both effects yielding higher source efficiency.

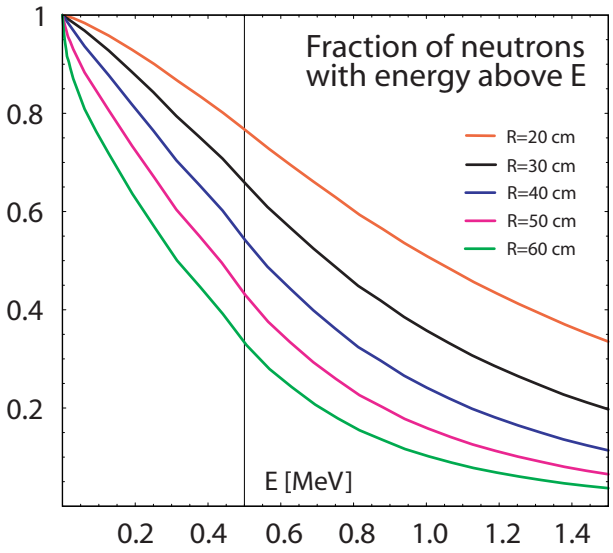

Figure 6.4. Fractions of source neutrons having energies above E when exiting a Pb/Bi target of different radii. With increasing target radius, the probability of source neutrons to induce fission sharply decreases. Figure adapted from **Paper II**.

6.2.3 Coolants

The external neutron multiplication was also estimated for different Pb/Bi-target radii of the Pb/Bi and Na-cooled ADSs. In **Paper IV**, scoping calculations were performed for a radially infinite lattice, see Figure 6.5, while **Paper V** investigated a realistic 3-D configuration of a TRU ADS burner.

Both studies showed that Pb/Bi-cooled systems yield higher source efficiency. The reason is mainly the contribution from (n,xn) reactions which occur in Pb/Bi. For smaller target radii, there is still an appreciable number of neutrons (about 6%) able to induce (n,2n) reactions in lead (threshold energy is ~ 7 MeV). Together with decreased neutron axial leakage in Pb/Bi in comparison to Na, Pb/Bi system yields higher source efficiency than Na-cooled counterpart. However, as the target radius increases, the fraction of the high-energy neutrons entering the core would decrease, and both Pb/Bi and Na-cooled ADS would have similar source efficiencies.

6.3 Neutronic performance

ZrN, HfN, YN, and BN have been investigated in **Paper II** as candidate diluent matrices for TRU ADS burner, see Table 6.1. Performance of fertile matrices (UN,

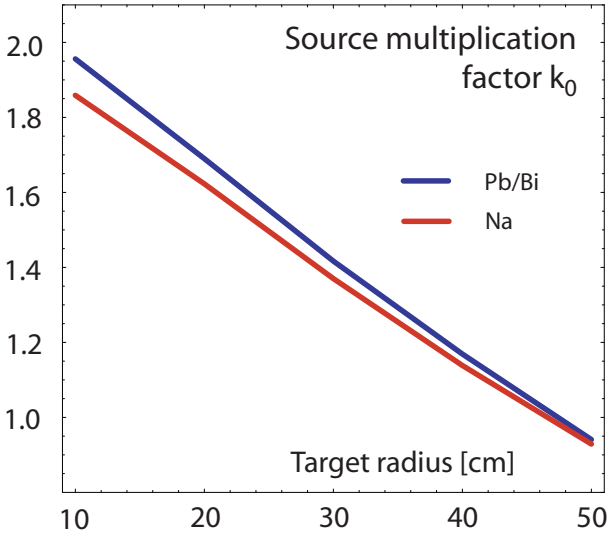

Figure 6.5. The external source multiplication factor k_0 as function of target radius for a model infinite lattice of TRU ADS cooled by lead/bismuth and sodium. Nitride fuel without a diluent matrix was applied. P/D = 1.7. Figure redrawn from **Paper IV**.

Fuel	E_{n} [keV]	E_{ϕ} [keV]	ψ^*	^{241}Am $\sigma_{\mathrm{f}}/\sigma_{\mathrm{a}}$
(TRU,Zr)N	87.4	396	29.7	0.104
(TRU,Hf)N	201	524	28.2	0.196
(TRU,Y)N	89.9	398	28.6	0.106
(TRU,B)N	407	811	25.2	0.376
(U,TRU)N	138	438	28.9	0.136
(Th,TRU)N	157	477	28.7	0.161
(U,Pu)N	121	416	28.6	0.121
(Pu,Zr)N	63.7	358	30.8	0.080
(TRUMOX,Zr)N	82.5	384	28.7	0.098
(TRUMOX,Hf)N	195	514	27.7	0.190
(MA,Zr)N	176	515	26.4	0.183

Table 6.1. Number (E_{n}) and flux (E_{ϕ}) weighted spectra average energies, proton source efficiencies (ψ^*), and fission probabilities of ^{241}Am in single zone ADS cores with P/D=1.6. Table is adopted from **Paper II**.

ThN) was also evaluated. Different types of TRU vectors were used in the simulations, denoted as TRU (Pu/Am = 4/1) and TRUMOX (Pu/Am = 0.86/0.14). Values for MA ADS burners working in the frame of a double-strata scenario (Pu/Am

ratio equal to 2/3) are also given. One-zone, homogeneous core configurations were used in order to facilitate a systematic comparison of different design options. In each case, the volume fraction of diluent matrix were adjusted to obtain k_{eff}=0.96. The calculations were performed by the Monte Carlo code MCNP [59]. JEF-2.2 nuclear data library was processed with NJOY [154] in order to account for temperature dependence. See **Paper II** for a detail description of the calculation model.

It appeared that the inert diluent matrices as ZrN and YN significantly moderate the neutron spectrum by inelastic neutron scattering, which results in low probabilities for direct fissioning of ^{241}Am. The use of fertile matrices in the fuel yields slightly harder neutron spectrum due to increased absorption in the resonance and thermal regions, which also somewhat improves $\sigma_{\text{f}}/\sigma_{\text{a}}$ for ^{241}Am. Hardening of the neutron spectra due to increased competing absorption in the even-neutron number/fertile actinides is also apparent when comparing values for (U,Pu)N with (U,TRU)N and (Pu,Zr)N with (TRU,Zr)N. BN-based fuels proved to be most efficient in suppressing slow neutron capture in americium, raising the fission probabilities of ^{241}Am to *0.38*. Another absorbing matrix, HfN, increased the ^{241}Am fission-to-absorption probability twice in comparison to ZrN. Hence, understandably, operating the reactor on a fast neutron spectrum is beneficial for limiting MA inventories in the fuel cycle.

In TRUMOX-based fuels, the fraction of strongly absorbing americium isotopes is actually lower than in TRU fuel, due to shorter cooling times than assumed for LWR UOX discharges. TRUMOX gives a slightly softer spectrum and thus also lower ^{241}Am fission probabilities. At the same time, due to the lower quality of the plutonium vector, the fraction of even-neutron number nuclides in TRUMOX fuel is higher, both effects resulting in diminished proton source efficiency.

For fertile matrices (ThN and UN), the source efficiency is slightly lower than for (TRU,Zr)N fuel. The reason is larger probability of parasitic absorption of spallation neutron in fertile matrices than in ZrN (macroscopic absorption cross-section for UN is roughly a factor of eight higher than for ZrN). Absorption of neutrons in BN causes a significant drop of the source efficiency. Interestingly, HfN does not seriously deteriorate the multiplication of source neutrons in the system, keeping ϕ^* well above unity ($\psi^* \sim 28$).

In **Paper IV**, the external source multiplication factor k_0 was investigated as a function of ZrN, UN and B_4C content in the sodium cooled TRU ADS core. Similarly to results obtained in **Paper II**, (TRU,Zr)N fuel provided better multiplication of the source neutrons than (U,TRU)N. B_4C absorbs neutrons very efficiently and gave significantly lower value of the source multiplication factor. The source efficiency of TRUN-fuelled, Pb/Bi-cooled ADS employing B_4C neutron absorber appeared to be very low. **Paper III** reports a value of $\phi^* \sim 0.85$ that corresponds to $\psi^* \sim 22{-}23$.

6.4 Safety performance

In **Papers I** and **II** we have investigated the reactivity changes upon the introduction of the coolant void reactivity into the reactor cores, both critical and sub-critical, fuelled with oxide and nitride fuels and cooled by liquid metals - lead/bismuth eutectic, lead, and sodium.

6.4.1 Coolant void worth

The coolant void worth is given as the difference in the k-eigenvalue between the flooded and voided states

$$W = \quad \Delta k_{\text{eff}} = k_{\text{eff}}^{\text{void}} - k_{\text{eff}}^{\text{flood}} = \overline{\nu}_{\text{void}} L_{\text{f}}^{\text{void}} - \overline{\nu}_{\text{flood}} L_{\text{f}}^{\text{flood}}. \tag{6.14}$$

where L_{f} is neutron loss to fission in one neutron generation for the respective core state - flooded or voided.

The average fission neutron yield can be considered as constant ($\overline{\nu} \equiv \overline{\nu}_{\text{flood}} \simeq \overline{\nu}_{\text{void}}$) in fast neutron systems. Therefore,

$$W = \overline{\nu}\ (L_{\text{f}}^{\text{void}} - L_{\text{f}}^{\text{flood}}), \tag{6.15}$$

which gives $W = \overline{\nu}\Delta L_{\text{f}}$.

Normalising the neutron balance equation in an eigenstate for *one neutron fission generation* we obtain

$$1 + C_{\text{x}} - L_{\text{x}} = L_{\text{c}} + L_{\text{e}} + L_{\text{f}}, \tag{6.16}$$

where L_{x} denotes the neutron loss rate in non-fission multiplication reactions, $C_{\text{x}} = \overline{\nu_{\text{x}}} L_{\text{x}}$ is the neutron creation rate in non-fission multiplication reactions, $\overline{\nu_{\text{x}}}$ is the average neutron yield in non-fission multiplication reactions ($\overline{\nu_{\text{x}}} \simeq 2$), L_{e} denotes the loss rate to leakage, L_{c} the loss rate to capture reactions, and L_{f} is the loss rate to fission.

Upon coolant voiding, $\Delta C_{\text{x}} \leq 10^{-3}$ in most of the cases. The coolant void worth can be subsequently decomposed in the infinite pin lattice 2-D model ($L_{\text{e}} = 0$) as

$$W = \overline{\nu} \cdot \Delta L_{\text{f}} = -\overline{\nu}(\Delta L_{\text{c}}^{\text{fuel}} + \Delta L_{\text{c}}^{\text{coolant}} + \Delta L_{\text{c}}^{\text{clad}}). \tag{6.17}$$

where $L_{\text{c}}^{\text{fuel}}$, $L_{\text{c}}^{\text{coolant}}$, and $L_{\text{c}}^{\text{clad}}$ is neutron capture rates to fuel, coolant, and cladding, respectively.

The neutron balance equation was further evaluated in realistic three dimensional core configurations, where the system geometry also included reflectors and plena. The void worth was then determined as

$$W = \quad -\overline{\nu}(\Delta L_{\text{c,fuel}} + \Delta L_{\text{c,coolant}} + \Delta L_{\text{c,clad}} + \tag{6.18}$$

$$\Delta L_{\text{e}} - \Delta G_{\text{x}}), \tag{6.19}$$

where L_{e} quantifies a rate of neutron leakage from the system, and $G_{\text{x}} = C_{\text{x}}$ - L_{x} is the neutron gain from non-fission multiplication reactions. Note that $G_{\text{x}} < 10^{-3}$.

Fuel − Coolant	ΔL_{f}	$\Delta L_{\mathrm{c,fuel}}$	$\Delta L_{\mathrm{c,cool}}$	$\Delta L_{\mathrm{c,clad}}$	$(\frac{\sigma_{\mathrm{f}}}{\sigma_{\mathrm{a}}})_{\mathrm{voided}}/(\frac{\sigma_{\mathrm{f}}}{\sigma_{\mathrm{a}}})_{\mathrm{flooded}}$
(U,Pu)O_2 − Na	+0.078	-0.059	-0.012	-0.007	1.20
(TRU,Zr)N − Na	+0.108	-0.090	-0.011	-0.007	1.22
(MA,Zr)N − Na	+0.119	-0.111	-0.005	-0.003	1.33
(TRU,Zr)N − Pb/Bi	+0.090	-0.039	-0.048	-0.003	1.11

Table 6.2. Infinite pin lattice void worth analyses. Pitch-to-diameter ratio is 2.0. The neutron loss rates are normalised per one fission neutron generation. Table redrawn from **Paper I**.

Infinite lattice analyses

The infinite lattice analysis, the effect of the spectrum hardening and changes in the neutron capture upon the coolant voiding was investigated for three types of fuels: standard FBR fuel (U,Pu)O_2, a plutonium based - TRU mononitride fuel (TRU,Zr)N, and minor actinide based ADS double strata fuel (MA,Zr)N, see **Paper I** for details. The results of the study decomposed into individual components are summarised in Table 6.2.

A reduction in fuel capture rate with concurrent increase of fission probability of even-neutron number actinides appeared to be the main contributor to the void worth. While capture reduction in the fuel provides about 76% of the void worth for (TRU,Zr)N fuel, it is more then 93% for the fuel containing 60% of minor actinides, i.e., (MA,Zr)N. The spectral gradient accompanying removal of the coolant from the lattice is also strongest for (MA,Zr)N fuel due to the significant increase of fission probabilities of the even-neutron number nuclides. The capture rate in the cladding is less significant and constitutes less than 10% of the void worth. Comparison of the sodium and Pb/Bi coolant void worths for (TRU,Zr)N fuel shows that Pb/Bi provides *smaller* spectral gradient upon coolant voiding limiting the change in the probability of neutrons being captured in fuel, which gives lower void worth.

3-D system analyses

Investigating the coolant void worth in realistic 3-D system configurations illustrates the influence of leakage effect upon coolant removal. Note that in contrast to the standard notion of the leakage term [32], L_{e} in our case denotes the neutrons leaking out of the *whole reactor system* to the surrounding shielding. The probability of these neutrons to enter the core and induce fission is rather remote and the reason why we list the leakage component separately in our study is merely phenomenological. Such neutrons can hence be effectively perceived as captured in the cladding and structural material of the reflector. The effect of the enhanced neutron leakage *from the core* upon coolant voiding is then exhibited as a change in the capture of neutrons in coolant and structural material of plena and reflectors.

Coolant	ΔL_{f}	$\Delta L_{\mathrm{c,fuel}}$	$\Delta L_{\mathrm{c,cool}}$	$\Delta L_{\mathrm{c,clad}}$	ΔL_{e}
Na	Core void worth, $(U,Pu)O_2$				
	+0.0071	-0.0908	+0.0265	+0.0428	+0.0156
	Core & upper plenum void worth, $(U,Pu)O_2$				
	-0.0166	-0.1282	+0.0471	+0.0397	+0.0598
	Core void worth, (TRU,Zr)N				
	-0.0102	-0.0839	+0.0205	+0.0524	+0.0214
Pb/Bi	Core void worth, radial reflector with steel pins, $(U,Pu)O_2$				
	+0.0114	-0.0709	-0.0129	+0.0677	+0.0039
	Core void worth, Pb/Bi radial reflector, $(U,Pu)O_2$				
	+0.0216	-0.0555	+0.0124	+0.0060	+0.0163
	Core void worth, radial reflector with steel pins, (TRU,Zr)N				
	-0.0226	-0.0650	-0.0104	+0.0903	+0.0060

Table 6.3. Void worth analyses in a model FBR and ADS, employing $(U,Pu)O_2$ and (TRU,Zr)N fuel, respectively. Pitch-to-diameter ratio is 2.0. $\Delta L_{\mathrm{c,clad}}$ includes capture in the structural material of the reflectors. Results according to **Paper I**.

In contrast to the infinite pin lattice analyses the changes in the capture probability in cladding introduces therefore a *negative* reactivity upon coolant voiding. In the case of the Pb/Bi-cooled core, we investigate two different radial reflector configurations

a) similar to the one used for sodium cooled systems, i.e. consisting of steel pins, immersed in the coolant; coolant volume ratio being 20 vol%,

b) with the whole radial reflector region filled by lead/bismuth eutectic only. Such radial reflector configurations have been proposed in a number of studies [108].

In Table 6.3, we display the coolant void worth for a model FBR with $(U,Pu)O_2$ fuel and an ADS employing (TRU,Zr)N fuel cooled by sodium and lead/bismuth (P/D = 2.0). Three (interconnected) results are interesting here. First, the Pb/Bi void worth for $(U,Pu)O_2$ fuel is actually *larger* than that of sodium-cooled system for realistic Pb/Bi pitches ($P/D \gtrsim 1.4$), see also Figure 6.8. Due to the better neutronic characteristics of Pb/Bi, the fraction of uranium in the (U,Pu) vector is higher than that for sodium. Hence, during coolant voiding, the spectral gradient becomes more pronounced in Pb/Bi due to higher content of fast fission thresholds isotopes in fuel, resulting in higher void worths. Second, varying the fraction of whole TRU vector in (TRU,Zr)N fuel leads to the opposite effect for the void worths of the respective coolants, as the inert matrix fraction is larger in the Pb/Bi system than for the Na-counterpart. Third, the negative reactivity feedback is supplied in Pb/Bi systems by the increase of neutron capture in the *structural material of reflector* only, while in the case of sodium, the capture in both reflector

coolant and structure introduces negative reactivity. When the steel pin reflector is replaced by Pb/Bi, the only significant effect on negative reactivity feedback is the increased neutron capture in coolant and surrounding reactor shielding material (manifested in our study as an increased leakage term L_e), resulting in excessive void reactivities. Introducing an absorbing material into the core reflector in order to increase the neutron capture upon coolant voiding would consequently also reduce void worth [155].

An extension of the coolant void worth study for a Pb/Bi-cooled, nitride fuelled ADS with different types of the diluent and fertile matrix fuels was performed in **Paper II**. A brief description of the modelling approach was given in Section 6.3. The high sensitivity of the void worth on the content of americium in the fuel was again shown: compare the core coolant void worths for (TRU,Zr)N and (Pu,Zr)N, which are −4300 and −7000 pcm, respectively. MA-based fuel again yielded very high positive void worth, of the order of +8000 pcm.

6.4.2 Cladding worth

At accidental conditions, melting of cladding may result in flush-out of structural material from the core, inserting a positive reactivity due to the decreased parasitic absorption in steel. The corresponding effect was calculated in **Paper II** by substituting pin cladding with coolant.

Again, the highest positive reactivity increase was observed for absorbing matrices and fuels with large content of even-neutron number actinides. For (MA,Zr)N, the cladding flush-out results in an extensive reactivity insertion larger than 5000 pcm. Thus, optimisation of the cladding (and duct) thickness is the imperative in order to improve the safety of the ADS cores.

Consider that in our heterogenous core designs employing 2.5-mm thick duct, the cladding void worth was elevated by about +2800 pcm when larger amount of the structural material was introduced to the system by decreasing the sub-assembly flat-to-flat from 18.3 cm to 10.8 cm (**Paper II**).

6.4.3 Reactivity temperature feedbacks

Reactivity temperature coefficients were investigated in detail in **Paper II** for the same set of fuel compositions as described in Section 6.3.

Coolant reactivity feedback

The coolant reactivity temperature coefficient was investigated by varying the Pb/Bi density in the reactor core from 10 g·cm^{-3} to 9 g·cm^{-3}, corresponding to a temperature change from 810 to 1540 K. Density of Pb/Bi as a function of temperature is shown in Figure 6.6 [50]. Sodium and lead values are given as a reference.

In summary, a strong negative feedback was understandably exhibited by fertile-free fuels with inert diluent matrices (ZrN and YN). Addition of fertile elements

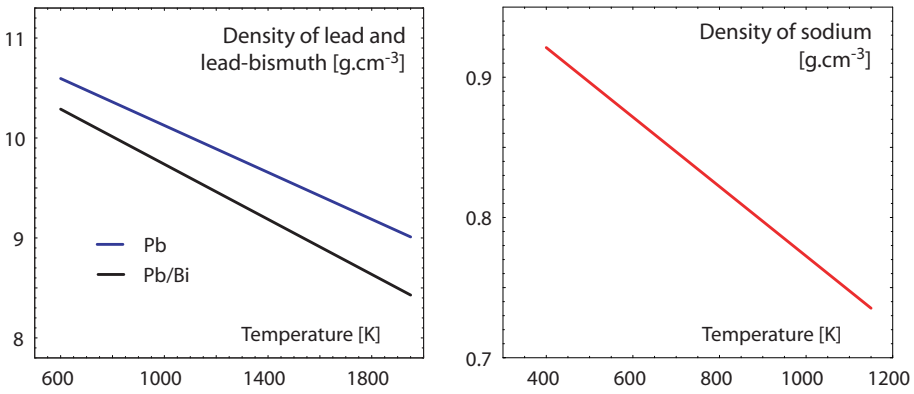

Figure 6.6. Coolant density as a function of temperature for liquid metal coolants - Pb, Pb/Bi and Na.

and/or employment of absorbing matrices elevates the coolant temperature reactivity feedback, which becomes positive. The effect of coolant voiding in high minor actinide content cores is further pronounced by the increased reactivity worth of americium being more significant than that of ^{238}U, see fast fission thresholds in Figure 3.2. Similarly, due to the spectral hardening during coolant temperature increase, the parasitic capture in absorbing materials as BN is significantly diminished, resulting in very large reactivity insertion.

Material dilatation

The system response to material dilatation was calculated for two distinctive events - axial dilatation of the fuel column, providing prompt reactivity feedback, and the expansion of the core lattice grid, providing somewhat delayed response to the fuel temperature changes. We assume that the thermal dilatation of the core components was not restricted.

The system response to the **axial fuel expansion** was calculated by increasing the pin length by 1 cm. In the case of ZrN and HfN-based fuels it corresponds to a temperature change from 1000 to 2070 K and from 1000 to 2050 K, respectively. The resulting reactivity coefficients were then -0.21 pcm/K for (TRU,Zr)N and -0.19 pcm/K for (TRU,Hf)N. For other types of fuels the axial expansion temperature feedback was in the interval from -0.18 to -0.28 pcm/$(10^{-5}\Delta H/H)$.

The reactivity change due to expansion of the **core lattice grid** was calculated by increasing the lattice pitch by 2%. For all fuels investigated, the reactivity change was rather similar, being in the range from -0.35 to -0.47 pcm/$(10^{-5}\Delta P/P)$. As expected, the grid expansion gives about a factor of two larger temperature feedback than axial elongation of the fuel (Chapter 3).

Doppler temperature reactivity

The Doppler reactivity coefficient is considered as "prompt" feedback, almost instantly following changes in the fuel temperature. In fuels with fertile support, the strongest Doppler was provided by fuels with ^{238}U and ^{232}Th matrices. In U/Th-free fuels, the largest contributor was apparently ^{240}Pu. A negative effect of the absorber material or americium on the fuel reactivity feedback was again revealed. As these materials compete with resonant capture on ^{240}Pu, a sharp cut-off in the spectrum below 1 keV may further suppress the Doppler feedback. Substituting Zr with Hf or mixing Am into the fuel thus decreases the Doppler constant by more than a factor of three. In the BN-bearing fuels, Doppler feedback is completely non-existent.

6.4.4 Effective delayed neutron fractions

Comparing individual core design configurations in **Paper II**, the highest effective delayed neutron fractions were observed for (U,TRU)N fuel, where the major contributor to β_{eff} is ^{238}U. When uranium is removed from the fuel, β_{eff} can be partly regained by introduction of ^{232}Th, or in fuels with soft spectrum, by large fractions of ^{242}Pu. Since a significant fraction of delayed neutrons is rather absorbed in ^{10}B than inducing fission, BN-based fuels provide very low β_{eff}. For (TRU,Hf)N fuel, β_{eff} is ∼160 pcm, which is 82% of the value observed for (TRU,Zr)N fuel or about one-half of β_{eff} for the CAPRA 04/94 core.

6.5 Burnup performance

Following the static analyses of neutronic and safety performance of different fuels for TRU ADS, we investigated their burnup merits. A summary of the results is presented in Table 6.4.

In the case of (U,Pu)N fuel, breeding of ^{239}Pu from ^{238}U somewhat diminishes the burnup reactivity swing. However, it is interesting to note that an admixture of 20% americium in the TRU vector significantly reduces reactivity burnup loss due to the production of additional plutonium via

$$^{241}\text{Am} + \text{n} \;\rightarrow (\sim 80\%)\; ^{242g}\text{Am} \;\rightarrow\; ^{242}\text{Cm} \;\rightarrow\; ^{238}\text{Pu}$$

channel, compare results for (U,Pu)N with (U,TRU)N. Actual burnability of the absorbing matrices (HfN & BN) showed to be questionable, as the reactivity swing per percent burnup appeared to be *larger* for these fuels than for inert diluents. In the faster spectrum, capture in fertile nuclides is suppressed leading to decreased production of fissile isotopes. A similar observation was also made by Yang & Khalil [43]. The 25% decrease in the reactivity swing as reported in **Paper III** for our TRU ADS design with a neutron absorber (B_4C) is therefore due to the introduction of uranium into the core, rather than due to burnability of boron carbide pins.

Fuel	m_{act}^{BOL} [kg]	Burnup rate [%FIMA/fpd]	$\Delta k_{eff}^{c}/\beta_c$ [pcm/%]	$^{242}Cm/\beta_c$ [%/%]	Doubling of I_p [fpd]
(TRU,Zr)N	942	0.076	-750	0.20	60
(TRU,Hf)N	1751	0.043	-780	0.12	115
(TRU,Y)N	919	0.078	-750	0.18	65
(TRU,B)N	2900	0.027	-780	0.06	190
(U,TRU)N	5513	0.014	-230	0.07	>1000
(Th,TRU)N	4810	0.016	-330	0.08	≈const
(U,Pu)N	5525	0.014	-690	0.001	300
(Pu,Zr)N	631	0.116	-930	0.002	40
(TRUMOX,Zr)N	950	0.078	-930	0.11	55
(TRUMOX,Hf)N	1822	0.042	-870	0.07	105

Table 6.4. Burnup characteristics of different single zone ADS cores with P/D=1.6. $\Delta I_p = I_p^{EOC} - I_p^{BOC}$. The reactivity swing and ^{242}Cm fractions per percent FIMA burnup are given for 5% FIMA. Table is adopted from **Paper II.**

On the other hand, the absorbing matrices perform well when it comes to the task of limiting the amount of minor actinides in the spent fuel. The fraction of ^{242}Cm in the actinide vector is almost halved when ZrN matrix is exchanged for HfN in the case of transuranics fuel. Using BN is even more effective in cutting the thermal parts of the spectra thus promoting *direct* fissioning of americium.

The accelerator power swing is one of the decisive factors limiting the effective length of one irradiation batch. The thermal constraints imposed by the cladding material (power peaking) and target module (ability to dissipate heat from the accelerator beam) play the major role. The accelerator power is doubled in about two full power months for (TRU,Zr)N, while for (TRU,Hf)N fuel it is in approximately 115 full power days. Use of the fertile material can notably prolong the length of the batch, but on the other hand, also effectively destroys the transmutation capability of the reactor, significantly diminishing burnup rates.

6.6 Influence of increased pitch-to-diameter ratio

The effect of large coolant fractions on the neutronics, safety, and burnup performance of the burner was investigated in **Paper I** and **Paper II** by varying reactor lattice pitch-to-diameter ratios between 1.2 and 2.4 corresponding to a change of coolant volume fractions from 37% to 84%. Due to the enhanced heat removal capabilities, the safety margins and grace time to fuel and cladding damage increase at transients (beam overpower, loss-of-flow, and loss-of-heat sink). The obvious drawback of the large volume fractions is, however, an increase in the neutron leakage, adversely affecting neutron economy and higher specific fuel inventories as the

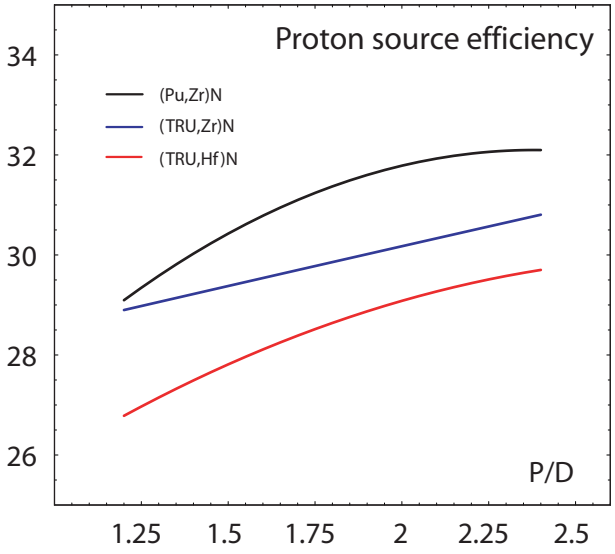

Figure 6.7. The proton source efficiency ψ^* as a function of P/D in Pb/Bi-cooled single zone ADS. Figure is adopted from **Paper II.**

amount of the diluent matrix has to be decreased in order to keep the reactivity constant.

6.6.1 Source efficiency

The proton source efficiency was calculated as a function of P/D in **Paper II**. Non-intuitively, the source efficiency increases as a function of P/D, see Figure 6.7. This phenomenon is a result of the mutual interplay of three processes. First, the actinide fuel fraction in the fuel is larger for increased P/D which elevates the neutron absorption probability in fuel. Second, the probability of the fission chain to be accommodated within the core increases with increasing core dimensions. Third, the difference in the neutron spectra of the source and eigenmode neutrons increases with P/D (remember: $\phi^* > 1$).

In **Paper IV**, we reported a *decrease* of the external source multiplication coefficient k_0 while increasing P/D, for both sodium and Pb/Bi. However, in contrast to the modelling approach applied in **Paper II**, the amount of the inert matrix was **not** adjusted in order to keep constant reactivity. The results presented there hence illustrate the sole effect of the spectrum thermalisation with a consequent decrease in fission-to-absorption probabilities due to the increased pin pitches leading to the gradual decrease of k_0 with increasing P/D. We again remind the reader that the external source multiplication factor k_0 does not describe the real multiplication

in the system and our results are to be seen merely in terms of comparison of the performance of the two coolants, Pb/Bi and sodium.

6.6.2 Coolant void and cladding worth

As the spectral effect (reduced capture in fuel) is a major contributor to the positive reactivity insertion during coolant voiding, the appropriate choice of heavy metal coolants (Pb, Pb/Bi) or low density gas coolants (He, steam) might somewhat alleviate the void worth. Understandably, the void worth is not only a function of coolant, but also of the type of fuel applied in the system and the lattice geometry. While lead-alloy coolants would be a favourable choice to reduce void worth for $(U,Pu)O_2$ fuel for small P/Ds only, see Figure 6.8, the choice of Pb/Bi appeared to be preferable for the transmutation related fuels as (TRU,Zr)N and (MA,Zr)N in the whole range of realistic P/Ds. Details are presented in **Paper II**.

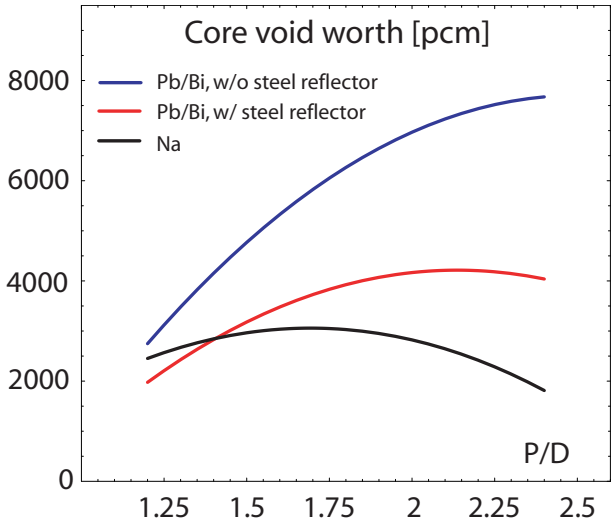

Figure 6.8. Coolant void worth in a critical FBR employing $(U,Pu)O_2$ fuel. The $Pu/(U + Pu)$ ratio was varied with P/D in order obtain $k_{\text{eff}} \sim 1$, for Na in the range between 17% and 33%, for Pb/Bi without steel pin reflector between 16% and 26%, and in the case of Pb/Bi with steel reflector between 17% and 27%. Figure adapted from **Paper I.**

Enlarging the pin lattice in order to reduce the void worth can prove successful only in systems with inert matrix fuel, see Figure 6.9. In cores with a significant amount of fertile isotopes and/or with substantial presence of absorbing materials, the coolant void worth is significantly elevated due to the increased spectral hardening which accompanies larger P/D. The cladding worth appeared to be a decreasing function of the lattice pitch. The parasitic absorption in the structural

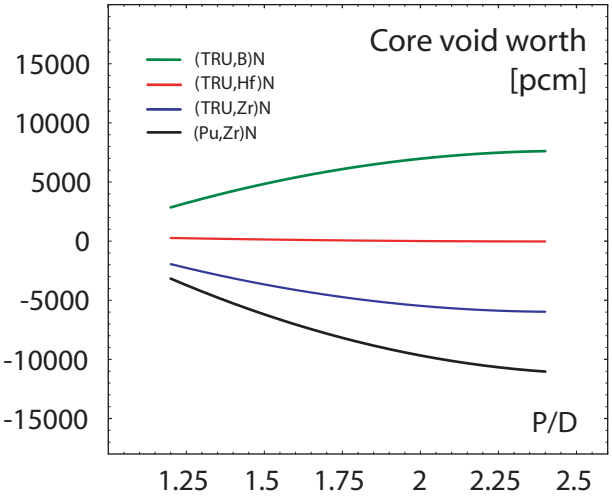

Figure 6.9. Core void worths in Pb/Bi-cooled TRU burners. Introduction of strongly absorbing materials to the fuel has an adverse effect on the coolant void reactivity. Figure redrawn from **Paper II**.

Fuel	P/D	^{241}Am σ_f/σ_a	Clad worth [pcm]	Coolant $\Delta k/\Delta T$ [pcm/K]	m_{act} at BOL [kg]	Burnup rate [%/fpd]	Doubling of I_p [fpd]
(TRU,Zr)N	1.2	0.106	+3700	−0.19	746	0.094	50
	2.0	0.101	+2300	−0.35	1155	0.063	85
	2.4	0.097	+1800	−0.38	1400	0.053	90
(TRU,Hf)N	1.2	0.214	+4300	+0.13	1532	0.048	95
	2.0	0.178	+2900	+0.27	1981	0.038	115
	2.4	0.163	+2400	+0.43	2244	0.034	120
(TRU,B)N	1.2	0.432	+5600	+0.17	2621	0.030	140
	2.0	0.328	+3400	+0.79	3179	0.025	190
	2.4	0.286	+2400	+0.90	3442	0.023	200

Table 6.5. Neutronic and burnup performance of the transuranium ADS Pb/Bi-cooled burner with ZrN, HfN, and BN as a function of pitch-to-diameter ratio. Table adopted from **Paper II**.

material is less and less significant with larger P/D, and likewise the reactivity which is introduced into the system during flush out, see Table 6.5.

6.6.3 Burnup performance

When enlarging pin pitch, the probability of neutrons to induce fission decreases due to the increased leakage and spectrum softening, This, in turn, implicates higher specific fuel inventories and consequently lower burnup rates which are approximately inversely proportional to the actinide masses. Decrease of the burnup rates consequently diminishes the accelerator proton beam swing. For ZrN and HfN matrices, the reactivity swing is approximately independent of P/D, while it decreases slightly for BN (see **Paper II**). With larger pitch, the neutron spectrum becomes softened, which increases the actual burnability of the matrix.

6.7 Homogeneous vs. heterogeneous modelling

In a separate, parametric study we also investigated the sensitivity of our results to the modelling approximation of the system geometry. The self-shielding effects observed in standard fast reactor design can be even more pronounced in reactor cores with heavy presence of heterogeneously distributed neutron absorbers.

A full pin-by-pin core geometry model of a refined TRU ADS core with heterogeneously distributed neutron absorber (B_4C), see **Paper III**, was compared with the homogeneous approximation, where fuel and absorber pins were smeared together with the coolant and cladding material. The structure in axial and radial reflectors were also smeared. A similar comparison was made for a model Pb/Bi-cooled core employing (TRU,Zr)N smearing core fuel, structural and coolant material. The results of these simulations are displayed in Table 6.6.

System	Design	k_{eff}	$M^{\text{f}}_{\text{ext}}$
(TRU,Zr)N	Homogeneous	0.96204 ± 0.00049	29.280 ± 0.0236
	Heterogeneous	0.95963 ± 0.00056	28.195 ± 0.0238
TRUN + B_4C	Homogeneous	0.94079 ± 0.00054	18.463 ± 0.0049
	Heterogeneous	0.96086 ± 0.00053	27.461 ± 0.0055

Table 6.6. Comparison of eigenvalue and source calculations for homogeneous and heterogeneous designs together with corresponding 1-σ relative statistical errors. In the case of eigenvalue calculations, totally 1 million of neutrons have been simulated in 100 active histories, while 5000 protons were used in a source multiplication run. Simulations have been performed on a single 1 GHz Pentium III processor PC running Linux operating system.

In order to dispatch our studies and match realistic calculation times, the homogeneous modelling approach would clearly be preferable as calculation times are increased by more than a factor of five in the case of heterogeneous modelling in order to reach similar 1-σ relative statistical errors. However, the homogeneous approximation implies the strong underestimation of the neutron multiplication in

a system with heterogeneously placed absorber pins. Sub-criticality level is also underestimated by ∼2000 pcm. Note that with respect to uncertainties of our Monte Carlo calculations, the change in the source efficiency is not significant, $\phi^* = 1.162 \pm 0.009$ (for homogeneous model) and $\phi^* = 1.119 \pm 0.014$ (for heterogeneous configuration).

Chapter 7

Design of a TRU ADS burner

The physical characteristics and challenges interconnected with transuranic burning in a nuclear reactor have been reviewed in previous chapters. The neutronic, safety & burnup performance of any incineration system will depend not only on the composition of the reactor's fuel but also on the choice of the core materials and geometry. Different diluent materials, core lattice configurations and coolants have been assessed in order to identify suitable fuel concepts and core design configurations for accelerator-driven transuranium burners. The results of these parametric, scoping studies were summarised in Chapter 6. Here, by appropriate choice of materials and by optimising fuel and core design, we aim at achieving favourable neutronic, burnup and safety characteristics of the transuranium ADS burner while respecting key thermal hydraulic and material-related constraints.

7.1 Core concept

Our concept is based on the introduction of neutron-absorbing materials into the core of accelerator-driven systems incinerating TRU nuclides in the frame of a two-component scenario, see Figure 3.10 - strategy e) and f). The system studies refer to a scenario of ADS-startup and introduction into the nuclear reactor park, assuming therefore a TRU composition being that of spent LWR UOX fuel (burnup 41.2 GWd/tHM) after 30 years of cooling, see Table 2.1.

The use of absorbing material was considered also for the CAPRA design [83] in order to dilute highly reactive plutonium fuel. Due to the severe degradation of Doppler and sodium void reactivity coefficients this option was, however, substituted by the dilution strategy. Requirements on safety margins (concerning reactivity coefficients) are somewhat relaxed in sub-critical reactors and a considerable

amount of neutron absorbers can be introduced. Absorbing materials can accommodate higher TRU inventories, which somewhat alleviate reactivity loss, reduce accelerator power swing and limit production of higher actinides in fuel cycle. Our extensive scoping and feasibility studies identified two candidate absorbing materials, hafnium nitride and boron carbide. Their merits were evaluated in two separate studies - **Paper II** and **Paper III**.

7.2 Down-selections of core materials

7.2.1 Fuel

The nitride fuels have been adopted as the primary option. As discussed in Section 5.1.1, nitrides feature good compatibility with liquid metal coolants and combine high thermal conductivity with acceptable solubility in nitric acid.

7.2.2 Diluent material

Boron carbide was chosen as a heterogenous diluent material in **Paper III** especially for its good thermal and irradiation stability in fast spectrum. Boron carbide features superior neutronic characteristics allowing to cut the thermal parts of the neutron spectra and thus attain high fission-to-absorption probabilities (~ 0.4 for ^{241}Am). The boron (19.82% ^{10}B isotopic abundance) was enriched up to 95% in order to avoid neutron moderation on ^{11}B nuclei and minimise absorber inventory.

In **Paper II**, an innovative absorbing material, HfN, was proposed to be homogeneously mixed with actinide nitrides. HfN has excellent thermophysical properties: very high melting temperature and favourable thermal conductivity. (Hf,Zr)N pellets have been produced by carbothermic reduction from mixed oxides and a solid solution was obtained [126]. Due to the similarity of the lattice parameters, actinide nitrides are assumed to form a homogeneous solution also with HfN. Hafnium is a good absorber of neutrons in the thermal and resonance energy regions, effectively hardening the neutron spectrum. Our scoping studies showed that HfN-based fuels provide a good combination of the neutronic, safety and burnup characteristics: a) maintaining hard neutron spectra and thus minimising the production of higher actinides in the fuel cycle, b) providing acceptable coolant void reactivity, hence reducing necessary sub-criticality margin at BOC, c) attaining a reasonable value of the source efficiency, thus limiting the requirements on the accelerator beam power, d) decreasing the burnup reactivity swing, thus alleviating power peaking.

7.2.3 Coolant

Lead-bismuth eutectic is investigated as a candidate coolant, combining low melting and high boiling temperatures with favourable voiding characteristics (see Section 6.4.1). Pb/Bi also features low chemical activity with outer environments (water, air) excluding the possibility for fire or explosions. However, Pb/Bi flow

rates are limited by erosion to about 2.5 m/s - eventuating in higher pitches than usual for sodium. Liquid lead-bismuth eutectic is also highly corrosive in contact with cladding and structural materials at higher temperatures. Silicon modified ferritic/martensitic steels like Russian EP-823 may reach temperatures up 890 K. However, recent experiments have however shown that these steels feature reduced radiation resistance [142], see Section 5.3 for detailed discussion.

7.3 Design constraints

Design constraints taken into account include

- maximum coolant velocity in order to limit corrosion and erosion of structural materials ($v_{\max} = 2.5$ m/s),
- peak linear power and minimum P/D as limited by requirements to maintain stability of the structural materials at steady state ($T_{\max} \approx 890$ K) and in transients ($T_{\max} \approx 1140$ K) as well as to keep nitride fuel temperature below the decomposition/melting limit,
- peak fluence in the pin cladding (~ 100 dpa-NRT) and maximum internal gas pressure, both effectively limiting the discharge burnup,
- minimum fuel pin diameter (fabricability limit) & maximum fuel column height, attaining reasonable pressure drop and limiting thermal bowing,
- maximum TRU fraction in the fuel (~ 50 vol%), respecting the requirements as posed by stability and fabricability considerations,
- minimum target radius, providing sufficient heat removing capabilities to dissipate heat generated by accelerator beam at steady state and in transients,
- allowing only double-fold increase in the accelerator power beam,
- ensuring acceptable safety characteristics of the core, namely preventing the system from an instantaneous damage.

As we discussed in Chapters 3 and 6, the actinide discharge burnup has to be maximised in order to minimise losses to the waste streams. Simultaneously, the number of recycling steps should be minimised. What follows below is an extended summary of the results presented in **Papers II** and **III**. The reader is advised to consult the respective papers for details.

7.4 Design employing HfN

A cross section of the conceptual core design of (TRU,Hf)N-fuelled Pb/Bi-cooled ADS, as presented in **Paper II**, is displayed in Figure 7.1. The core is subdivided

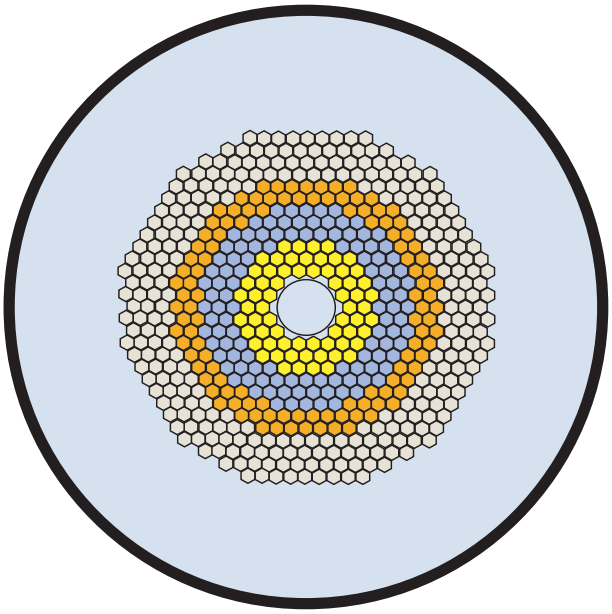

Figure 7.1. Cross section of the conceptual core design of Pb/Bi-cooled ADS employing (TRU,Hf)N. The core consists of three enrichment zones with the different matrix fractions. Radial steel reflector sub-assemblies are depicted in grey. The thickness of the radial reflector is optimised such that the coolant void reactivity is minimised. Pitch-to-diameter ratio is 1.75. Figure adapted from **Paper II**.

Sub-assembly row/zones	1-3	4-6	7-8	9-12
Actinide fraction (vol%)	32	37	45	–
Number S/As	66	114	114	282

Table 7.1. TRU volume fractions in fuel and a number of S/As in each enrichment zone yielding a radial power peaking factor less than 1.3 at BOL. There is 282 sub-assemblies in the radial reflector. Table adapted from **Paper II**.

radially into three enrichment fuel zones surrounded by four S/A rows of steel reflector (the steel volume fraction being 80%). The fraction of the matrix was adjusted so that a radial power peaking factor less than 1.3 is obtained at BOL, see Table 7.1.

The pellet, pin, sub-assembly, and system design parameters can be seen in Table 7.2. The flat-to-flat (FTF) of the S/A is adjusted such that the core fits a ∼20 cm radius target module. In this design, a relatively small sub-assembly FTF of 10.8 cm is chosen, thus allowing finer distribution of fuel in the core and facilitating symmetric reloading patterns. The power of the system was kept constant at the

Pellet density (% TD)	0.85
Pellet outer radius R_{fuel} (mm)	2.4
Cladding inner radius R_{gap} (mm)	2.5
Cladding outer radius R_{pin} (mm)	3.0
Pin bond	Pb/Bi
Active pin length (cm)	100
Length of upper fission gas plenum (cm)	150
Length of lower fission gas plenum (cm)	10
Length of bottom plenum spacer (cm)	10
S/A outer flat-to-flat (cm)	10.8
S/A pitch (cm)	11.0
Thickness of the duct (cm)	0.25
Pins per S/A	91
Pitch-to-diameter ratio	1.75
Number of core S/As	294
Length of radial reflector S/As (cm)	140
Length of upper reflector (cm)	200
Length of lower reflector (cm)	230
Spallation target outer radius (cm)	22.5
Radius of accelerator beam tube (cm)	15
Distance of target window from centreplane (cm)	20

Table 7.2. Pellet, pin, sub-assembly, and system design specifications of the (TRU,Hf)N-fuelled Pb/Bi-cooled ADS. A triangular pin lattice is adopted. The initial level of sub-criticality was set to $k_{\text{eff}} = 0.962$. Table adapted from **Paper II**.

level of 800 MW_{th} as limited by availability of the target coolant to remove the heat evolved by the accelerator beam. The proton beam impact window was placed 20 cm above the midplane of the core in order to minimise the number of neutrons leaking out of the spallation target into the axial reflectors and hence maximise the source efficiency. At the same time, almost axially symmetric power distribution is yielded. The gas plenum is located in the upper part of the core, reducing risks associated with positive reactivity insertion due to gas release from ruptured cladding. The length of the upper plenum was assumed to be relatively large, 150 cm, sufficient to accommodate released fission gases (mainly Xe, Cs, and Sr) and all helium from decayed ^{242}Cm.

Basic characteristics of the conceptual design of (TRU,Hf)N-fuelled Pb/Bi-cooled ADS are given in Table 7.3. Observe that despite the presence of absorbing matrix in the core, a slightly negative void reactivity (-270 pcm) could be obtained

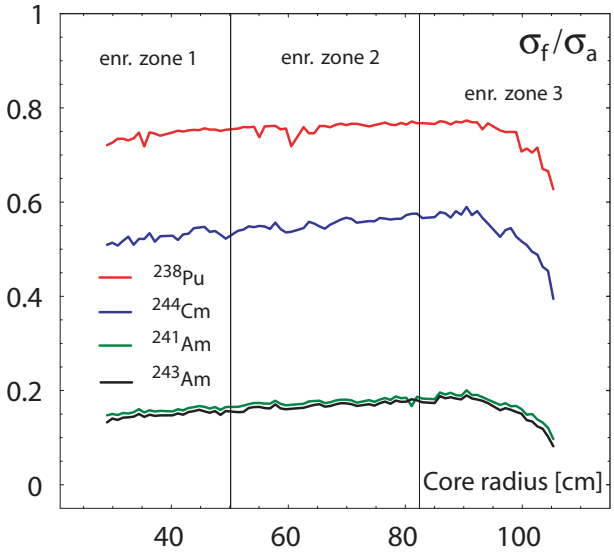

Figure 7.2. Pin-by-pin calculated radial distribution of fission probabilities. Fission-to-absorption fraction of ^{241}Am reaches 20%. Adapted from **Paper II.**

in the present design. Voiding the core together with the upper plenum and radial reflector brings the system additional negative reactivity (−3500 pcm).

Radial distribution of fission-to-absorption probabilities for even-neutron number nuclides is then presented in Figure 7.2. The fission probability is increased by a factor of two in the case of ^{241}Am and ^{243}Am in comparison to the CAPRA and Energy Amplifier figures (see also Table 7.4), resulting in a significant reduction of the He-producing nuclides ^{242}Cm and ^{238}Pu.

Irradiating the fuel for 100 days at the constant thermal power of 800 MW yielded a reactivity swing of 3300 pcm which was compensated for by an increase of accelerator power from 16 to 30 MW. The average cycle burnup reached 3.6%, with local burnups ranging from 5.5% in zone one to 2.5% in zone eight. The burnup calculations were accomplished by the MCB code [156].

The maximum achievable burnup of fuel pin was consequently determined by respecting cladding radiation damage and pin burst limits. The gas pressure in the fuel pin was calculated assuming that all fission gases (elements with boiling temperature lower than 2150 K) together with all helium from ^{242}Cm decay are released from the fuel. The maximum pressure in the most exposed pin in the S/A closest to the target is 3.7 MPa at the end of one irradiation cycle/batch (100 fpd), generating a hoop stress of 18.5 MPa. In order to keep this figure under the limiting value of 100 MPa, measured for irradiated rods at the temperature of 1140 K [140], the maximum residence time of the most exposed sub-assembly is 540 fpd.

Parameters	Unit	Conceptual design
Averaged linear power	kW/m	29.9
Proton efficiency ψ^* (BOC/EOC)		26.9/26.0
Coolant void worth at BOL	pcm	-270
Cladding and duct worth at BOL	pcm	$+6390$
Flooding of the accelerator tube	pcm	$+200$
Doppler T$\Delta k_{\text{eff}}/\Delta T$	pcm	-47
Axial fuel expansion $\Delta k_{\text{eff}}/(\Delta H/H)$	pcm/10^{-5}	-0.21
Grid expansion $\Delta k_{\text{eff}}/(\Delta P/P)$	pcm/10^{-5}	-0.52
Coolant density change $\Delta k_{\text{eff}}/\Delta T$	pcm	$+0.13$
β_{eff} at BOL	pcm	230
m_{act} at BOL	kg	2140
Burnup rate	%FIMA/fpd	0.036
Reactivity loss	pcm/batch	-3300
$\Delta k^{\text{c}}_{\text{eff}}/\beta_{\text{c}}$	pcm/%FIMA	-850
Doubling of the accelerator power I_{p}	fpd	100
^{242}Cm fraction in fuel	%/%FIMA	0.12
Number of batches		5
Batch length	days	100
Average burnup w/o core reshuffle	%FIMA	$\sim$20
Maximum radiation damage at EOL	dpa-NRT	100
Net Pu consumption	kg/efpy	188
Net MA consumption	kg/efpy	21

Table 7.3. Neutronic, safety and burnup performance of the conceptual ADS core design employing (TRU,Hf)N fuel and Pb/Bi coolant. P is the lattice pitch, H is the active core length. A capacity factor of 0.75 was assumed. Table is adapted from **Paper II**.

The radiation damage has been estimated using the formula suggested by Garner [157], relating 200 dpa-NRT damage rate to the damage neutron fluence (E_{n} > 0.1 MeV) of $4{\cdot}10^{23}$ n/cm^2. The highest exposure is found for high-burnup pins placed closest to the spallation target. There, 69% of the neutron flux is above the 100 keV, with a cycle/batch averaged fast flux of $4.2{\cdot}10^{15}$n/cm^2/s. Considering an axial power peaking factor of 1.28, the maximum fast fluence in cladding after 540 fpd is $2{\cdot}10^{23}$ n/cm^2 $\sim$ 100 dpa-NRT, which could be a reasonable estimate of the dose limit of Si-modified ferritic steels like EP-823 [142]. Thus, a sub-assembly burnup of 0.55%FIMA/fpd $\cdot$ 540 fpd $\sim$ 30%FIMA is in principle possible.

The fuel cycle our conceptual TRU ADS design thus consist of five 100-days long irradiation cycles. During the outages a few reflector sub-assemblies in the

core perimeter will be substituted with fuel S/As. Even without fuel reshuffling, an average burnup of the first, BOL core of ∼20% can be reached neutronically. Due to the burnup of TRU fuel and consequently increasing fractions of fission products, proton source efficiency decreases. The k_{eff} in the beginning of each irradiation batch is thus increased from 0.962 at BOL to 0.970 at the fifth irradiation cycle in order to keep the accelerator beam power at approximately 16 MW at BOC. The reactivity drop during one irradiation batch is compensated by an increase in accelerator beam by less than a factor of 2.0.

The linear power ratings are 39 kW/m at the beginning of life (power peaking 1.3 in the first S/A row) and rise up to 54 kW/m at EOC (100 full power days) when the burnup of the core has to be interrupted due to the limitation in maximum cladding temperatures (890 K). In Figure 7.3, the radial power profile is displayed at the beginning and at the end of the irradiation cycle, respectively.

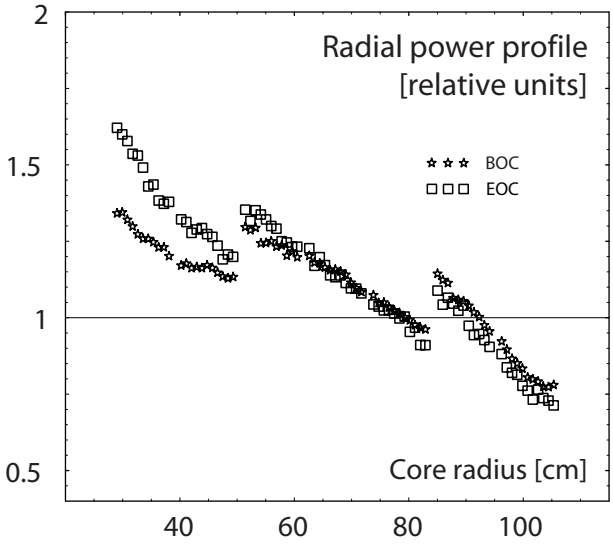

Figure 7.3. Radial power profile at BOC and EOC as reported on in **Paper II**. The maximum steady-state linear power remains bellow 60 kW/m, ensuring thermal stability of the structural material.

The beneficial effect of the HfN matrix in terms of the limitation of higher actinides in the fuel cycle is illustrated by evaluating the concentration of curium in the equilibrium fuel cycle. The qualitative analyses showed that curium inventory in mass-constrained equilibrium is about 1% for the present conceptual design, which is to be compared to more than 4% in a CAPRA type spectrum.

The lattice pitch of the reactor was chosen so that instant decomposition of nitride fuel or cladding damage are prevented under accidental conditions involving unprotected beam overpower transient, unprotected loss-of-flow, and unprotected

loss-of-heat sink. The thermal conductivity of the fuel is enhanced by HfN hence the peak centerline steady state temperature of the fuel remains below 1510 K at the EOC in the most exposed fuel pin. The corresponding coolant temperature difference is 220 K, which is a 60 K increase in comparison to BOC. At accidental conditions, when the accelerator beam is increased by a factor of two at BOC, the peak fuel temperature remains under 2150 K, still leaving a 250 K margin to the fuel decomposition limit.

In summary, our conceptual design of (TRU,Hf)N-fuelled Pb/Bi-cooled ADS features good combination of the neutronic and burnup characteristics - providing slightly negative coolant void worth, low burnup reactivity swing, and reasonable value source efficiency. However, excessive coolant volumes are required in order to guarantee cladding integrity under unprotected loss-of-flow accidents as the burst limit of ferritic steels is low (about 200 K below that for austenitic). Because austenitic steels feature very low (high temperature) corrosion resistance towards lead-alloys, it appears that, at present, there is no obvious choice of cladding material for our system.

Moreover, further studies are required in order to investigate the system transient behaviour in more detail and analyse its characteristics during an approach and in the equilibrium. Safety merits of increased TRU inventories being a consequence of HfN matrix have to be assessed, too. Finally, the high temperature material and irradiation performance of the Hf-based fuels needs to be established.

7.5 Design employing B_4C

In **Paper III**, the feasibility of employing a strong neutron absorber (B_4C) in the TRU ADS was investigated. We showed that one can achieve a significant increase in fission-to-absorption probabilities by a factor of 2.5 in the case of ^{241}Am and by a factor of three for ^{237}Np in comparison to the CAPRA and Energy Amplifier figures, see Table 7.4.

However, the introduction of boron carbide into the core yielded adverse effects on core safety parameters, particularly fuel temperature and coolant void coefficients. Due to the hard neutron spectrum, the Doppler coefficient virtually disappeared as hardly any neutrons reached the resonances. At the same time, spectral hardening upon the coolant voiding diminishes the parasitic capture in absorbing materials, which resulted in very large reactivity insertion, +3500 pcm.

The results of the burnup calculations are presented in Table 7.5. Fuel irradiation time was 300 days.

The reactivity decrease of 5600 pcm had to be compensated by an increase of accelerator power from 20 to 75 MW. Observe that the latter value would not be acceptable with respect to the ability of the 20-cm radius target to dissipate heat generated by proton beam. Hence, shorter irradiation cycle of about 50 full power days should be applied instead. Alternatively, total core power should be decreased, increasing also margins to the fuel/cladding damage. In the original

Nuclide	zone 1	zone 2	zone 3	zone 4	CAPRA	EA
^{237}Np	0.22	0.30	0.47	0.46	0.15	0.15
^{238}Pu	0.72	0.78	0.86	0.85	0.64	0.69
^{240}Pu	0.48	0.58	0.73	0.72	0.37	0.40
^{242}Pu	0.43	0.55	0.72	0.71	0.33	0.32
^{241}Am	0.14	0.20	0.33	0.33	0.12	0.12
^{243}Am	0.13	0.19	0.34	0.33	0.10	0.11
^{244}Cm	0.50	0.59	0.73	0.72	0.40	0.36

Table 7.4. Fission-to-absorption probability ratios for quickly decaying α-emitters and their predecessors in the fuel zones of nitride-fuelled Pb/Bi-cooled TRU ADS employing a B_4C absorber presented in **Paper III**. These values are compared to corresponding values of CAPRA and Energy Amplifier designs. The benefit of introducing neutron absorbers to reduce α activity and helium accumulation in fuel pins is clear.

Property	BOL	100 d	200 d	300 d
k_{eff}	0.972	0.955	0.936	0.916
ϕ_n^*	0.877	0.870	0.850	0.802
ϕ_f^*	0.875	0.867	0.847	0.797
Target power (MW)	20.5	36.9	54.9	75.1
Power peaking in zone 1	1.08	1.29	1.49	1.70
Average flux (10^{19} m^{-2}s^{-1})	3.86	4.14	4.45	4.78
Flux peaking in zone 1	1.97	2.27	2.57	2.88

Table 7.5. Burnup characteristics of nitride-fuelled Pb/Bi-cooled TRU ADS with B_4C neutron absorbers. Thermal power of the system is 1200 MW. Table adapted from **Paper III.**

design, presented in **Paper III**, the total burnup reached 8.7% in one irradiation cycle, local burnups were ranging from 7.3% in zone three to 11.5% in zone one and two. All transuranics were homogeneously dispersed throughout the whole core.

In this study, nitrogen alone was proposed to be used as pin bonding gas in order to suppress the decomposition of the nitride fuel. However, nitrogen has very low thermal conductivity, yielding extensive temperature gradients in the pellet-clad gap, of the order of 1000 K, before the gap is closed. In **Paper III**, the peak fuel temperature was estimated to be kept below 2100 K during the whole irradiation cycle at the steady state conditions. However, if the whole accelerator beam power margin would be accidently inserted into the system at BOL when pellet-clad gap is open, the fuel dissociation limit could be surpassed. Recent studies show that admixing of only small portions of the nitrogen into the inert gas is sufficient to delay the onset of the fuel dissociation by several hundreds Kelvin [116]. Hence, a

remedy would be to exchange nitrogen bonding with He-1%N_2 gas or apply liquid-metal bond, as was proposed for the (TRU,Hf)N burner (**Paper II**).

Chapter 8

Papers

Abstracts of the appended papers are summarised below.

8.1 Paper I

Liquid metal coolant void worths have been calculated as a function of fuel composition and core geometry for several model fast breeder reactors and accelerator-driven systems. The Monte Carlo transport code MCNP with continuous energy cross-section libraries was used for this study. With respect to the core void worth, lead/bismuth cooled FBRs appear to be inferior to those employing sodium for pitch-to-diameter ratios exceeding 1.4. It is shown that in reactor systems cooled with lead/bismuth eutectic, radial steel pin reflectors significantly lower the void worth. The void worth proves to be a strong function of the fuel composition, reactor cores with high content of minor actinides in fuel exhibiting larger void reactivities than systems with plutonium based fuel. Enlarging the lattice pitch in ADS burners operating on Pu rich fuel decreases the void worth while the opposite is true for ADSs employing americium based fuels.

8.2 Paper II

We have studied the neutronic & burnup characteristics of an accelerator-driven transuranium burner in a start-up mode. Different inert and absorbing matrices as well as lattice configurations have been assessed in order to identify suitable fuel and core design configurations. Monte Carlo transport and burnup codes were used in the analyses. The pin pitch was varied in order to optimise the source efficiency and coolant void worth while respecting the fuel and cladding limits during steady-state conditions and at transients. HfN provides a good combination of safety characteristics (negative coolant void worth and prompt reactivity feedback) and reasonable values of source efficiency and burnup reactivity swing. HfN-based fuels

yield twice higher neutron fission-to-absorption probabilities in americium isotopes compared to reactor designs relying on inert matrices, thus limiting the production of higher actinides in the fuel cycle. A safety analysis of the conceptual core design shows that the system withstands an unprotected accelerator overpower transient.

8.3 Paper III

The application of burnable absorbers (BA) for minimisation of power peaking, reactivity loss and capture to fission probabilities in an accelerator driven waste transmutation system (ADS, ATW) has been investigated. ^{10}B enriched B_4C absorber rods were introduced into a lead/bismuth cooled core fuelled with TRU discharges from light water reactors in order to achieve the smallest possible power peakings at a BOL sub-criticality level of 0.97. Detailed Monte Carlo simulations show that a radial power peaking equal to 1.2 at BOL is attainable using a four zone differentiation in BA content. Using a newly written Monte Carlo Burnup code (MCB), reactivity losses were calculated to be 640 pcm per percent transuranium burnup for unrecycled TRU discharges. Compared to corresponding values in BA free cores, BA introduction diminishes reactivity losses in TRU fuelled sub-critical cores by about 20%. Radial power peaking after 300 days of operation at 1200 MW thermal power was less than 1.75 at a sub-criticality level of $\sim$0.92, which appears to be acceptable with respect to limitations in cladding and fuel temperatures. In addition, the use of BA yields significantly higher fission to capture probabilities in even neutron number nuclides. A fission to absorption probability ratio for ^{241}Am equal to 0.33 was achieved in the configuration studied here. Hence, production of the strong α-emitter ^{242}Cm is reduced, leading to lower fuel swelling rates and pin pressurisation. Disadvantages following BA introduction, such as increase of void worth and decrease of Doppler feedback in conjunction with small values of β_{eff}, need to be addressed by detailed studies of sub-critical core dynamics.

8.4 Paper IV

The introduction of accelerator driven systems (ADS) is believed to be of importance for efficient and safe transmutation of americium and curium. Among the problems related to the use of ADS in this context are comparatively high power peakings and high helium accumulation rates in fuel pins. The present study shows that radial power peakings similar to those of critical configurations ($\sim$1.1) can be achieved in sub-critical cores by adequate distribution of fuel, burnable absorbers and diluents. The introduction of strong neutron absorbers in sub-assemblies containing americium increases fission to absorption ratios up to $\sim$0.50, which reduces helium production due to ^{242}Cm decay by a factor of two. In order to maintain a source importance reasonably close to unity, neutron poisons should be placed in

the periphery of the core, and diluent materials with small cross sections for capture and inelastic scattering should be used in the vicinity of the spallation target.

8.5 Paper V

In order to study the beam power amplification of an accelerator driven system (ADS), a new parameter, the proton source efficiency (ψ^*) is introduced. ψ^* represents the average importance of the external proton source, relative to the average importance of the eigenmode production, and is closely related to the neutron source efficiency (ϕ^*), which is frequently used in the ADS field. ϕ^* is commonly used in the physics of sub-critical systems driven by any external source (spallation source, (d,d), (d,t), ^{252}Cf spontaneous fissions etc.). On the contrary, ψ^* has been defined in this paper exclusively for ADS studies, where the system is driven by a spallation source. The main advantage with using ψ^* instead of ϕ^* for ADS is that the way of defining the external source is unique and that it is proportional to the core power divided by the proton beam power, independently of the neutron source distribution.

Numerical simulations have been performed with the Monte Carlo code MCNPX in order to study ψ^* as a function of different design parameters. It was found that, in order to maximise ψ^*, and therefore minimise the proton current needs, a target radius as small as possible should be chosen. For target radii smaller than about 30 cm, lead-bismuth is a better choice of coolant material than sodium, regarding the proton source efficiency, while for larger target radii the two materials are equally good. The optimal axial proton beam impact was found to be located approximately 20 cm above the core centre. Varying the proton energy, ψ^*/E_{p} was found to have a maximum for proton energies between 1200 and 1400 MeV. Increasing the americium content in the fuel decreases ψ^* considerably, in particular when the target radius is large.

Chapter 9

Conclusions

Accelerator-driven systems (ADS) have been proposed to deal with the excess of americium and curium in P&T schemes closed for entire transuranic vector. In countries without developed fast reactor programmes or with politically motivated proliferation concerns, the ADS are envisioned to operate together with light-water reactors in the so called two-component scheme. A major difficulty associated with this scenario is, however, high reactivity losses due to rapid burnout of fissile isotopes, which simultaneously exacerbates power peaking.

In this work, we addressed the issue of extensive burnup reactivity swing in transuranium ADS, while also achieving good neutronic, burnup and safety characteristics of the reactor. Series of parametric, scoping studies were performed in order to identify promising coolant candidates, fuel concepts and core designs.

The economy of the source neutrons was first investigated as a function of core and target design. For these analyses, a novel, generalised framework was presented in order to describe the source multiplication in ADS. This parameter is defined independently of the distribution of the *neutron* source, allowing for a fair mutual intercomparison of different ADS designs. The source efficiency showed to be a strong decreasing function of target radius due to inelastic slowing down of neutrons in the target.

We furthermore focused on the evaluation of the coolant void worth in the model FBR and ADS designs. Most importantly, it appeared that in reactor systems cooled by lead/bismuth eutectic, radial steel pin reflectors have to be applied in order to significantly lower the coolant void reactivity. The void worth proved to be a strong function of the fuel composition - reactor cores with high content of fertile material or minor actinides in fuel exhibiting larger void reactivities than systems with plutonium-based inert matrix fuels.

For transuranic fuel, fertile and strongly absorbing matrices yielded higher void worth when increasing P/D, while the opposite was valid for inert matrices. Moreover, large pitches appeared to be favourable for limiting the reactivity worth of the cladding material and improving the source efficiency.

HfN-based fuels were subsequently identified as an attractive option for transuranium ADS burners. (TRU,Hf)N appeared to have a good combination of neutronic, burnup and thermal characteristics: maintaining hard neutron spectra, yielding acceptable coolant void reactivity and source efficiency, and providing small burnup reactivity swing. HfN appears to have a stabilising effect on the fuel, improving its thermal conductivity and thus its margin to failure.

Considering key material-related and thermal hydraulic design constraints, we presented a conceptual design of a lead/bismuth eutectic cooled ADS burner employing (TRU,Hf)N fuel. The design featured a hard neutron spectrum yielding a factor of two higher ^{241}Am and ^{243}Am fission probabilities than are typical for systems employing inert matrix fuel. Hence, the production of higher actinides in the fuel cycle is minimised. The burnup reactivity swing and associated power peaking were managed by an appropriate choice of cycle length (100 days) and by core enrichment zoning. The average discharge burnup of 20% fissions per initial atom was reached. The conceptual core design features favourable safety characteristics - core coolant void worth being slightly negative. A safety analysis shows that the system is protected from an instant damage during unprotected beam overpower transient.

In conclusion, it seems that the principal merits of accelerator-driven systems in terms of their potential to reduce radiotoxic inventory of spent nuclear fuel are well established. However, several important issues have to be resolved in the near future before they are implemented. The choice of core and target materials - fuel matrix, coolant, and structural material - is still an open question alluding to their long-term mechanical, thermal and irradiation performance. E.g. while the well established oxide fuel seems to be the most natural choice for ADS-demo, the advanced fuel types as e.g. nitrides appear to be a more favourable option for gigawatt-size ADS units. Nevertheless, it might be completely other factors than technological, which would decide about the future fate of ADS and P&T technologies, e.g. political and social one. In this regard, an increase of easily apprehended, short-term risks which are associated with P&T could play an important role.

Bibliography

[1] C. Bennett et al., Astrophysical Journal Supplement Series **148**, 1 (2003).

[2] A. Becquerel, Comptes Rendus de l'Académie des Sciences (Paris) **122**, 501 (1896).

[3] O. Hahn and F. Strassmann, Naturwissenschaften **27**, 11 (1939).

[4] L. Meitner and O. Frisch, Nature **143**, 239 (1939).

[5] F. Joliot et al., Nature **143**, 470 (1939).

[6] F. Joliot et al., Nature **143**, 680 (1939).

[7] J. Lewellen, *The Mighty Atom*, Knopf, 1955.

[8] http://howard.engr.siu.edu/mech/faculty/hippo/lecture16a.htm, September 17, 2004.

[9] L. Brown et al., *State of the World*, W.W. Norton & Company, 1992.

[10] *Actinide and Fission Product Partitioning and Transmutation, Status and Assessment Report*, OECD/NEA, 1999.

[11] JEF-PC, version 2.0, OECD/NEA.

[12] P. de Marcillac et al., Nature **422**, 876 (2003).

[13] *Council directive lying down basic safety standards for the protection of the health*, Number 96/29/EUROATOM, 1996.

[14] B. Gautier, Innovative fuel physics: Reactor core design and high burnup fuel performance, in *Lecture notes: The 1999 Frédéric Joliot/Otto Hahn Summer School*, CEA/FZK, 1999.

[15] K. Fukuda et al., IAEA overview of global spent fuel storage, Technical Report IAEA–CN–102/60, IAEA, 2003.

[16] N. Oi, Plutonium challenges: Changing dimensions of global cooperation, 40/1/1998, IAEA Bulletin, 1998.

[17] Post-closure safety of a deep repository for spent nuclear fuel, Technical Report TR-99-06, Swedish Nuclear Fuel and Waste Management Co., 1999.

[18] A EU roadmap for developing accelerator driven systems (ADS) for nuclear waste incineration, Technical report, The European Technical Working Group on ADS, ENEA, 2001.

[19] *Dose Coefficients for Intakes of Radionuclides by Workers*, ICRP Publication 68, 1994.

[20] *Age Dependent Doses to Members of the Public from Intake of Radionuclides: Part 5 - Compilation of Ingestion and Inhalation Dose Coefficients*, ICRP Publication 76, 1995.

[21] H. Gruppelaar et al., Advanced technologies for the reduction of nuclear waste, Technical Report ECN-R-98-008, ECN, Petten, 1998.

[22] Nuclear waste: technologies for separations and transmutations, Technical report, National Research Council, 1996.

[23] G. Volckaert et al., Long-term environmental impact of underground disposal of P&T waste, in *Proceedings of the Fifth International Information Exchange Meeting on Actinide and Fission Product Partitioning and Transmutation*, page 463, OECD/NEA, Mol, Belgium, November 25-27, 1998.

[24] N. Cadelli et al., *Performance Assessment of Geological Isolation Systems for Radioactive Waste*, Commission of the European Communities, 1988.

[25] *Accelerator-driven Systems (ADS) and Fast Reactors (FR) in Advanced Nuclear Fuel Cycles, A Comparative Study*, OECD/NEA, 2002.

[26] T. Pigford, Reprocessing incentives for waste disposal, in *Transactions of the American Nuclear Society*, volume 62, page 97, ANS, 1990.

[27] A. Croff et al., Actinide partitioning-transmutation program final report, Technical Report ORNL-5566, Oak Ridge National Laboratory, 1980.

[28] Evaluation of actinide partitioning and transmutation, Technical Report 214, IAEA, 1982.

[29] *The Enviromental and Ethical Basis of Geological Disposal of Long-Lived Radioactive Wastes*, OECD/NEA, 1996.

[30] A. Croff, A reexamination of the incentives for actinide burning, in *Transactions of the American Nuclear Society*, volume 62, page 76, 1990.

[31] *The Future of Nuclear Power, An interdisciplinary MIT study*, Massachusetts Institute of Technology, U.S.A., 2003.

[32] A. Waltar and A. Reynolds, *Fast Breeder Reactors*, Pergamon Press, 1981.

[33] M. Steinberg et al., Neutron burning of long-lived fission products for waste disposal, Technical Report BNL-8558, Brookhaven National Laboratory, 1964.

[34] Y. Shubin et al., Evaluations of photoneutron reaction cross sections of radioactive fission product nuclei, Technical Report INDC(CCP)-408, IAEA, 1997.

[35] M. Gregory and M. Steinberg, A nuclear ransmutation system for disposal of long-lived fission product waste in an expanding nuclear power economy, Technical Report BNL-11915, Brookhaven National Laboratory, 1967.

[36] H. Harada et al., Fusion technology **24(2)**, 161 (1993).

[37] J. Wallenius, Fusion technology **33**, 456 (1998).

[38] I. Slessarev et al., On neutron consumption requirements for long-lived fisson products (LLFP) transmutation and lanthanides, in *Proceedings of the International Conference on Future Nuclear Systems, GLOBAL'99*, ANS, 1999.

[39] M. Salvatores, Transmutation and innovative options for the back-end of the fuel cycle, in *Proceedings of the International Conference on Future Nuclear Systems, GLOBAL'99*, ANS, Jackson Hole, USA, August 29 - September 3, 1999.

[40] Y. Sakamura et al., Studies on pyrochemical reprocessing for metallic and nitride fuels: behaviour of transuranium elements in LiCl-KCl/liquid metal systems, in *Proceedings of the International Conference on Future Nuclear Systems, GLOBAL'99*, ANS, Jackson Hole, USA, August 29 - September 3, 1999.

[41] M. Salvatores et al., Nuclear Science and Engineering **116**, 1 (1994).

[42] F. Venneri et al., The physics design of accelerator-driven transmutation system, in *Proceedings of the International Conference on Evaluation of Emerging Nuclear Fuel Cycle Systems, GLOBAL'95*, page 474, ANS, Versailles, France, September 11-14, 1995.

[43] W. Yang and H. Khalil, Neutronics design studies of an LBE cooled ATW blanket, in *Proceedings of the IAEA Technical Committee Meeting on Core Physics and Engineering Aspects of Emerging Nuclear Energy Systems for Energy Generation and Transmutation, IAEA-TECDOC-1356*, Argonne National Laboratory, USA, November 28 - December 1, 2000.

[44] T. Takizuka et al., Dedicted accelerator-driven system for nuclear waste transmutation, in *Proceedings of the Third International Conference on Accelerator-Driven Transmutation Technologies and Applications, ADTTA'99*, Praha, Czech Republic, June 7-11, 1999.

[45] M. Eriksson, J. Wallenius, M. Jolkkonen, and J. Cahalan, Inherent safety of fuels for accelerator-driven systems, Submitted to Nuclear Technology, 2004.

[46] T. Thompson and J. Beckerley, editors, *The Technology of Nuclear Reactor Safety*, volume 1, The M.I.T. Press, 1964.

[47] B. Pershagen et al., *Snabba bridreaktorer*, NE 1982:6, Nämnden för energiproduktionsforskning, Sweden (in Swedish), 1982.

[48] E. Adamov et al., *White book of nuclear energy*, MINATOM, Russia (in Russian), 2001.

[49] W. Satcey, *Nuclear Reactor Physics*, John Wiley & Sons, Inc., 2001.

[50] H. Etherington, editor, *Nuclear Engineering Handbook*, McGraw-Hill Book Company, 1958.

[51] H. Kleykamp, Journal of Nuclear Materials **275**, 1 (1999).

[52] H. Pierson, *Handbook of Refractory Carbides and Nitrides*, William Andrew Publishing/Noyes, 1996.

[53] R. Thetford and M. Mignanelli, Journal of Nuclear Materials **320**, 44 (2003).

[54] H. H. Hummel and D. Okrent, *Reactivity Coefficients in Large Fast Power Reactors*, American Nuclear Society, 1970.

[55] S. Glasstone and A. Sesonske, *Nuclear Reactor Engineering*, volume 1, Chapman and Hill, 1994.

[56] C. Lombardi et al., Journal of Nuclear Materials **274**, 181 (1999).

[57] A. Conti et al., CAPRA exploratory studies of U-free fast Pu burner cores, in *Proceedings of the International Conference on Evaluation of Emerging Nuclear Fuel Cycle Systems, GLOBAL'95*, page 1316, ANS, Versailles, France, September 11-14, 1995.

[58] G. Keepin, *Physics of nuclear kinetics*, Addison-Wesley,Reading,USA, 1965.

[59] J.F. Briesmeister, editor, MCNP – A general Monte Carlo N-Particle transport code, version 4C, Technical Report LA–13709–M, Los Alamos National Laboratory, USA, 2000.

[60] International handbook of evaluated criticality safety benchmark experiments, Technical Report NEA/NSC/DOC(95)03, OECD/NEA, 2003.

[61] M. Asty, A review of the collaborative programme on the European Fast Reactor (EFR) and on the CAPRA activities, in *27. meeting of the International Working Group on Fast Reactors*, IAEA-TECDOC-791, IAEA, Vienna, 1994.

[62] D. Wade and R. Hill, Progress in Nuclear Energy **31**, 13 (1997).

[63] K. Hesketh et al., Multiple recycle of plutonium in PWR - a physics code benchmark study by the OECD/NEA, in *Proceedings of the International Conference on Future Nuclear Systems, GLOBAL'97*, page 287, 1997.

[64] W. Bernnat et al., PWR benchmarks from OECD working party on physics of plutonium recycling, in *Proceedings of the International Conference on Evaluation of Emerging Nuclear Fuel Cycle Systems, GLOBAL'95*, page 627, ANS, Versailles, France, September 11-14, 1995.

[65] J. Kloosterman, Multiple recycling of plutonium in advanced PWRs, in *RECOD'98*, page 266, 1998.

[66] M. Delpech, Innovative fuel physics: Innovative concepts, in *Lecture notes: The 1999 Frédéric Joliot/Otto Hahn Summer School*, CEA/FZK, 1999.

[67] A. Puill and S. Aniel-Buchheit, Full MOX core for PWRs, in *Proceedings of the International Conference on Future Nuclear Systems, GLOBAL'97*, page 274, 1997.

[68] A. Puill et al., Mastery of the plutonium inventory in PWRs: The APA concept, in *Proceedings of the International Conference on Future Nuclear Systems, GLOBAL'99*, ANS, Jackson Hole, USA, August 29 - September 3, 1999.

[69] H. Golfier et al., Plutonium and minor actinide recycling in PWRs with new APA concepts, in *Proceedings of the International Conference on Future nuclear systems, GLOBAL 01*, Paris, France, September 9-13, 2001.

[70] A. Vasile et al., Feasibility studies of the CORAIL subassembly for Pu multirecycling in PWRs, in *Proceedings of the International Conference on Future Nuclear Systems, GLOBAL 2003*, ANS, New Orleans, USA, November 16-20, 2003.

[71] G. Youinou et al., Plutonium management and multirecycling in LWRs using an enriched uranium support, in *Proceedings of the International Conference on Future Nuclear Systems, GLOBAL'99*, ANS, Jackson Hole, USA, 1999.

[72] G. Youinou et al., Plutonium and americium multirecycling in the European Pressurized Reactor (EPR) using slightly over-moderated U-235 enriched MOX fuel assemblies, in *Proceedings of the International Conference on Future Nuclear Systems, GLOBAL 2003*, ANS, New Orleans, USA, November 16-20, 2003.

[73] M. Delpech et al., Scenarios of plutonium and minor actinide recycling, in *Proceedings of the International Conference on Future Nuclear Systems, GLOBAL'97*, page 731, 1997.

[74] J. Kloosterman and H. Gruppelaar, Multi-recycling of actinides in thorium based fuels, in *Proceedings of the International Conference on Future Nuclear Systems, GLOBAL'99*, ANS, Jackson Hole, USA, August 29 - September 3, 1999.

[75] M. Delpech et al., The Am and Cm transmutation, physics and feasibility, in *Proceedings of the International Conference on Future Nuclear Systems, GLOBAL'99*, ANS, Jackson Hole, USA, August 29 - September 3, 1999.

[76] D. Haas et al., The EFTTRA European collaboration for development of fuels and targets for transmutation: Status of recent developments., in *Proceedings of the International Conference on Future Nuclear Systems, GLOBAL'99*, ANS, Jackson Hole, USA, August 29 - September 3, 1999.

[77] K. Richter et al., Journal of Nuclear Materials **249**, 121 (1997).

[78] R. Konings et al., Nuclear Science and Engineering **128**, 70 (1998).

[79] A. Conti et al., Long-lived fission product transmutation studies, in *Proceedings of the International Conference on Future Nuclear Systems, GLOBAL'99*, ANS, Jackson Hole, USA, August 29 - September 3, 1999.

[80] T. Mukaiyama et al., Minor actinide transmutation in fission reactors and fuel cycle considerations, in *Second international information exchange meeting*, page 320, OECD/NEA, 1992.

[81] L. Baetslé et al., Impact of advanced fuel cycles and irradiation scenarios of final disposal issues, in *Proceedings of the International Conference on Future Nuclear Systems, GLOBAL'99*, ANS, Jackson Hole, USA, August 29 - September 3, 1999.

[82] M. Salvatores et al., Nuclear Instruments and Methods in Physics Research **A414**, 5 (1998).

[83] A. Languille et al., CAPRA core studies - the oxide reference option, in *Proceedings of the International Conference on Evaluation of Emerging Nuclear Fuel Cycle Systems, GLOBAL'95*, page 874, ANS, Versailles, France, September 11-14, 1995.

[84] D. Leliévre, Nuclear science and technology – perspectives and costs of partitioning and transmutation of long-lived radionuclides, Technical Report EUR-17485, European Communities, 1996.

[85] N. Budylkin et al., Journal of Nuclear Materials **329-333**, 621 (2004).

[86] C. D. Raedt and L. Baetslé, Impact of high burnup irradiation and multiple recycling in fast burner reactors on the plutonium and minor actinide inventories, in *Proceedings of the International Conference on Evaluation of Emerging Nuclear Fuel Cycle Systems, GLOBAL'95*, page 922, ANS, Versailles, France, September 11-14, 1995.

[87] T. Mukaiyama, OMEGA program in Japan and ADS development in JAERI, in *Proceedings of the Third International Conference on Accelerator-Driven Transmutation Technologies and Applications, ADTTA'99*, Praha, Czech Republic, June 7-11, 1999.

[88] H. Murata and T. Mukaiyama, Atomkernenergie-Kerntechnik **45**, 23 (1984).

[89] D. Foster et al., Review of PNL study on transmutation processing of high level waste, Technical Report LA–UR–74–74, Los Alamos National Laboratory, USA, 1974.

[90] F. Venneri et al., The Los Alamos accelerator-driven transmutation of nuclear waste (ATW) concept - development of the ATW target/blanket system, in *Proceedings of the Second International Conference on Accelerator-Driven Transmutation Technologies and Applications*, page 758, Uppsala University, 1996.

[91] M. Mizumoto et al., Proton linac development for neutron science project, in *Proceedings of the Third International Conference on Accelerator-Driven Transmutation Technologies and Applications, ADTTA'99*, Praha, Czech Republic, June 7-11, 1999.

[92] C. Rubbia and J. Rubio, A tentative programme towards a full scale Energy Amplifier, Technical Report CERN/LHC/96–11(EET), 1996.

[93] M. Salvatores et al., Nuclear Science and Engineering **124**, 280 (1996).

[94] T. Sasa et al., Conceptual design study and code development for accelerator-driven transmutation system, in *Proceedings of the International Conference on Future Nuclear Systems, GLOBAL'97*, page 435, 1997.

[95] H. Oigawa et al., Research and development program on accelerator driven system in JAERI, in *Proceedings of the International Conference on Future Nuclear Systems, GLOBAL 2003*, ANS, New Orleans, USA, November 16-20, 2003.

[96] M. Viala et al., The SPIN program - assets and prospects, in *Proceedings of the International Conference on Future Nuclear Systems, GLOBAL'97*, page 706, 1997.

[97] M. Salvatores, Advanced options for transmutation strategies, in *Proceedings of the Fifth International Information Exchange Meeting on Actinide and Fission Product Partitioning and Transmutation*, OECD/NEA, Mol, Belgium, November 25-27, 1998.

[98] J. Garnier et al., Feasibility study of an advanced GFR, in *Proceedings of the International Conference on Future Nuclear Systems, GLOBAL 2003*, ANS, New Orleans, USA, November 16-20, 2003.

[99] A technology roadmap for Generation IV nuclear energy systems, Technical report, U.S. DOE Nuclear Energy Research Advisory Committee and the Generation IV International Forum, 2002.

[100] S. Pillon, Design of a moderated target for transmutation of americium, in *Proceedings of the Seventh Information Exchange Meeting on Actinide and Fission Product Partitioning and Transmutation*, OECD/NEA, Jeju, Korea, October 4-16, 2002.

[101] G. Imel et al., The TRADE experiment and progress, in *Proceedings of the International Conference on Future Nuclear Systems, GLOBAL 2003*, ANS, New Orleans, USA, November 16-20, 2003.

[102] C. Bowman et al., Nuclear Instruments and Methods in Physics Research **A320**, 336 (1992).

[103] W. Sailor et al., Progress in Nuclear Energy **28**, 359 (1994).

[104] F. Venneri, Disposition of nuclear waste using sub-critical accelerator driven systems, Technical Report LA-UR-98-985, Los Alamos National Laboratory, 1998.

[105] A roadmap for developing accelerator transmutation of waste (ATW) technology: A report to Congress, 1999.

[106] F. Carminati et al., An Energy Amplifier for cleaner and inexhaustible nuclear energy production driven by a particle beam accelerator, Technical Report CERN/AT/93–47(ET), CERN, 1993.

[107] C. Rubbia et al., Conceptual design of a fast neutron operated high power Energy Amplifier, Technical Report CERN/AT/95–44(ET), CERN, 1995.

[108] C. Rubbia et al., Fast neutron incineration in the Energy Amplifier as alternative to geologic storage: The case of Spain, Technical Report CERN/LHC/97–01(EET), 1997.

[109] H. A. Abderrahim et al., Nuclear Instruments and Methods in Physics Research **A463**, 487 (2001).

[110] H. Beaumont et al., Heterogeneous minor actinide recycling in the CAPRA high burnup core with target sub-assemblies, in *Proceedings of the International Conference on Future Nuclear Systems, GLOBAL'99*, ANS, Jackson Hole, USA, August 29 - September 3, 1999.

[111] J. Wallenius, Journal of Nuclear Materials **320**, 142 (2003).

[112] K. Richter and C. Sari, Journal of Nuclear Materials **184**, 167 (1991).

[113] H. Matzke, *Science of Advanced LMFBR fuels*, North-Holland, 1986.

[114] R. Margevicius, AFC fuels development update: 2003 semi-annual meeting, LA-UR-03-0415, Los Alamos National Laboratory, 2003.

[115] M. Takano et al., Study on the stability of AmN and (Am,Zr)N, in *Proceedings of the International Conference on Future Nuclear Systems, GLOBAL 2003*, ANS, New Orleans, USA, November 16-20, 2003.

[116] M. Jolkkonen, M. Streit, and J. Wallenius, Journal of Nuclear Science and Technology **41**, 457 (2004).

[117] M. Akabori et al., in *International symposium on nitride fuel cycle technology*, JAERI, Tokai-mura, August 2004.

[118] B. Rogozkin, N. Stepennova, and A. Proshkin, Atomnaya Energiya **95**, 208 (2003).

[119] Y. Suzuki and Y.Arai, Journal of Alloys and Compounds **271–273**, 577 (1998).

[120] Y. Arai et al., J. Nucl. Mater. **195**, 37 (1992).

[121] J. Wallenius and S. Pillon, N-15 requirement for 2^{nd} stratum ADS nitride fuels, in *AccApp'01 & ADTTA'01 Nuclear Applications in the New Millennium*, ANS, Reno, USA, November 11-15, 2001.

[122] N. Cocuaud et al., Inert matrices, uranium-free plutonium fuel and americium target. Synthesis of CAPRA, SPIN, EFTTRA studies, in *Proceedings of the International Conference on Future Nuclear Systems, GLOBAL'97*, page 1044, 1997.

[123] J. Wallenius, CONFIRM: status and perspectives, in *Eight international information exchange meeting on P&T*, OECD/NEA, Las Vegas, November 2004.

[124] M. Mignanelli, Stability of U and U,Zr nitrides at high temperatures, in *CONFIRM progress meeting, 27-28 September 2001.*

[125] M. Streit et al., Journal of Nuclear Materials **319**, 51 (2003).

[126] M. Streit, Personal communication, 2004.

[127] G. Hofman et al., Progress in Nuclear Energy **31**, 83 (1997).

[128] C. Degueldre and J. Paratte, Journal of Nuclear Materials **274**, 1 (1999).

[129] N. Chauvin et al., Optimisation of minor actinide fuels for transmutation in conventional reactors (PWR, FR), in *Proceedings of the International Conference on Future Nuclear Systems, GLOBAL'99*, ANS, Jackson Hole, USA, August 29 - September 3, 1999.

[130] H. Matzke et al., Journal of Nuclear Materials **274**, 47 (1999).

[131] R. Konings et al., Journal of Nuclear Materials **274**, 84 (1999).

[132] A. Languille et al., Journal of Alloys and Compounds **271–273**, 517 (1998).

[133] J. Kloosterman and P. Damen, Journal of Nuclear Materials **274**, 112 (1999).

[134] J. Wallenius and M. Eriksson, Neutronic design of sub-critical minor actinide burners, submitted to Nuclear Technology, 2004.

[135] N. Novikova, Y. Pashkin, and V. Chekunov, Some features of sub-critical blankets cooled with lead-bismuth, in *Proceedings of the Third International Conference on Accelerator-Driven Transmutation Technologies and Applications, ADTTA'99*, Praha, Czech Republic, June 7-11, 1999.

[136] A. Rousanov et al., Developing and studying the cladding steels for the fuel elements of the NPIs with heavy coolant, in *Proceedings of the Conference Heavy liquid metal coolants in nuclear technology, HLCM'98*, Institute of Physics and Power Engineering, Obninsk, Russia, October 5-9, 1998.

[137] F. Barbier and A. Rusanov, Journal of Nuclear Materials **296**, 231 (2001).

[138] D. Pankratov et al., Polonium problem in nuclear power plants with lead-bismuth as a coolant, in *Proceedings of the Conference Heavy liquid metal coolants in nuclear technology, HLCM'98*, Institute of Physics and Power Engineering, Obninsk, Russia, October 5-9, 1998.

[139] T. Mihara, Y. Tanaka, and Y. Enuma, Conceptual design studies on various types of HLMC fast reactor plants, in *Power reactors and sub-critical blanket systems with lead and lead-bismuth as coolant and/or target material. Utilization and transmutation of actinides and long lived fission products*, IAEA-TECDOC-1348, 2003.

[140] N. Cannon et al., Transient and static mechanical properties of D9 fuel pin cladding and duct material irradiated to high fluence, in *Effects of Radiation on Materials: 15$^{\text{th}}$ International Symposium, ASTM STP 1125*, edited by R. Stoller, A. Kumar, and D. Gelles, American Society for Testing and Materials, Philadelphia, USA, 1992.

[141] J. Séran et al., Behaviour under neutron irradiation of the 15-15Ti and EM10 steels used as standard materials of the pénix fuel subassembly, in *Effects of Radiation on Materials: 15$^{\text{th}}$ International Symposium, ASTM STP 1125*, edited by R. Stoller, A. Kumar, and D. Gelles, American Society for Testing and Materials, Philadelphia, USA, 1992.

[142] S. Porollo et al., Journal of Nuclear Materials **329-333**, 314 (2004).

[143] B. Gromov et al., The analysis of operating experience of reactor installations using lead-bismuth coolant and accidents happened, in *Proceedings of the Conference Heavy liquid metal coolants in nuclear technology, HLMC'98*, Institute of Physics and Power Engineering, Obninsk, Russia, October 5-9, 1998.

[144] H. Khalil and R. Hill, Nuclear Science and Engineering **109**, 221 (1991).

[145] T. Hamid and K. Ott, Nuclear Science and Engineering **113**, 109 (1993).

[146] H. Choi and T. Downar, Nuclear Science and Engineering **133**, 1 (1999).

[147] P. Hejzlar, M. Driscoll, and M. Kazimi, Nuclear Science and Engineering **139**, 138 (2001).

[148] T. Takizuka et al., Studies on accelerator driven transmutation systems, in *Proceedings of the Fifth international information exchange meeting*, page 383, OECD/NEA, Mol, Belgium, November 25-27, 1998.

[149] W. Maschek et al., Safety analyses for ADS cores with dedicated fuel and proposals for safety improvements, in *Proceedings of the IAEA Technical Committee Meeting on Core Physics and Engineering Aspects of Emerging Nuclear Energy Systems for Energy Generation and Transmutation, IAEA-TECDOC-1356*, Argonne National Laboratory, USA, November 28 - December 1, 2000.

[150] M. Eriksson et al., Safety analysis of Na and Pb-Bi coolants in response to beam instabilities, in *Proceedings of the Third International Workshop on Utilisation and Reliability of High Power Proton Accelerators*, Santa Fe, USA, May 2002.

[151] K. Tuček et al., IAEA accelerator driven system neutronic benchmark, in *Feasibility and motivation for hybrid concepts for nuclear energy generation and transmutation*, IAEA–TC–903.3, 1998.

[152] M. Chadwick et al., Nuclear Science and Engineering **131**, 293 (1999).

[153] Y. Kim, W. S. Park, T. Y. Song, and C. K. Park, Nuclear Science and Engineering **143**, 141 (2003).

[154] R. MacFarlane and D. Muir, *The NJOY nuclear data processing system, version 91*, LA-12740-M, Los Alamos National Laboratory, USA, 1994.

[155] S. Kessler, Nuclear Science and Engineering **117**, 254 (1994).

[156] J. Cetnar et al., Transmutation calculations with Monte Carlo continuous energy burnup system MCB, in *Proceedings of the Third International Conference on Accelerator-Driven Transmutation Technologies and Applications, ADTTA'99*, Praha, Czech Republic, June 7-11, 1999.

[157] R. Cahn, P. Haasen, and E. Kramer, *Materials Science and Technology: a comprehensive treatment*, volume 10A, VCH, 1994.